



UFBA

UNIVERSIDADE FEDERAL DA BAHIA
ESCOLA POLITÉCNICA
PROGRAMA DE PÓS GRADUAÇÃO EM
ENGENHARIA INDUSTRIAL - PEI

DOUTORADO EM ENGENHARIA INDUSTRIAL

Normane Mirele Chaves da Silva

Desenvolvimento e caracterização de filmes biodegradáveis utilizando amido produzidos por extrusão termoplástica visando aplicação como embalagens





**Desenvolvimento e caracterização de filmes biodegradáveis utilizando
amido produzidos por extrusão termoplástica visando aplicação como
embalagens**

Normane Mirele Chaves da Silva

Salvador - Bahia

2018

NORMANE MIRELE CHAVES DA SILVA

**Desenvolvimento e caracterização de filmes biodegradáveis utilizando
amido produzidos por extrusão termoplástica visando aplicação como
embalagens**

Tese apresentada ao Programa de
Pós-Graduação em Engenharia
Industrial da Universidade Federal da
Bahia, em cumprimento às exigências
para obtenção do título de Doutor.

Orientadores:

Prof^a Dr^a Elaine C. de M. Cabral Albuquerque

Prof^a. Dr^a. Rosana Lopes Lima Fialho

Salvador – Bahia

2018

Ficha catalográfica elaborada pelo Sistema Universitário de Bibliotecas (SIBI/UFBA),
com os dados fornecidos pelo(a) autor(a).

Chaves da Silva, Normane Mirele
Desenvolvimento e caracterização de filmes
biodegradáveis utilizando amido produzidos por
extrusão termoplástica visando aplicação como
embalagens / Normane Mirele Chaves da Silva. --
Salvador, 2018.
145 f. : il

Orientador: Elaine C. de M. Cabral Albuquerque.
Coorientador: Rosana Lopes Lima Fialho.
Tese (Doutorado - Engenharia Industrial) --
Universidade Federal da Bahia, UFBA, 2018.

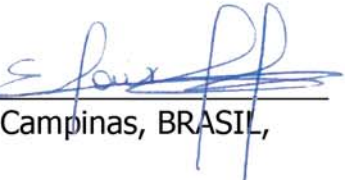
1. reforço polimérico,. 2. blendas biodegradáveis,.
3. extrusão. 4. gelatina reciclada.. I. Albuquerque,
Elaine C. de M. Cabral. II. Fialho, Rosana Lopes
Lima. III. Título.

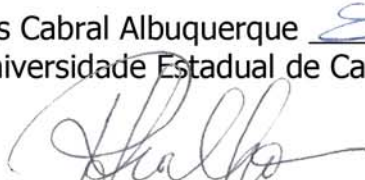
**DESENVOLVIMENTO E CARACTERIZAÇÃO DE FILMES BIODEGRADÁVEIS
UTILIZANDO AMIDO PRODUZIDOS POR EXTRUSÃO TERMOPLÁSTICA
VISANDO APLICAÇÕES EM EMBALAGENS**

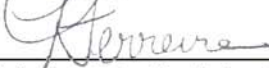
NORMANE MIRELE CHAVES DA SILVA

Tese submetida ao corpo docente do programa de pós-graduação em Engenharia Industrial da Universidade Federal da Bahia como parte dos requisitos necessários para a obtenção do grau de doutor em Engenharia Industrial.

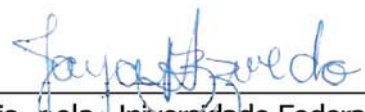
Examinada por:

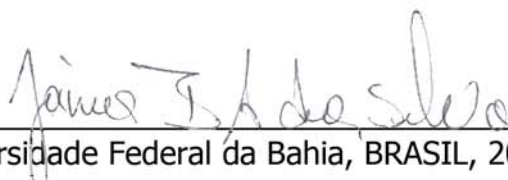
Prof. Dra. Elaine Christine de Magalhães Cabral Albuquerque 
Doutora em Engenharia Química, pela Universidade Estadual de Campinas, BRASIL,
2005.

Prof. Dra. Rosana Lopes Lima Fialho 
Doutora em Engenharia Química, pela Universidade Federal do Rio de Janeiro, BRASIL,
1998.

Prof. Dr. Classius Ferreira da Silva 
Doutor em Engenharia Química, pela Universidade Estadual de Campinas, BRASIL,
2006.

Profa. Dra. Farayde Matta Fakhouri 
Doutora em Tecnologia de Alimentos, pela Universidade Estadual de Campinas,
BRASIL, 2009.

Profa. Dra. Joyce Batista Azevedo 
Doutora em Ciência e Engenharia de Materiais, pela Universidade Federal de Campina Grande, BRASIL, 2013.

Profa. Dra. Jania Betania Alves da Silva 
Doutora em Engenharia Química, pela Universidade Federal da Bahia, BRASIL, 2013.

Salvador, BA - BRASIL
Agosto/2018

Dedico:

À Minha mãe;

Uma mulher incrível, que possui uma vontade de viver que dificilmente encontrarei em alguma outra pessoa.

AGRADECIMENTOS

À professora orientadora Drª. Elaine Christine de Magalhães Cabral-Albuquerque, pela orientação, carinho e por confiar a mim a execução desse trabalho. À professora Drª. Rosana Lopes Lima Fialho pela parceria e ensinamentos.

À professora Drª. Farayde Matta Fakhouri pelo acompanhamento, incentivo, motivação, revisão dos artigos e por ter aberto as portas para mim na Universidade Estadual de Londrina (UEL).

Aos colegas e amigos do Laboratório de Polímeros e Bioprocessos (LPB) e do Programa em Engenharia Industrial (PEI), Bruno, Ian, Eron e Juliano pela colaboração durante a pesquisa.

À professora Drª. Janice Izabel Druzian por permitir que grande parte dessa pesquisa fosse realizada no Laboratório de Pescados e Cromatografia Aplicada - LAPESCA FAR/UFBA e com isso possibilitou que grandes amigos surgissem em minha vida como Johnson, Paulo Leonardo, Denílson, Cris Rasta, Paulo Romano, Jamille, Carol, Lucas, Luciana.

Aos técnicos da secretaria do PEI, especialmente Tatiane, pelo apoio e atenção durante todo esse período.

Ao meu pai, minha mãe, meus irmãos, meus sobrinhos e meus amigos de longe, pelo amor, amizade e apoio incondicional.

Ao meu marido, companheiro e confidente Lucas Landim, pelo incentivo, apoio, amor e atenção em todos os momentos. Definitivamente essa trajetória não seria a mesma sem você ao meu lado. Amo-te eternamente!

Ao Instituto Federal Baiano (IF BAIANO) por todo apoio necessário;

À Fundação de Amparo à Pesquisa do Estado da Bahia (FAPESB) pelo apoio financeiro concedido através de uma bolsa de doutorado;

À todos que de alguma forma contribuíram para a realização deste trabalho, aqui fica o meu agradecimento.

SILVA, Normane Mirele Chaves da. Desenvolvimento e caracterização de filmes biodegradáveis utilizando amido produzidos por extrusão termoplástica visando aplicação como embalagens. 2018 (Tese de Doutorado). Programa de Pós-graduação em Engenharia Industrial. Universidade Federal da Bahia, Salvador, 2018.

RESUMO

O uso de polímeros sintéticos para a produção de embalagens plásticas tem impulsionado as pesquisas e o desenvolvimento de novos materiais. Neste contexto, o objetivo desse trabalho foi desenvolver e caracterizar filmes biodegradáveis a base de amido termoplástico com diferentes materiais de reforço, através do processo de extrusão e sopro visando aplicação como embalagem. Para tanto, dividiu-se o trabalho em duas etapas: a primeira etapa foi a produção filmes de poli(butileno adipato co-tereftalato) (PBAT) e amido termoplástico (ATP) incorporado com nanopartículas de amido (SNP), a segunda etapa foi direcionada para a produção de filmes de amido termoplástico e gelatina reciclada. Os resultados obtidos nos filmes de PBAT/ATP/SNP mostraram que os filmes que foram incorporados com 1% de SNP apresentaram redução da permeabilidade ao vapor de água e as propriedades mecânicas foram significativamente melhoradas, apresentando assim características similares aos filmes produzidos apenas com o PBAT. No que diz respeito aos filmes produzidos com amido e gelatina reciclada, foi possível constatar que o processo de reciclagem que a gelatina passou não interferiu em suas propriedades físicas, uma vez que, filmes com maiores concentrações de gelatina reciclada (12,5%) apresentaram características mecânicas superiores quando comparados a aqueles com menores concentrações. Além disso, a análise de biodegradabilidade mostrou que após 17 semanas esse mesmo filme apresentou uma perda de massa total de 50 %. Portanto, este trabalho mostra que é possível produzir filmes de amido termoplástico por extrusão com diferentes materiais de reforço com boas propriedades mecânicas e de barreira, apresentando assim como uma alternativa as embalagens plásticas convencionais.

Palavras-chaves: reforço polimérico, blendas biodegradáveis, extrusão, gelatina reciclada.

ABSTRACT

The use of synthetic polymers for the production of plastic packaging has propelled the researches and development of new materials. In this context, the objective of this work was the development and characterization of biodegradable films based on thermoplastic starch with different reinforcement materials, through the extrusion and blowing process for packaging application. The first step was to study the incorporation of starch nanoparticles (SNP) produced by ultrasound in blends of poly (butylenes adipate-co-terephthalate)-PBAT and thermoplastic starch (TPS). The second step aimed to the production of thermoplastic starch films and recycled gelatin. The results obtained in the PBAT/ATP/SNP films showed that the films that were incorporated with 1% SNP showed a reduction in water vapor permeability and the mechanical properties were significantly improved, thus presenting similar characteristics to the films produced only with the PBAT. About the films produced with recycled starch and gelatin, it was possible to observe that the recycling process which gelatin was subjected did not interfere in the physical properties, since, films with higher concentrations of recycled gelatin (12.5%) presented improved mechanical characteristics when compared to those with lower concentrations. Also the biodegradability analysis showed that after 17 weeks the same film showed a weight loss of 50%. Therefore, this work shows that it is possible to produce thermoplastic starch films by extrusion with different reinforcing materials with good mechanical and water vapor barrier properties, thus presenting as an alternative to the conventional plastic packaging.

Keywords: polymer reinforcement, biodegradable blends, extrusion, recycled gelatin.

Lista de Figuras

Capítulo 2

Figura 1 - Classificação de polímeros biodegradáveis	7
Figura 2 - Estrutura química do poli(butileno adipato co-tereftalato) (PBAT).....	9
Figura 3 - Estrutura química do amido: amilose (a) e amilopectina (b)	11
Figura 4 – Estrutura química da gelatina.....	14
Figura 5 - Esquema dos principais componentes de uma extrusora.....	17
Figura 6 – Diferentes métodos de produção de nanopartículas de amido	22

Capítulo 3

Figura 1 - a) Suspensão inicial b) Dispersão coloidal sonicada por 75 minutos (SNP) c) Nanopartículas de amido após o processo de secagem por congelamento (liofilização).....	26
Figura 2 - Extrusora dupla-rosca de matriz plana.....	27
Figura 3 - Pellets de PBAT/ATP/SNP.....	28
Figura 4- <i>Pellets</i> de amido e gelatina.....	29
Figura 5 - Extrusão por sopro.....	29

Capítulo 4

Artigo I

Figure 1. SNP images obtained by transmission electronic microscope (TEM). Magnification 1000x.	45
Figure 2. SEM of the surface of the films. PBAT (a), PBAT/TPS (b), 70/30/1% (c), 70/30/2% (d), 70/30/3% (e), 70/30/4% (f) and 70/30/5% (g). Magnification 5000x.	46
Figure 3. X-ray diffraction patterns for cassava starch (CS) and starch nanoparticles (SNP).	47
Figure 4. X-ray diffraction patterns and relative crystallinity (RC) of the films. .	48

Figure 5. Thermogravimetric analysis (TG) and derivative thermogravimetric (DTG) curves cassava starch (CS) and starch nanoparticles (SNP).....	49
Figure 6. Thermogravimetric analysis of the films.....	50
Figure 7. Differential thermal analysis of cassava starch (CS) and starch nanoparticles (SNP).....	51
Figure 8. Differential thermal analysis for films.....	52
Figure 9. Water absorptio n of the films.....	55

Artigo II

Fig. 1a - SEM features of the surface of the composite films.	72
Fig. 1b - Micrograph of native cassava starch (a) and SEM features of cross section of the composite films containing 2.5% (b) and 12.5% (c) of recycled gelatin.....	73
Fig. 2. X-ray diffractograms for starch, recycled gelatin and composite films... ..	75
Fig. 3. Thermogravimetric (TG) (a) and derivative TG (DTG) (b) of starch, recycled gelatin and composite films.....	76
Fig. 4. DSC thermograms of starch, recycled gelatin and composite films.....	78
Fig. 5. Water solubility of composites films.....	79
Fig. 6. Effect of gelatin concentration on mechanical properties of the composite films: Elongation at break (a); Tensile strength (b); Elasticity modulus (c). ..	80
Fig. 7. Stress- strain curves for the composite films.	81
Fig. 8. Evolution of biodegradation of the composite films buried under solid composting material.	82

Lista de Tabelas

Capítulo 2

Tabela 1 - Exemplos de pesquisas que utilizaram o PBAT e o amido para a produção de filmes biodegradáveis..... 18

Capítulo 3

Tabela 1 - Composição dos filmes poliméricos para 100g de amostra. 27

Tabela 2 - Composição das formulações dos filmes elaborados a partir de blendas de amido e gelatina..... 29

Capítulo 4

Artigo I

Table 1 - Values of thickness, water vapor permeability (WVP) and opacity of the films..... 53

Table 1 - Mechanical properties of PBAT, PBAT/TPS and PBAT/TPS/SNP films.
..... 55

Artigo II

Table 1 - Thermal Stability of films. 76

Sumário

RESUMO.....	iii
ABSTRACT	iv
Lista de Figuras.....	v
Lista de Tabelas	vii
CAPÍTULO 1- INTRODUÇÃO	1
1.1 Objetivos	4
1.2 Estrutura e organização	4
CAPÍTULO 2 – REVISÃO DE LITERATURA	5
2.1. Embalagens para alimentos	5
2.2. Polímeros biodegradáveis	6
2.2.1 Poli(butileno adipato co-tereftalato) (PBAT) Erro! Indicador não definido.	
2.2.2 Amido	10
2.2.3 Gelatina.....	13
2.3 Produção de filmes poliméricos biodegradáveis visando embalagens alimentícias	15
2.3.1 Casting	15
2.3.2 Extrusão a quente	16
2.4 Filmes à base de amido produzidos por extrusão	17
2.5 Reforço em filmes poliméricos visando aplicação na industria alimentícia.	20
CAPÍTULO 3 – MATERIAL E MÉTODOS	25
3.1 Materiais.....	25
3.2 Métodos.....	25
3.2.1 Produção das nanopartículas de amido	25
3.2.2 Produção dos filmes poliméricos de PBAT/AMIDO/SNP.....	26
3.2.3 Produção dos filmes poliméricos de amido e gelatina.....	28
3.3 Caracterização das nanopartículas de amido	29
3.3.1 Diâmetro médio, índice de polidispersão e potencial zeta das SNP	29
3.3.2 Morfologia.....	30
3.3.3 Cristalinidade.....	30
3.3.4 Análises térmicas das SNP	30
3.4 Caracterização dos filmes poliméricos	31

3.4.1 Caracterização dos filmes de PBAT/AMIDO/SNP	31
3.4.2 Caracterização dos filmes de amido e gelatina reciclada.....	33
CAPÍTULO 4 – RESULTADOS	36
Artigo I	36
Artigo II.....	64
CAPÍTULO 5 – CONCLUSÕES FINAIS E SUGESTÃO PARA TRABALHOS FUTUROS	87
CAPÍTULO 6 – REFERÊNCIAS BIBLIOGRÁFICAS	89
APÊNDICE A.....	105
APENDICE B.....	118
APÊNDICE C	129
APENDICE D	134

CAPÍTULO 1- INTRODUÇÃO

Um dos grandes desafios da população atual é destinar adequadamente as embalagens plásticas convencionais oriundas de polímeros sintéticos, uma vez que essas apresentam um processo de degradação lento. Assim, discussões sobre resíduos sólidos, sustentabilidade, biodegradabilidade e reciclagem dessas embalagens estão se tornando cada vez mais frequentes em meios científicos e jurídicos. Nesse contexto, os materiais poliméricos biodegradáveis são uma escolha ideal para substituir as embalagens de plásticos convencionais, pelo menos parcialmente, que possam ser dispostas com segurança no meio ambiente (WEI et al., 2015). Assim, novos polímeros comerciais à base de recursos renováveis em um curto prazo, ou derivados de petróleo, mas de caráter biodegradável, estão sendo desenvolvidos (LUCKACHAN; PILLAI, 2011).

Entre os polímeros provenientes de recursos renováveis, o amido tem sido considerado como um dos candidatos mais promissores, principalmente por sua disponibilidade e baixo custo (FAMÁ et al., 2005; COSTA, 2008). Além disso, ao ser misturado com plastificantes, como água e glicerol, dá origem a um novo material conhecido como amido termoplástico (ATP), o qual apresenta propriedades de processamento superiores ao amido nativo, sendo, por exemplo, utilizado na produção de filmes por extrusão (SARAZIN et al., 2008; THUNWALL et al., 2008). Entretanto, filmes produzidos somente de ATP apresentam fragilidade e sensibilidade à umidade o que limita sua utilização. Portanto, faz-se necessário a busca por alternativas que minimizem tais limitações.

Nesse contexto, uma das formas mais eficientes de melhorar as propriedades do amido termoplástico é a sua mistura com outros polímeros (formando as blendas poliméricas), como o poli (butileno adipato co-tereftalato) (PBAT) e a gelatina, com o objetivo de melhorar ou modificar as suas propriedades mecânicas e de permeação ao vapor de água, além de contribuir para a redução do custo de produtos a base de polímeros. No entanto, os

filmes produzidos a partir de blendas entre alguns polímeros biodegradáveis e amido ainda apresentam propriedades mecânicas e de barreira ao vapor de água inadequadas para embalagens alimentícias (ZULLO; IANNACE, 2009; BRANDELERO; GROSSMANN; YAMASHITA, 2011). Na literatura várias pesquisas descrevem a incorporação de fibras naturais, proteínas, óleos essenciais, entre outros, em filmes de amido com o objetivo de melhorar suas propriedades. Entre essas alternativas, destaca-se a, a incorporação de nanocargas a blendas de polímeros, visando aplicação em embalagens alimentícias, uma vez que essas, por apresentarem tamanho em escala nanométrica, têm a capacidade de preencher os espaços da matriz polimérica, possibilitando assim a produção de filmes mais estruturados, melhorando propriedades mecânicas e de barreira ao vapor de água.

Pesquisas que abrangem o uso desses nanomateriais como reforço em filmes poliméricos biodegradáveis são citadas na literatura (TEIXEIRA et al., 2009; SILVA; PEREIRA; DRUZIAN, 2012; ZAINUDDIN; AHMAD; KARGARZADEH, 2013; SLAVUTSKY; BERTUZZI, 2014). Entretanto, esses relatos descrevem a utilização de nanofibras ou nanocrystalis (*nanowhiskers*) de celulose. O uso de nanopartículas de amido (SNP) como material de reforço em filmes ainda é pouco explorada, o que possibilita novas abordagens.

As SNP podem ser produzidas por diferentes métodos, com destaque para a técnica de ultrassom que não gera resíduo (ecologicamente verde), apresenta alto rendimento e não necessita de qualquer tratamento para purificação (BEL HAAJ; MAGNIN; BOUFI, 2014). Além da aplicação como reforço, as SNP também podem ser utilizadas como nanosistemas de encapsulação de substâncias ativas, como pigmentos naturais com propriedades antioxidantes ou compostos indicadores da alteração do material, como alteração pH, contaminação microbiana e inativação de oxigênio, mostrando que as nanopartículas podem incorporar características que a transformem em sistemas capazes de melhorar a estabilidade do alimento. Em geral, os pigmentos naturais são instáveis, quimicamente, na presença de luz ou altas temperaturas e a encapsulação em SNP pode melhorar sua

estabilidade em processos alimentícios que usam temperaturas elevadas (FANG; BHANDARI, 2010; CORTÉS-ROJAS, 2015).

A produção de blendas de ATP e gelatina, também é uma opção para a produção de filmes biodegradáveis, principalmente porque a gelatina, que é um polímero natural, apresenta excelentes propriedades filmogênicas, abundância e biodegradabilidade (NUR HANANI; ROOS; KERRY, 2012). Entretanto, a depender do seu processo de produção, tipo e características desejadas, a gelatina pode apresentar um custo relativamente alto, o que restringe o seu uso grande proporção. Assim, uma das alternativas de reduzir o custo do processo que envolve a produção de filmes que contenham gelatina em sua composição, é a substituição da gelatina convencional pela gelatina reciclada. A incorporação de gelatina reciclada, além de contribuir com a redução dos custos da matéria-prima para produção de filmes, diminui a disposição de resíduos poliméricos no meio ambiente.

Portanto, este trabalho visa contribuir com a produção de filmes poliméricos à base de amido que apresentem características físicas desejáveis e com isso possam ser aplicados na indústria alimentícia.

1.1 Objetivos

Objetivo geral

Desenvolver filmes biodegradáveis a base de amido termoplástico, através do processo de extrusão e sopro visando aplicação como embalagem para indústria alimentícia.

Objetivos específicos

- Produzir filmes poliméricos a base de amido e PBAT;
- Produzir filmes poliméricos a base de amido e gelatina;
- Caracterizar os filmes produzidos quanto a morfologia, permeabilidade ao vapor d'água e propriedades mecânicas;
- Reforçar os filmes a base de amido com nanopartículas poliméricas;
- Avaliar o efeito da incorporação das nanopartículas de amido nas propriedades físicas e mecânicas de filmes biodegradáveis a base de amido;

1.2 Estrutura e organização

Este trabalho está estruturado em 6 (seis) capítulos, incluindo este. O segundo capítulo refere-se à fundamentação teórica que deu suporte a esta tese e as estratégias de produção de filmes a base de amido. O terceiro capítulo aborda a metodologia utilizada na parte experimental do trabalho, enquanto o quarto apresenta os resultados e sua discussão no formato de artigos que já foram publicados nas revistas International Journal of Polymer Science e Journal of Applied Polymer Science intitulados “PBAT/TPS composite films reinforced with starch nanoparticles produced by ultrasound” e “Starch/recycled gelatin composite films produced by extrusion: physical and mechanical properties”.

O quinto capítulo deste documento apresentam a conclusão e sugestão para trabalhos futuros, respectivamente. Por fim, o sexto capítulo apresenta as referências bibliográficas utilizadas neste trabalho. Também consta de um apêndice dedicado à produção de nanopartículas de amido contendo curcumina e outro apêndice que foi publicado na forma de capítulo de livro intitulado Production and Characterization of Starch Nanoparticles.

CAPÍTULO 2 – REVISÃO DE LITERATURA

2.1. Embalagens para alimentos

A embalagem é de fundamental importância para os alimentos, pois facilita sua manipulação, transporte, protege contra danos físicos e mecânicos, além de preservar a segurança e a qualidade do alimento, evitando a contaminação externa, química ou microbiológica e prolongando sua vida de prateleira (DAINELLI et al., 2008; RESTUCCIA et al., 2010). Segundo LAUTENSCHLÄGER (2001), o conceito de embalagem varia conforme a perspectiva em que é observada.

Para o consumidor, a embalagem é um meio de satisfazer o desejo de consumo do produto; para o marketing, a embalagem se torna o meio mais próximo do consumidor ser atraído para a compra do produto; para o setor de design, a embalagem é a forma de proteção até chegar ao consumidor; para a engenharia industrial é o meio de proteção do produto no transporte e armazenamento.

As embalagens podem ser classificadas, segundo sua utilização, em primárias, secundárias e terciárias. As primárias estão em contato direto com o produto, enquanto as secundárias têm a função de agrupar para facilitar a manipulação e a apresentação do produto. As embalagens secundárias também podem proteger a embalagem primária, evitando choques excessivos e vibrações do produto no seu interior. As embalagens terciárias protegem a mercadoria durante as fases do transporte e assim por diante (LANDIM et al., 2016). As embalagens para alimentos podem ser produzidas a partir de vários materiais. A escolha do material vai depender, entre outros fatores, das características do alimento a ser comercializado.

Os materiais mais utilizados na produção de embalagens alimentícias são o vidro, metal, papel/papelão e o plástico, sendo esse último o que domina o mercado de embalagens para alimentos. Esse domínio de embalagens

plásticas se deve ao fato deste apresentar menores custos de produção, flexibilidade de operação, leveza, transparência, boas propriedades mecânicas e barreiras ao vapor de água e oxigênio. Os polímeros mais usados em embalagens plásticas são: poliamidas (PA) (em filmes simples ou multicamadas), polietileno tereftalato (PET) (em garrafas para envase de bebidas), polietileno de baixa densidade (PEBD), polipropileno (PP), policloreto de vinila (PVC) entre outros (NASSER et al., 2005; FÉLIX; MANZOLI; PADULA, 2008).

Ainda que esses polímeros apresentem uma série de benefícios como matéria-prima básica para produção de embalagens alimentícias plásticas, esses materiais são provenientes do petróleo e decompõem-se lentamente no meio ambiente. Por apresentarem um longo período de decomposição (em geral, maior que 50 anos) e considerando que as embalagens possuem ciclo de vida curto, esses materiais contribuem para a geração significativa de resíduos sólidos urbanos (SCAPIN, 2009). No Brasil, segundo a ABRELPE – Associação Brasileira de Empresas de Limpeza Pública e Resíduos Especiais, a quantidade de plásticos pós-consumo gerado em 2016 foi de aproximadamente 3.300 toneladas, sendo que 23% desse total foram destinados à reciclagem. Assim, cerca de 80% de todo o material plástico produzido e/ou consumido é descartado em lixões ou no meio ambiente (ABRELPE, 2016).

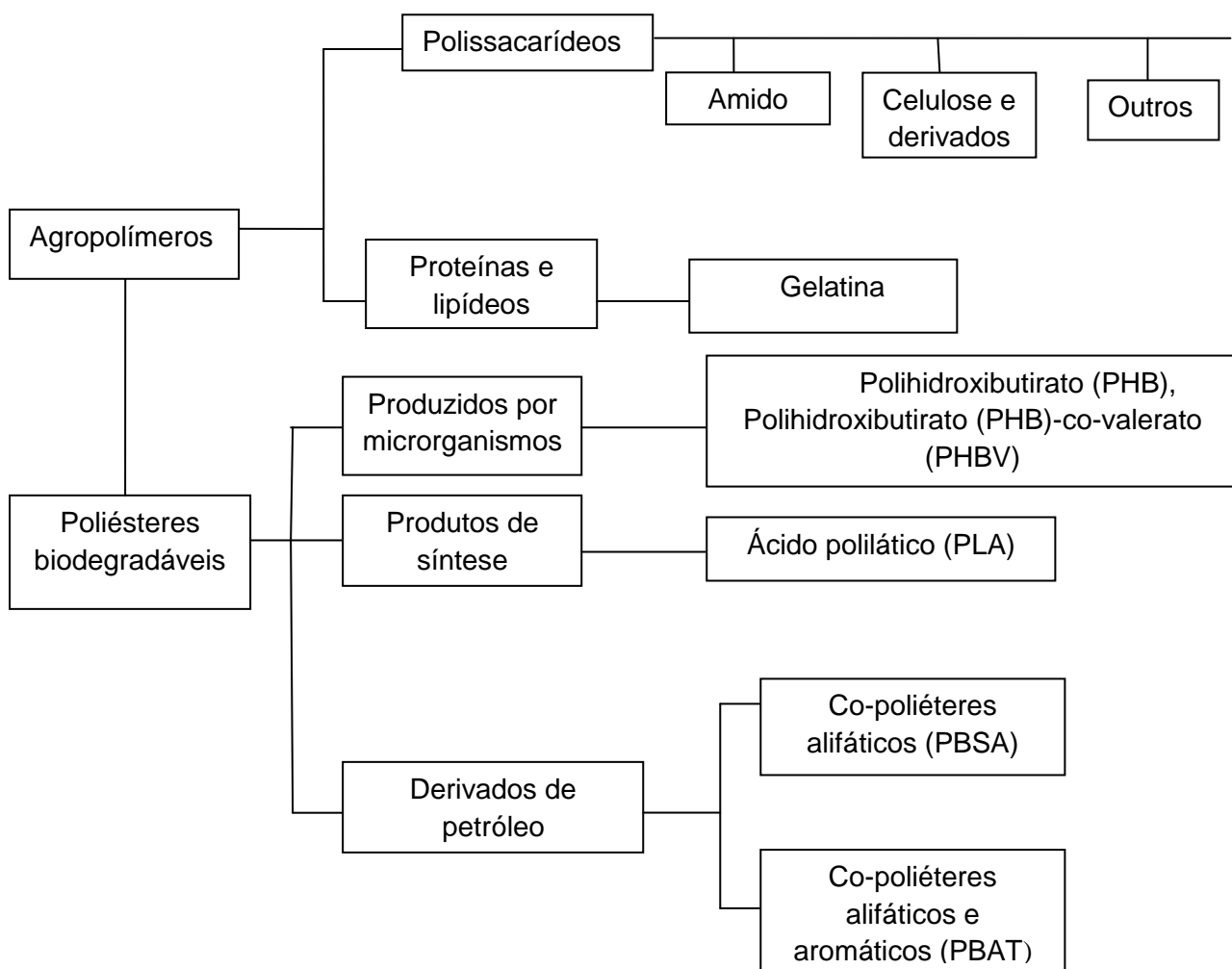
Nesse contexto faz-se necessário a busca por novas fontes de materiais, que tenham propriedades mecânicas semelhantes aos atuais polímeros utilizados na produção de embalagens alimentícias plásticas e que sejam rapidamente degradados, em semanas ou meses, no meio ambiente (AURAS, R., SINGH, S., SINGH J., 2006; DEL NOBILE et al., 2008; BRITO et al. 2011).

2.2. Polímeros biodegradáveis

Segundo a *American Society for Testing and Materials* (ASTM) e a *International Standards Organization* (ISO) polímeros biodegradáveis são aqueles que sofrem alterações nas propriedades químicas e mecânicas pela ação de agentes presentes no ambiente (RAMANI; CHARLES, 1999). Avérous

e Boquilon (2004) propuseram uma classificação de polímeros biodegradáveis em duas grandes famílias, os agropolímeros e os poliésteres biodegradáveis (Figura 1).

Figura 1 - Classificação de polímeros biodegradáveis.



Fonte: Adaptado de Avérous e Boquillo (2004).

Dentre os agropolímeros biodegradáveis, aqueles mais estudados são os polissacarídeos (amido) e as proteínas (gelatina). Esses são provenientes de fontes renováveis e possuem um ciclo de vida mais curto comparado com polímeros obtidos do petróleo (PETERSSON; STADING, 2005; BRITO et al., 2011). Além disso, apresentam boa capacidade de formar filmes flexíveis que

podem vir a serem utilizados como embalagens (WANG et al. 2007; MALI et al. 2010).

Entre os poliésteres biodegradáveis o PLA - poli(ácido lático); PHB - poli(hidroxibutirato); PHBV - poli(hidroxibutirato-co-hidroxivalerato) e copoliésteres alifáticos aromáticos (AAC) biodegradáveis, tais como: Ecoflex® - poli(butileno adipato co-tereftalato), são os que recebem maior atenção. Eles podem ser sintetizados por bactérias a partir de pequenas moléculas como o ácido butírico ou o ácido valérico ou obtidos de fontes fósseis, petróleo, ou da mistura entre biomassa e petróleo. A degradação destes resulta da ação de microorganismos de ocorrência natural como bactérias, fungos e algas, podendo ser consumidos em semanas ou meses sob condições ideais de biodegradação (BRITO et al., 2011). Por apresentarem alta resistência à umidade, à gordura, à mudança de temperatura e propriedade de barreira a gases, estes polímeros apresentam ótimas aplicações no setor de embalagens e filmes (PELICANO; PACHEKOSKI; AGNELLI, 2009), sendo, portanto destinados para a produção de diversos materiais, como sacos plásticos, copos, pratos, talheres, embalagens industriais (laminados, espumas), embalagens para a agricultura e para produtos de higiene e cosméticos (BASTIOLI, 2001) e também utilizados de forma isolada ou em combinação com outros materiais (blendas poliméricas) para a produção de filmes poliméricos (REIS et al., 2008; ARRIETA et al., 2014; MA et al., 2014; PACHEKOSKI; DALMOLIN, 2014; MALWELA; SINHA, 2015; AKRAMI et al., 2016; FERRI; FENOLLAR; BALART, 2016; LORIOT; VANNINI; POUSTKA, 2017; NOFAR et al., 2017). Entretanto, esses polímeros apresentam altos custos de produção e comercialização, o que inviabiliza a sua utilização em larga escala na indústria de alimentos. Os agropolímeros, por sua vez, como o amido, celulose e gelatina apresentam alta disponibilidade e renovabilidade quando convertidos em um material termoplástico, mantém seu caráter biodegradável e constitui uma interessante alternativa para polímeros sintéticos (SAVADEKAR; MHASKE, 2012).

Estes quando são usados para a produção de filmes resultam em materiais que apresentam propriedades de barreira adequadas contra o oxigênio, umidade relativa baixa e intermediária resistência mecânica.

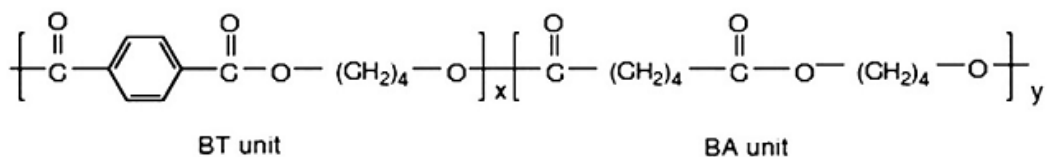
Entretanto, possuem elevada permeabilidade ao vapor de água, em razão da sua alta natureza hidrofílica, o que impede a sua utilização em escala industrial. Para contornar tais desvantagens, incluem-se modificações químicas, adição de plastificantes, mistura com outros polímeros, inserção de nanopartículas e adição de compatibilizantes. Assim, esses polímeros tornam-se mais aplicáveis em comparação com os polímeros à base de petróleo para fins de embalagens alimentícias (GARAVAND et al., 2017).

2.2.1 Poli(butileno adipato co-tereftalato) (PBAT)

O poli(butileno adipato co-tereftalato) (PBAT) é um copoliéster alifático aromático produzido a partir do petróleo, oriundo do ácido tereftálico, ácido adípico e 1,4-butanodiol (Figura 3). Segundo a norma ASTM D6400-04 é compostável, além de ser biodegradável em solo e meio aquoso, variando seu tempo de degradação em função do comprimento médio da cadeia dos blocos aromáticos (AL-ITRY; LAMNAWAR; MAAZOUZ, 2012; PALSIKOWSKI, 2015).

O caráter biodegradável do PBAT é devido a sua estrutura química, que apresenta uma parte alifática que é susceptível a ação biológica. Além disso, possui compostos aromáticos, que são resistentes a ação de bactérias e fungos, permanecendo praticamente intactos no ambiente, mas são tem excelentes propriedades físicas. Sendo assim, o PBAT combina biodegradabilidade e bom desempenho (RUDNIK, 2008; FUKUSHIMA et al., 2012).

Figura 2 - Estrutura química do poli(butileno adipato co-tereftalato) (PBAT).



Fonte: FUKUSHIMA et al., 2012.

O nome comercial do PBAT é Ecoflex ® e é produzido pela BASF AG (Alemanha) sendo considerado um polímero versátil e que permite a fabricação

desde filmes para embalar alimentos até artefatos termomoldados, injetados, soprados e extrusados (BASF, 2015). O PBAT apresenta propriedades comparáveis ao polietileno de baixa densidade (PEBD), com boas propriedades mecânicas e térmicas. Essa é uma das principais vantagens para a indústria transformadora, pois os filmes de PBAT podem ser fabricados e impressos em equipamentos tradicionais para polietileno (PE) não exigindo investimentos em novas máquinas (BIASUTTI, 2011; FUKUSHIMA et al., 2012). Apesar de apresentar essas vantagens, seu alto custo de produção e comercialização ainda dificulta a sua utilização em larga escala. Apesar disso, o PBAT ainda é combinado com outros polímeros para a produção de filmes (AL-ITRY; LAMNAWAR; MAAZOUZ, 2012; FUKUSHIMA et al., 2012; ARRUDA et al., 2015; NOFAR et al., 2017; OLIVEIRA et al., 2017).

A Tabela 1 apresenta resumidamente as principais propriedades do PBAT comercializado pela BASF.

Tabela 1 - Propriedades gerais do Ecoflex ®

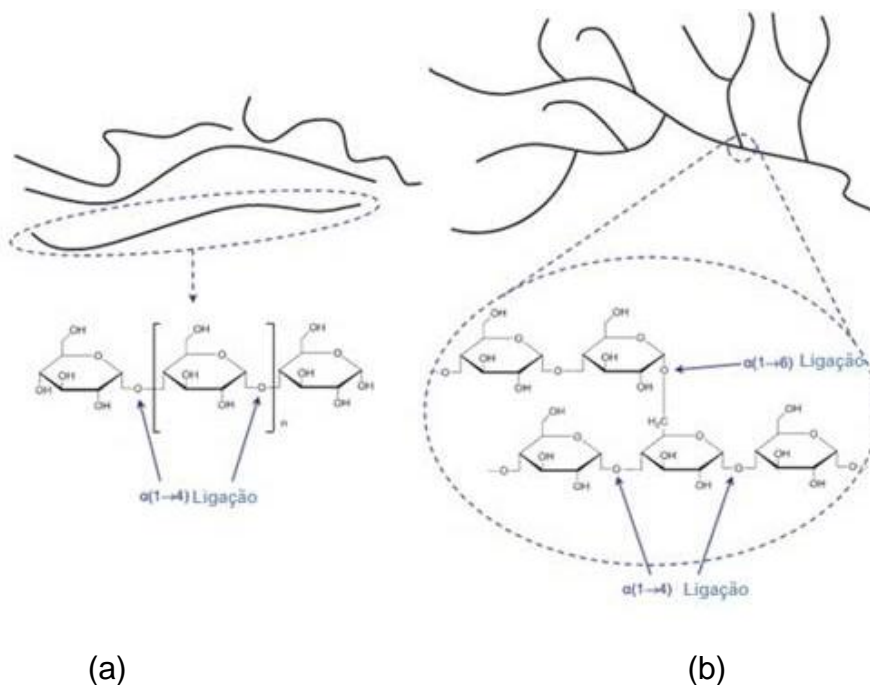
Propriedades	Valores
Densidade (g/cm ³)	1,25-1,27
Temperatura de fusão (°C)	110-120
Temperatura de transição vítreia (°C)	-30
Transparência (%)	82
Permeabilidade ao vapor de água (g/m ² . d)	170

2.2.2 Amido

O amido é um produto amiláceo, que pode ser extraído de partes comestíveis de cereais, raízes e tubérculos. Na indústria alimentícia, os amidos extraídos de tubérculos, raízes e rizomas podem ser designados como fécula. Suas propriedades químicas variam de acordo com sua fonte botânica, mas também são afetadas por outros fatores como pH, modificações químicas, composição do sistema, e força iônica do meio (FAMÁ et al., 2005).

O amido (Figura 2) é considerado uma importante fonte de energia na alimentação humana. Além disso, desempenha um papel essencial na melhoria das propriedades tecnológicas dos alimentos, como a solubilidade, viscosidade, força de gelatinização ou adesão nos produtos alimentares. O amido nativo é parcialmente cristalino ou semicristalino, com cristalinidade na faixa de 20-45%. É constituído de duas macromoléculas principais: a amilose (20-30%) que é uma molécula essencialmente linear e a amilopectina (70-80%) que é uma molécula ramificada, ambas com elevada massa molar. A cristalinidade dos grânulos de amido está relacionada principalmente à amilopectina, devido ao seu conjunto de ramificações que formam agregados cristalinos (SEBIO, 2003; CORRADINI et al., 2005; LIU et al., 2009).

Figura 3 - Estrutura química do amido: amilose (a) e amilopectina (b).



Fonte: XIE et al., 2013.

A amilose e amilopectina possuem dois importantes grupos funcionais: o grupo hidroxila ($-OH$), susceptível às reações de substituições; e as pontes oxídicas ou ligações glicosídicas (C-O-C), favorável à ruptura de cadeias. No primeiro grupo, a hidroxila da glicose atua como nucleófilo e através das

ligações com esse grupo, modificações na estrutura do amido podem ser feitas, originando polímero com diferentes propriedades.

Os grânulos de amido não são solúveis em água a temperatura ambiente (20-25°C). Entretanto, intumescem ao serem aquecidos (60-75°C) devido à difusão e absorção de água, perdendo ou reduzindo seu grau de cristalinidade e, consequentemente, favorecendo a dissolução parcial do amido em meio aquoso. Na sua forma nativa, o granulo de amido é caracterizado por sua baixa estabilidade sob tensão, hidroficiabilidade e ausência de plasticidade. Isso ocorre devido a presença de grupos hidroxilas em sua estrutura que corroboram para fortes interações intermoleculares, essas características fazem com o que o amido não seja uma boa opção para substituir os plásticos petroquímicos, não constituindo um verdadeiro termoplástico (MUKERJEA; SLOCUM; ROBYT, 2007). Entretanto, sob a ação de altas temperaturas (90 – 180 °C), cisalhamento mecânico e presença de plastificantes (glicerol, água e outros polióis), o amido é transformado em um novo material conhecido como amido termoplástico (ATP), que pode ser facilmente utilizado em processos industriais como extrusão, sopro, injeção e moldagem por compressão (AZEVEDO, 2016; RODRIGUEZ-GONZALEZ; RAMSAY; FAVIS, 2004; TAJUDDIN et al., 2011).

Para a produção de ATP, a escolha do tipo e concentração do agente plastificante são fatores determinantes. Plastificantes são moléculas pequenas que interagem com cadeias poliméricas como um solvente, enfraquecendo as pontes de hidrogênio entre as cadeias e, assim, aumentando o volume molecular. Essas mudanças afetam diretamente a temperatura de transição vítreo do material (T_g), que é reduzida, favorecendo a transição de um material de um estado vítreo (menor mobilidade molecular), para um estado de maior mobilidade molecular e, consequentemente, maior flexibilidade (GONTARD; GUILBERT; CUQ, 1993; VAN SOEST; VLIEGENTHART, 1997; BIERHALZ, 2010). O glicerol é o plastificante mais empregado na composição do ATP devido ao seu caráter polar e sua estrutura molecular (volume reduzido), além de seu elevado ponto de ebulição (SHIMAZU; MALI; VICTÓRIA, 2007).

Geralmente, os plastificantes são adicionados em compósitos termoplásticos de amido na proporção de 10 a 30g/100g amido seco, dependo do grau de rigidez do material que se deseja produzir (SHIMAZU; MALI; VICTÓRIA, 2007). Ressalta-se que, dependendo da concentração em que são empregados, os plastificantes podem causar um efeito chamado antiplastificante, isto é, ao invés de aumentar a flexibilidade e hidrofilicidade, podem causar um efeito contrário (MALI et al., 2005; CHANG; ABD KARIM; SEOW, 2006). Esse efeito pode acontecer quando são empregadas pequenas concentrações de plastificante (até 20 g/100 amido), assim o plastificante interage com o biopolímero, mas não está presente em quantidade suficiente para aumentar a mobilidade molecular (LOURDIN et al., 1997).

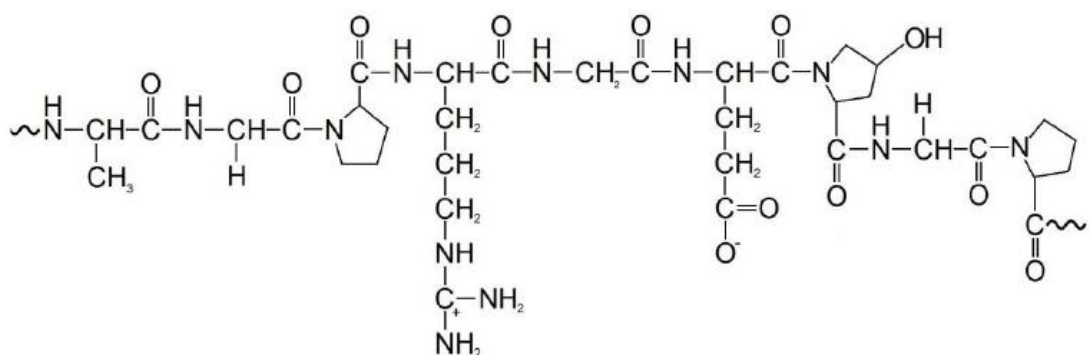
Embora o amido termoplástico seja um polímero de baixo custo, a sua aplicação como matéria-prima para produção de filmes poliméricos ainda é muito limitada, principalmente devido a sua baixa resistência mecânica, elevada sensibilidade a água, alteração de suas propriedades devido a cristalização durante o armazenamento e baixa compatibilidade com outros polímeros comerciais (NOSSA, 2014; MALI; GROSSMANN; YAMASHITA, 2010). Assim, a utilização deste termoplástico está associada à mistura com outros polímeros (blendas poliméricas) (REIS et al., 2008; MIRANDA; CARVALHO, 2011). A produção de blendas poliméricas tem por objetivo obter um determinado material polimérico com propriedades diferentes e superiores às dos polímeros puros, ou seja, melhorar propriedades físicas, químicas, mecânicas, além de acelerar o processo de biodegradação e reduzir o custo total do material, uma vez que o alto custo afeta a substituição dos polímeros sintéticos por polímeros biodegradáveis na área de embalagens.

2.2.3 Gelatina

A gelatina é uma proteína de origem animal, obtida pela desnaturação térmica do colágeno, que apresenta a propriedade de formar géis termo-reversíveis após ser aquecida, solubilizada e resfriada. Os aminoácidos predominantes, em sua estrutura, são principalmente a glicina (33%), prolina (13%) e a hidroxiprolina (9%). Apresenta massa molar média a partir de 65.000 até 300.000 g / mol, dependendo do grau de hidrólise que é submetida.

(FAKIROV e BHATTACHARYYA, 2007; BELITZ,, GROSCH, e SCHIEBERLE, 2009). Pode ser classificada em dois tipos, de acordo com o pré-tratamento aplicado: tipo A, obtida a partir do colágeno tratado com ácido (com pele e ossos de suínos) e tipo B obtida através do tratamento alcalino (com couro, ossos e aparas de couro) (HANANI et al., 2014). A sua estrutura química está representada da Figura 4.

Figura 4 – Estrutura química da gelatina



Fonte: Takinami, 2014.

A gelatina apresenta propriedades que podem ser divididas em dois grupos: as propriedades gelificantes (viscosidade, força do gel, texturização, espessamento e ligação de água) e as propriedades de superfície (formação e estabilização de emulsão, formação de filme e formação de espuma) (GOMEZ-GUILLEN et al., 2011).

Em sistemas aquosos a gelatina forma ligações de hidrogênio com a água devido a exposição de regiões polares, tornando-se intumescida (gel). A força dos géis (*Bloom*) formados depende da concentração e da força intrínseca da gelatina usada, que é em função da estrutura e da massa molar (SEBIO, 2003; GOMEZ-GUILLEN et al., 2011).

A gelatina desperta bastante interesse por ser uma matéria-prima abundante, por ter excelentes propriedades funcionais e filmogênicas, além de exibir baixa antigenicidade, elevada biocompatibilidade e absorbilidade

(MORAES; SILVA, 2008; GÓMEZ-ESTACA et al., 2009). Uma de suas aplicações mais estudadas nos últimos anos é o seu uso na produção de filmes biodegradáveis (RIVERO; GARCÍA; PINOTTI, 2010; KRISHNA; NINDO; MIN, 2012; NUR HANANI; ROOS; KERRY, 2012; NUR HANANI et al., 2013; WANG et al. 2017). Os filmes feitos de gelatina são transparentes, resistentes e fáceis de manusear, apresentam efetiva barreira a gases (CO_2 e O_2), porém, em função do seu caráter hidrofílico, possui alta permeabilidade ao vapor de água (DE CARVALHO; GROSSO, 2006; WU et al., 2017). Entretanto, a gelatina, pode ter seu custo muito elevado, dependendo do processo de produção, das características desejadas (*bloom* e viscosidade), bem como do Tipo (A ou B). Uma das formas de reduzir o custo de filmes elaborados a base de gelatina, bem como contribuir para a eliminação de resíduos, seria a utilização de gelatina reciclada como matéria-prima para a produção de filmes poliméricos.

2.3 Produção de filmes poliméricos biodegradáveis visando embalagens alimentícias

As técnicas mais comumente usadas para a produção de filmes a partir da mistura de polímeros ou blendas são “*casting*” e extrusão a quente. A literatura cita vários trabalhos referentes à produção de filmes via *casting* (AHMAD et al., 2015; FERNANDES et al., 2015; WANG et al. 2016) (MALI et al., 2002, 2004, 2005; 2006; ALVES et al., 2007; GALDEANO et al., 2009).

2.3.1 Casting

O método de *casting* é um método multi-etapas, onde os filmes são preparados pela evaporação do solvente de uma solução filmogênica sobre um suporte, essa técnica é considerada simples e de custo relativamente baixo (MALI, 2002). Embora apresente características de produção em pequena escala, muitos investimentos tem contribuído para tornar esta técnica de produção adequada para a utilização em larga escala. O desafio de transposição da escala está em controlar parâmetros operacionais de máquinas industriais, tais como tempo de secagem, velocidade de mistura, temperatura que refletam na qualidade do filme formado. Além disso, essa técnica usa solventes, produz filmes quebradiços ao longo do tempo de

estocagem e causa decréscimo no percentual de elongação devido à evaporação do solvente (KARK, KIM e NA et al., 2016).

2.3.2 Extrusão a quente

A extrusão é uma operação termomecânica de vasta aplicação, utilizada no processamento de alimentos, de rações animais, na modificação de amidos e no processamento de termoplásticos.

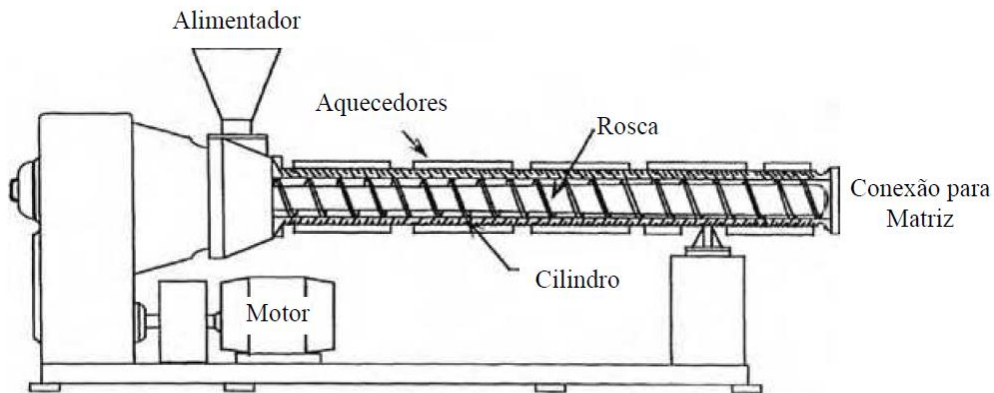
Dentre as suas principais vantagens estão: i) versatilidade, capaz de produzir uma grande variedade de produtos, tornando o processo extremamente flexível ii) baixo custo, a extrusão é um processo relativamente barato e produtivo comparado a outros processos que utilizam calor iii) processo automatizado que permite grande capacidade de produção (BERRIOS; ASCHERI; LOSSO, 2012). Além disso, o fato de utilizar pequenas quantidades de água apresenta a vantagem de não gerar efluentes, assim considerado de baixo impacto ambiental (SCAPIM, 2009).

O sistema de extrusão é constituído por uma rosca arquimediana, girando dentro de um barril aquecido, arrastando o material polimérico que é alimentado, por meio de um funil em uma de suas extremidades. Consequentemente, o material é aquecido, fundido e forçado, sob pressão a passar através de uma abertura na extremidade oposta, denominada matriz. O material extrudado é resfriado progressivamente, até tornar-se sólido. Dentre os componentes de uma extrusora, a rosca é considerada o mais importante pelo fato de transportar, fundir, homogeneizar e plastificar o polímero. É devido ao movimento, e consequente cisalhamento sobre o material, que a rosca única gera cerca de 80% da energia térmica e mecânica necessária para transformar os polímeros (MANRICH, 2005).

As máquinas extrusoras são do tipo de rosca única, conhecidas como monorosca e máquinas com dupla rosca, mas independente do tipo, a rosca deve ser projetada de tal maneira que sua geometria e elementos de rosca promovam a máxima eficiência, vazão constante, plastificação e homogeneização adequadas sem danos ao polímero, alinhadas com a

durabilidade da mesma (RICHART, 2013). A Figura 4 apresenta o esquema de uma extrusora.

Figura 5 - Esquema dos principais componentes de uma extrusora.



Fonte: Koopmans; Doelder; Molenaar, 2001.

2.4 Filmes à base de amido produzidos por extrusão

A produção de filmes poliméricos a base de amido tem o objetivo de encontrar uma solução para os problemas causados por plásticos, que levam séculos para se degradarem na natureza. A mistura com o amido acelera o ataque de microorganismos e garante pelo menos uma biodegradação parcial. Isso ocorre porque os microorganismos hidrolisam o amido circundante e o material polimérico estrutural perde sua integridade. Esse processo faz com que haja deterioração das propriedades mecânicas, facilitando a quebra do material por outros mecanismos de degradação (KIATKAMJORNWONG et al., 1999; THAKORE et al., 2001). Além disso, o amido por ser barato e abundante diminui os custos de produção das blendas. Entretanto, o amido por possuir elevada hidroficialidade, produz filmes com alta permeabilidade ao vapor de água e propriedades mecânicas pobres (quebradiços).

A produção de filmes biodegradáveis pelo processo de extrusão utilizando o amido como um dos seus componentes vem crescendo nos últimos anos, destaca-se a mistura do amido com poliésteres biodegradáveis, entre os mais estudados estão os poliésteres alifáticos e aromáticos como o poli(ácido láctico) (PLA), policaprolactona(PCL), poli(butileno adipato coteléftalato) (PBAT)

e poli(hidroxibutirato) (PHB) (KE; SUN; SEIB, 2003; LI; HUNEAULT, 2011; MINA-H; VALADEZ-G; TOLEDANO-T, 2013; SHIRAI et al., 2016), ou com polímeros naturais (PELISSARI; YAMASHITA; GROSSMANN, 2011; DANG; YOKSAN, 2016; MENDES et al., 2016).

Nesse contexto, o PBAT, que já foi relatado anteriormente (Item 2.2.2) como um polímero que apresenta uma série de características que o credencia como um material adequado para a produção de filmes poliméricos surge como uma das possibilidades mais estudadas para a produção de blendas com o amido. A mistura desses dois polímeros tem por objetivos principais melhorar a processabilidade e as propriedades do amido termoplástico (OLIVEIRA et al. 2017). A produção de blendas de amido e PBAT vêm sendo explorada nos últimos anos e com resultados satisfatórios (Tabela 1).

Tabela 1 - Exemplos de pesquisas que utilizaram o PBAT e o amido para a produção de filmes biodegradáveis.

Proporção PBAT/ATP	Resultados	Referências
70/30	Aumento linear nos valores de módulo de elasticidade em função da proporção de amido (até 30%) na matriz de PBAT.	Mohanty; Nayak (2010)
70/30	Aumento de 107% do módulo de elasticidade 20,81% do alongamento até a ruptura.	Nayak (2010)
50/50	Maiores valores de alongamento a ruptura quando comparado com outras proporções de PBAT/ATP (80/20 e 65/35).	Brandelero; Grossmann; Yamashita (2011)
70/30	Valores de alongamento até a ruptura iguais aos filmes de PBAT puro.	Stagner, Alves e Narayan (2012)
70/30	Aumento da resistência a tração dos filmes até a adição de 30% em peso de amido na matriz de PBAT.	Wei et al. (2015)

Vale frisar que a maioria desses relatos, que incluem PBAT e ATP, utiliza a proporção de 70/30 para a produção dos filmes. Segundo Wei et al. (2015), essa relação confere melhores resultados (propriedade mecânicas) devido a melhor dispersão e ao menor tamanho de partícula de ATP na matriz PBAT.

Essas pesquisas, além de comprovar a viabilidade tecnológica e econômica da união PBAT/ATP para a produção de filmes poliméricos, descrevem também que a baixa compatibilidade existente entre esses dois materiais ainda é uma desvantagem a ser contornada.

A baixa compatibilidade entre o amido (hidrofílico) e o PBAT (hidrofóbico) é devido à alta tensão interfacial existente entre si. Na tentativa de contornar essa incompatibilidade, utilizam-se agentes compatibilizantes, que são substâncias que possuem grupos funcionais que tem a capacidade de reagir simultaneamente com os componentes de uma blenda polimérica, modificando-os e desta forma melhorando a interação entre eles (ERMOLOVICH; MAKAREVICH, 2006).

Para sua função ser desempenhada de forma eficiente o compatibilizante deve estar localizado na interface entre os domínios de fase das blendas imiscíveis. Os compatibilizantes podem atuar segundo dois mecanismos distintos: o mecanismo de natureza termodinâmico, onde atua reduzindo a tensão interfacial entre as fases e o mecanismo de natureza cinética, onde o compatibilizante localizado na interface reduz a aglomeração dos domínios por estabilização estérica (MALIGER et al., 2006). Os ácidos orgânicos são uma das principais substâncias que podem ser usadas como agentes compatibilizantes por ser uma alternativa atóxica, com vantagens evidentes de segurança e compatibilidade com os alimentos, quando o objetivo é a embalagem alimentar (CARVALHO et al., 2005). Sendo o ácido adípico, cítrico, esteárico, anidrido malélico, mágico e tartárico os mais utilizados.

A gelatina, como já foi descrito no Item 2.2.3, é uma alternativa promissora para a produção de filmes poliméricos e também vem sendo estudada como uma opção para composição de blendas com ATP. Tongdeesoontorn et al. (2012) descreveram que filmes com 30% de gelatina

(produzidos por *casting*) apresentaram maior força de tração quando comparados com filme de ATP puro. Entretanto, menores valores de alongamento até a ruptura.

Fakhouri et al. (2013) ao comparar diferentes técnicas de obtenção de filmes de amido e gelatina concluíram que a composição do amido e o processo de obtenção interferem nas propriedades do filme. Soliman e Furuta (2014) desenvolveram, pela técnica de fundição com evaporação do solvente, filmes de gelatina com diferentes tipos de amido. Os autores concluíram que o aumento da concentração de gelatina proporcionou um aumento nos valores de tensão e de alongamento até a ruptura.

Acosta et al. (2015) ao analisarem as características físicas e microestruturais de filmes de amido de mandioca e gelatina bovina, pela técnica de *casting*, constataram que a adição de gelatina proporcionou um aumento nos valores de alongamento até a ruptura dos filmes.

Liu et al. (2014) produziram filmes de gelatina e amido de milho hidroxipropilado com alto teor de amilose (80%) plastificados com polietilenoglicol (PEG) 400 (400 g/mol) pelo método de *casting*. Segundo os autores a mistura de gelatina e amido formam duas fases separadas. As superfícies dos filmes com PEG tornaram-se muito mais suaves, o que indica a que a compatibilidade na interface entre a gelatina e o amido foi melhorada.

Vale salientar, que na literatura atual, a gelatina utilizada na produção de filmes biodegradáveis apresenta-se na sua forma nativa. O uso da gelatina reciclada como matéria-prima para a produção de filmes ainda não foi descrita por nenhum autor, concedendo a esse trabalho um perfil moderno e que adequado aos dias atuais.

2.5 Reforço em filmes poliméricos visando aplicação na indústria alimentícia

A inserção de nanopartículas ou nanocristais em uma matriz polimérica melhora não apenas as propriedades dessas matrizes, mas também seu custo-benefício, pois, o incremento das propriedades é obtido a concentrações muito baixas desses preenchedores.

Compósitos correspondem à combinação de polímeros e preenchedores inorgânicos ou orgânicos, separados entre si por uma interface e cujas propriedades e desempenho devem ser superiores aos seus constituintes quando atuam isoladamente. Já os nanocompósitos são obtidos através da incorporação física de pelo menos um componente, em uma matriz polimérica, com dimensões nanométricas (TEIXEIRA, 2010). Quando essa nanopartícula é de caráter biodegradável e é inserida em matrizes poliméricas também biodegradáveis essa composição é conhecida como bionanocompósito (CHEN et al., 2009).

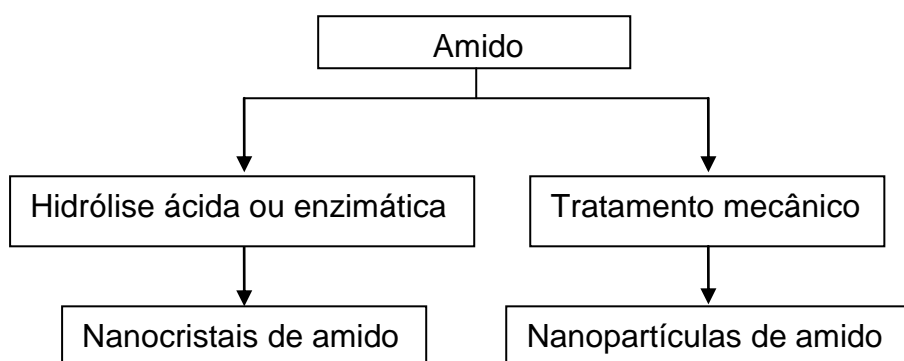
As propriedades dos bionanocompósitos dependem das características individuais de cada componente (matriz e reforço), da composição (fração volumétrica dos constituintes), da morfologia da partícula (dimensões) e arranjo espacial (grau de cristalinidade) e das propriedades da interface (PEREIRA et al., 2014).

Muitos trabalhos na literatura descrevem a produção de bionanocompósitos com matrizes biodegradáveis de origem natural como polissacarídeos (amido, alginato e quitosana) e com polímeros sintéticos biodegradáveis, com destaque para os polilactídeos – PLAs (também obtido por rota biotecnológica), a poli(ϵ -caprolactona) - PCL, o poli(ácido glicólico) - PGA, o poli(hidroxioctanoato) - PHO, o poli(hidroxibutirato) – PHB, e o seu copolímero poli(hidroxibutirato-co-hidroxivalerato) – PHBV. As pesquisas compreendem, sobretudo, o uso de nanofibras ou nanocristais (NCC) de celulose como nanocompósito, (GOFFIN et al., 2011; CHEN et al., 2012; LUZI et al., 2015; MIRANDA et al., 2015; MA; HU; WANG, 2016; CORSELLO et al., 2017). Essas nanocargas propiciam características únicas à matriz em função de sua adesão interfacial matriz-reforço, orientação na matriz, seu grau de dispersão, sua morfologia controlada e pequeno volume, por consequência grande área superficial (AZEREDO, 2013).

Nanopartículas de amido (SNP) são obtidas a partir da ruptura da região cristalina do amido por meio de tratamento mecânico, como por exemplo, microfluidiação, ultrassom, processos combinados, precipitação, entre outros, apresentando característica basicamente amorfa, já os nanocristais de amido

(SNC) são plaquetas cristalinas resultantes da hidrólise ácida ou enzimática e que durante a reação, as regiões amorfas, mais acessíveis, são mais rapidamente atacadas em comparação aos domínios cristalinos que permanecem intactos (Le Corre; Angellier-Coussy, 2014). Assim, os nanocristais e as nanopartículas, possuem propriedades, cristalinidade e formas diferentes. A Figura 5 mostra alguns meios de produção de nanopartículas de amido com perfil amorfo ou cristalino.

Figura 6 – Diferentes métodos de produção de nanopartículas de amido.



Fonte: Adaptado de Le Corre e Angellier-Coussy (2014).

Os nanocristais (SNC) ou as nanopartículas de amido (SNP) vêm sendo utilizados, em várias pesquisas, como enchimento em filmes de amido (SHI et al., 2013; DAI et al., 2015; LI et al., 2015; TEODORO et al., 2015; FAN et al., 2016; JIANG et al., 2016) e também em outras matrizes poliméricas (CHEN et al., 2008; RAJISHA et al., 2014; CONDÉS et al., 2015). Os resultados demonstraram uma melhoria das propriedades mecânicas e de barreira ao vapor de água desses filmes, além de acelerar o processo de degradação. Todas essas pesquisas foram desenvolvidas utilizando a tradicional técnica *casting* para a produção dos filmes.

Vale frisar que as SNP quando inseridas em matrizes poliméricas não proporcionam o mesmo reforço que os NCC ou os SNC (KIM; PARK; LIM, 2015; BEL HAAJ et al., 2016). A principal razão é a diferença na geometria das nanopartículas. Os nanocristais têm uma relação L/d (comprimento por

diâmetro) mais elevada (50-500 nm de comprimento, e 3-5 nm de diâmetro) quando comparadas com as nanopartículas (comprimento de 20-40 nm e diâmetro de 15-30 nm) (ANGELLIER-COUSSY et al., 2009; MOON et al., 2011), consequentemente os nanocristais tem a capacidade de preencher melhor os espaços e proporcionar uma melhoria nas propriedades mecânicas de permeabilidade ao vapor de água.

Praticamente não há na literatura pesquisas que tenham utilizado SNP ou SNC na produção de filmes poliméricos por extrusão. O único registro até o momento é o de Gonzalez-Seligra et al. (2016) que produziram filmes de PBAT/ATP, reforçados com 0,6% de SNP produzidas por radiação gama, os autores concluíram uma melhoria nas propriedades mecânicas do compósito.

Entre os diferentes processos para a produção de nanopartículas a hidrólise ácida é a mais utilizada. No entanto, esse método não é apropriado para aplicações industriais, pois requer um longo tempo para execução, além de gerar resíduos ambientais. O tratamento por ultrassom surge como uma alternativa para a produção de nanopartículas de amido, sendo considerada uma técnica ecologicamente verde e sem a necessidade de qualquer tratamento químico adicional (BEL HAAJ et al., 2013).

O ultrassom é um conjunto de ondas sonoras com vibrações mecânicas de alta freqüência, acima da capacidade do ouvido humano (18 kHz). (JAMBRAK et al., 2010; LI et al., 2016). As ondas são geradas por transdutores que criam vibrações com alta energia. Estas vibrações são amplificadas e transmitidas para sonotrodes ou probes, os quais entram em contato direto com o fluido, gerando vibrações que são capazes de formar cavidades cheias de gás ou de vapor (cavitação) (JAMBRAK et al., 2010; FENG, BARBOSA-CANOVAS; WEISS, 2011).

Normalmente esse método é utilizado para promover modificações químicas em polímeros (ALIYU; HEPHER, 2000; BAXTER; ZIVANOVIC; WEISS, 2005), inativação de microrganismos (CAMERON; MCMASTER; BRITZ, 2008) e em suspensões de amido para melhorar característica como solubilidade, inchaço e capacidade de absorção de água (IZIDORO et al., 2011; LUO et al., 2008).

Recentemente vem sendo utilizado para a produção de nanopartículas de amido (BEL HAAJ et al., 2013; BEL HAAJ; BOU, 2014; BEL HAAL et al., 2016). Entretanto, ainda não há relatos da utilização de nanopartículas de amido produzidas por ultrassom como enchimento polimérico, o que confere a essa pesquisa um caráter inovador.

CAPÍTULO 3 – MATERIAL E MÉTODOS

3.1 Materiais

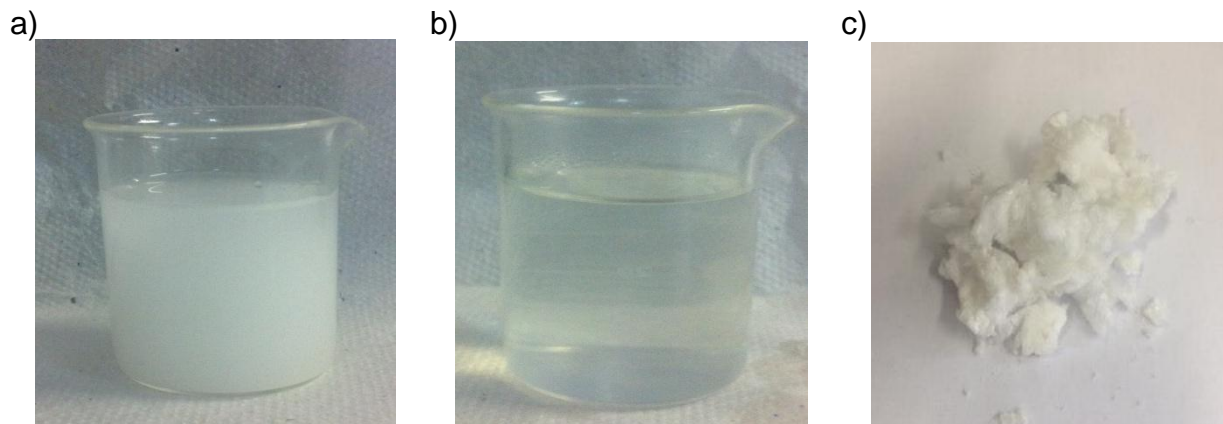
- Amido de mandioca cedido pela Cargil Agrícola S.A.
- Amido de mandioca adquirido junto a Yoki S.A.
- Glicerol comercial (Dinâmica-Brasil)
- Agentes compatibilizantes: ácido cítrico (Vetec Química Fina-LTDA) e o ácido esteárico (Dinâmica-Brasil).
- Poli(butileno adipato co-tereftalato)-PBAT adquirido junto a BASF.
- Gelatina bovina reciclada doada pela Universidade Estadual de Campinas (Unicamp).

3.2 Métodos

3.2.1 Produção das nanopartículas de amido

As nanopartículas de amido (SNP) foram produzidas segundo metodologia adaptada de Bel Haaj et al. (2013). A suspensão de amido (50 mL) com um teor de sólidos de 1,5% foi sonicada a 80% de potência (50 W) durante 75 min em um ultrassom com probe (modelo Q55, EUA). Em seguida, a suspensão coloidal foi submetida a secagem por congelamento (liofilização). A Figura 1 apresenta a suspensão de amido, a dispersão coloidal (SNP) e as SNP após a liofilização.

Figura 1 - a) Suspensão inicial b) Dispersão coloidal sonicada por 75 minutos (SNP) c) Nanopartículas de amido após o processo de secagem por congelamento (liofilização).



3.2.2 Produção dos filmes poliméricos de PBAT/AMIDO/SNP

O processamento dos filmes seguiu a metodologia proposta por Silva et al., (2012) com adaptações e consistiu em duas etapas. A primeira etapa foi a produção dos *pellets*. Inicialmente o amido, as SNP, o glicerol, os ácidos cítrico e esteárico foram misturados manualmente e processados em extrusora dupla-rosca marca AX (modelo DR1640, Brasil) localizada no Laboratório de Análises Aplicadas a Biomateriais do Departamento de Farmácia da Universidade Federal da Bahia. A velocidade da rosca foi mantida em 44 rpm, o programa de temperatura utilizado para a produção dos *pellets* foi de 80°C, 120°C, 130°C, 130°C, 140°C, 140°C, 145°C e 145°C para as zonas de aquecimento de 1 a 8 respectivamente. A segunda etapa foi a produção dos filmes, onde foram utilizados os mesmos parâmetros da produção dos *pellets*, com a inclusão da matriz formadora dos filmes que foi mantida a 130°C. A Tabela 1 apresenta a composição dos filmes.

Tabela 1 - Composição dos filmes poliméricos para 100g de amostra.

Filmes	Amido (g)	SNP(g)	PBAT(g)	Glicerol(g)	Ác. Cítrico(g)	Ác. Esteárico (g)
70/30	22,1	0	70,0	7,0	0,6	0,3
70/30/1%	21,87	0,22	70,0	7,0	0,6	0,3
70/30/2%	21,65	0,44	70,0	7,0	0,6	0,3
70/30/3%	21,43	0,66	70,0	7,0	0,6	0,3
70/30/4%	21,21	0,88	70,0	7,0	0,6	0,3
70/30/5%	20,99	1,10	70,0	7,0	0,6	0,3

A Figura 2 apresenta extrusora dupla-rosca utilizada na produção dos filmes e a Figura 3 os *pellets*.

Figura 2 - Extrusora dupla-rosca de matriz plana.

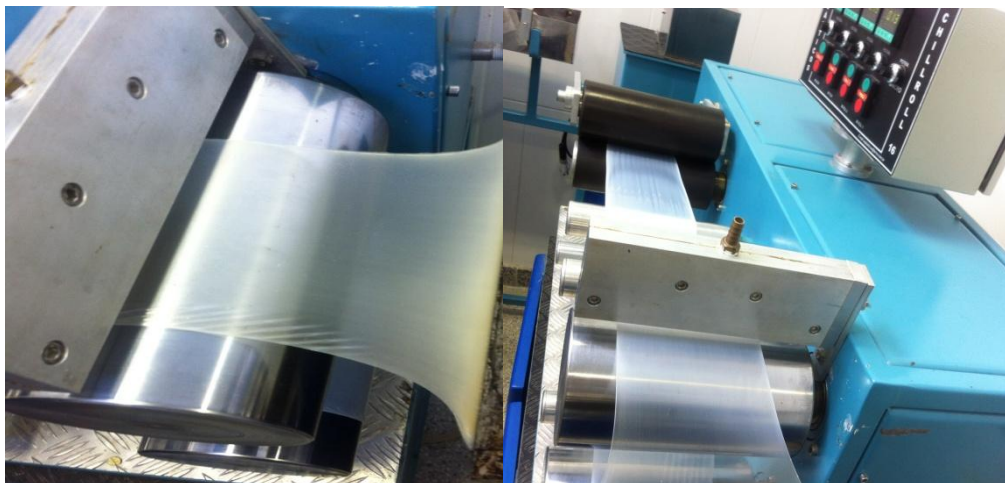


Figura 3 - Pellets de PBAT/ATP/SNP.



3.2.3 Produção dos filmes poliméricos de amido e gelatina

Os filmes foram obtidos utilizando-se extrusora marca BGM (modelo EL-25, São Paulo, Brasil) localizada no Departamento de Ciência e Tecnologia de Alimentos do Centro de Ciências Agrárias da Universidade Estadual de Londrina. A extrusora possui 3 (três) zonas de aquecimento no canhão, 1 zona de aquecimento no cabeçote para fio e duas zonas de aquecimento no cabeçote para produção de filmes por sopro. Novamente a produção dos filmes se deu em duas etapas.

A primeira etapa foi a produção dos *pellets*. Inicialmente foram misturados manualmente o amido de mandioca, o glicerol e a gelatina. A extrusora foi alimentada com esta mistura e o fio produzido cortado na forma de *pellets*. A temperatura utilizada foi de 120°C nas 3 zonas de aquecimento do canhão e 90°C no cabeçote para fio, com velocidade da rosca de 30 rpm. A extrusora foi alimentada manualmente com os *pellets* (blendas) e o filme foi formado pela técnica de sopro (balão). A Figura 5 apresenta os *pellets* e a Figura 6 o filme sendo soprado na extrusora.

Figura 4- Pellets de amido e gelatina.



Figura 5 - Extrusão por sopro dos filmes de amido e gelatina.



Foram produzidas 6 (seis) formulação de filmes contendo amido de mandioca, glicerol e gelatina. Na Tabela 2 encontra-se a composição utilizada para produzir os filmes.

Tabela 2 - Composição das formulações dos filmes elaborados a partir de blendas de amido e gelatina.

Filmes	Amido (g)	Glicerol(g)	Gelatina(g)
2.5GEL	500	100	12,5
5GEL	500	100	25,0
7.5GEL	500	100	37,5
10GEL	500	100	50,0
12.5GEL	500	100	62,5
15GEL	500	100	75,0

3.3 Caracterização das nanopartículas de amido

3.3.1 Diâmetro médio, índice de polidispersão e potencial zeta das SNP

As medidas de diâmetro médio e distribuição de tamanhos foram realizadas utilizando um equipamento Zetasizer Nano-ZS (Malvern Instruments, UK) através de medidas de espalhamento dinâmico da luz. Os valores reportados de diâmetro médio são médias de 3 (três) medidas.

3.3.2 Morfologia

A morfologia das SNP foi avaliada através de análises de microscopia eletrônica de transmissão (MET), realizada em Microscópio Eletrônico de Transmissão de 120kV Tecnai G2–12 Spirit (FEI) do Centro de Pesquisas Gonçalo Muniz da FIOCRUZ – Salvador – BA. Para visualização das nanoparticulas, a técnica de contraste negativo foi utilizada. A suspensão foi depositada em grade revestidas de carbono e, após cerca de 2min, o líquido em excesso foi absorvido com papel de filtro específico de secagem Uma gota de 2% de acetato de uranila foi depositada sobre a grade e, após retirar o excesso do corante, o fino filme resultante foi exposto a secagem para posterior visualização.

3.3.3 Cristalinidade

As análises das SNP foram realizadas em um Difratômetro de raios-X Rigaku, modelo Miniflex, com passo de 4°/min (SNP) ou 2°/min (filmes) e radiação de cobre $\lambda = 1,5433 \text{ \AA}$, operando com 40 kV e corrente de 30 mA, com varredura entre 5° e 40 °.

3.3.4 Análises térmicas das SNP

A análise termogravimétrica (TGA) foi realizada em um analisador térmico da marca Perkin Elmer, modelo STA 6000, assistido pelo software Pyris Series, foram utilizadas massas de aproximadamente 8 mg em atmosfera inerte de nitrogênio de 30 mL/min, com taxa de aquecimento de 10 °C/min, no intervalo de temperatura de 25 a 600 °C.

Para a técnica de Calorimetria Exploratória Diferencial (DSC) foi utilizado um calorímetro de TA Instruments (EUA-EUA), modelo TA 2010. Cerca de 8-10 mg de amostras pré-condicionadas (60%UR, 25°C) foram hermeticamente seladas em cadiños de alumínio, para prevenir a evaporação da água durante a varredura, as amostras foram aquecidas de 20°C até 250°C, numa taxa de 10°C/min

3.4 Caracterização dos filmes poliméricos

3.4.1 Caracterização dos filmes de PBAT/AMIDO/SNP

3.4.1.1 Morfologia

As características morfológicas das superfícies e a estrutura interna dos filmes foram analisadas por meio de análise de microscopia eletrônica de varredura (MEV) em um microscópio modelo Quanta 200 (FEI, Holanda). Para investigar a estrutura interna foi realizado um corte crioscópico, utilizando nitrogênio líquido. Todas as amostras foram metalizadas por deposição de uma fina camada de ouro em um metalizador Quorum 150R. Foi utilizada uma tensão de 5kV para evitar a degradação dos filmes.

3.4.1.2 Cristalinidade

As análises os filmes foram realizadas em um Difratômetro de raios-X Rigaku, modelo Miniflex, com passo de 4º/min (SNP) ou 2º/min (filmes) e radiação de cobre $\lambda = 1,5433 \text{ \AA}$, operando com 40 kV e corrente de 30 mA, com varredura entre 5º e 40 º.

3.4.1.3 Análises térmicas

A análise termogravimétrica (TGA) foi realizada em um analisador térmico da marca Perkin Elmer, modelo STA 6000, assistido pelo software Pyris Series. Foram usadas massas de aproximadamente 8 mg em atmosfera inerte de nitrogênio de 30 mL/min, com taxa de aquecimento de 10 °C/min, no intervalo de temperatura de 25 a 600 °C.

Para a técnica de Calorimetria Exploratória Diferencial (DSC) foi utilizado um calorímetro de TA Instruments (EUA-EUA), modelo TA 2010. Cerca de 8-10 mg de amostras pré-condicionadas (60%UR, 25°C) foram hermeticamente seladas em cadinhos de alumínio, para prevenir a evaporação da água durante a varredura. As amostras dos filmes foram resfriadas até 0°C e então aquecidas até 250°C, numa taxa de 10°C/min, para apagar o histórico térmico e depois resfriadas novamente à 0°C e então reaquecidas até 250°C a mesma taxa de aquecimento.

3.4.1.4 Espessura dos filmes

A espessura dos filmes foi determinada utilizando um micrometro digital Digimess de ponta plana (de 0-25 mm, com resolução de 0,001mm) e determinada pela média de 10 medidas aleatórios em diferentes partes de uma mesma amostra. Estas medidas foram obtidas após condicionamento dos filmes por 48 h a 25°C e 50% de umidade.

3.4.1.5 Permeação (P) e taxa de permeabilidade ao vapor de água (TPVA) dos filmes

A taxa de permeabilidade ao vapor d'água e a permeabilidade dos filmes foram determinadas segundo a norma ASTM E96 – 95 - *Standard test methods for water vapor transmission of materials* e calculadas segundo as seguintes equações:

$$TPVA = G/t \cdot Ap \quad (\text{Equação 1})$$

$$P = TPVA \cdot e/S(R1 - R2) \quad (\text{Equação 2})$$

Onde TPVA é a taxa de permeação de vapor de água, e a espessura do filme, S é a pressão de saturação do vapor de água na temperatura do ensaio, R1 e R2 são as umidades relativas do ar em cada uma das faces da amostra, G é a variação da massa, t é o tempo, Ap a área de permeação de S é uma constante.

3.4.1.6 Opacidade aparente

A opacidade dos filmes foi determinada em um espectrofotômetro PerkinElmer (modelo Lambda 35), segundo Shi et al. (2013). Os filmes foram cortados em quadrados e aderidos à parede interna da cubeta de modo a permanecer posicionado perpendicular ao feixe de luz. Uma cubeta vazia foi usada como referência. Varreu-se a faixa do comprimento de onda da luz visível, a 600 nm para cada filme e a opacidade foi calculada conforme a equação: Opacidade = A_{600} / T , onde A_{600} é a absorção a 600 nm e T é a espessura do filme em mm, a análise foi realizada em triplicata.

3.4.1.7 Análise estrutural do filme através de Espectroscopia de Infravermelho por Transformada de Fourier (FTIR)

As análises de FTIR foram realizadas com objetivo de verificar a formação de novas ligações químicas ou aumento na quantidade de ligações já existentes. Para isso, utilizou-se um espectrômetro Nicolet 6700 (Thermo Fisher Scientific Inc., Massachusetts, USA), com detector MCT/B SmartOrbit, resolução 4 e 128 varreduras, comprimento de onda de 4000 cm⁻¹ a 400 cm⁻¹.

3.4.1.8 Propriedades mecânicas

Os filmes foram caracterizados através de ensaios de tração, segundo a norma ASTM D-882- *Standard Test Method for Tensile Properties of Thin Plastic Sheeting*. Foram obtidos corpos de prova retangulares (com 25 mm de largura e 190 mm de comprimento) e submetidos a uma máquina de ensaios da Emic, modelo DL 2000, com célula de carga de 500N, à temperatura ambiente, caracterizando as propriedades de ruptura e módulo elasticidade.

3.4.2 Caracterização dos filmes de amido e gelatina reciclada

3.4.2.1 Morfologia

As características morfológicas das superfícies e a estrutura interna dos filmes dos filmes foram analisadas no microscópio eletrônico de varredura modelo VEGA 3LMU (Tescan, Holland). Para investigar a estrutura interna foi realizado um corte crioscópico, utilizando nitrogênio líquido. Todas as amostras foram metalizadas por deposição de uma fina camada de ouro em um metalizador Quorum 150R. Foi utilizada uma tensão de 5kV para evitar a degradação dos filmes.

3.4.2.2 Difração de Raios-X (DRX)

As análises dos filmes foram realizadas em um Difratômetro de raios-X Shimadzu modelo XRD-6100 (Japão), com passo de 0.1°/min e radiação de cobre $\lambda = 1,5433 \text{ \AA}$, operando com 40 kV e corrente de 30 mA, com varredura entre 5° e 30 °.

3.4.2.3 Espessura

A espessura dos filmes foi determinada utilizando um micrometro Digimess (Argentina) e determinada pela média de 10 medidas aleatórios em diferentes partes de uma mesma amostra. Estas medidas foram obtidas após condicionamento dos filmes por 48 h a 25°C e 50% de umidade.

3.4.2.4 Solubilidade em água e ácido

A solubilidade dos filmes em água foi determinada de acordo com o método proposto por Gontard et al. (1994). As amostras, em triplicata, foram preparadas recortando-se discos de 2 cm de diâmetro. A massa seca inicial das amostras foi obtida após a secagem das mesmas, por um período de 24 horas à temperatura de 105°C, em estufa de circulação e renovação de ar. Após a primeira pesagem, as amostras foram imersas em um recipiente contendo 50mL de água destilada e agitadas suavemente por 24 horas. Em seguida, as amostras solubilizadas foram retiradas da água e secas a temperatura de 105°C por mais 24 horas, para obtenção da massa seca final. A solubilidade dos filmes em ácido foi determinada como descrito para a água. No entanto, após a determinação do peso seco inicial, as amostras foram imersas em um recipiente contendo ácido clorídrico (1 mol equi / L).

3.4.2.5 Análises térmicas

A análise termogravimétrica (TGA) foi realizada em um analisador térmico da marca Perkin Elmer, modelo STA 6000, assistido pelo software Pyris Series. Nos ensaios foram usadas massas de aproximadamente 8 mg em atmosfera inerte de nitrogênio de 30 mL/min, com taxa de aquecimento de 10 °C/min, no intervalo de temperatura de 25 a 800 °C.

Para a análise de Calorimetria Exploratória Diferencial (DSC) foi utilizado um calorímetro de TA Instruments (EUA-EUA), modelo TA 2010. Cerca de 8-10 mg de amostras pré-condicionadas (60%UR, 25°C) foram hermeticamente seladas em cadiños de alumínio, para prevenir a evaporação da água durante a varredura. Aproximadamente 10 mg de amostras pré-condicionadas (60% UR, 25 ° C) foram hermeticamente seladas em um cadiño de alumínio para

evitar a evaporação da água durante a varredura. As amostras de filmes foram aquecidas de 20 a 250°C a uma taxa de 10° / min.

3.4.2.6 Propriedades mecânicas

Os filmes foram caracterizados através de ensaios de tração, segundo a norma ASTM D-882. Corpos de prova retangulares (com 25 mm de largura e 190 mm de comprimento) foram obtidos com o auxílio de uma tesoura. Os testes foram realizados utilizando uma máquina de ensaios da Emic, modelo DL 2000, com célula de carga de 500N, à temperatura ambiente, caracterizando as propriedades de ruptura e o módulo elasticidade.

3.4.2.7 Teste de biodegradação

O solo simulado utilizado no ensaio de biodegradabilidade foi preparado misturando partes iguais de solo fértil, areia de praia seca e peneirada (40 mesh), e esterco de cavalo seco ao sol por dois dias, seguindo a norma ASTM G-160-03.

Os filmes foram cortados em pedaços de 2 cm X 2 cm, acondicionados em bandejas plásticas e cobertos pelo solo simulado, mantidas a 30°C ($\pm 2^{\circ}\text{C}$) em uma estufa (para cultura bacteriológica com circulação de ar e refrigeração), sendo umidificada a cada 2 dias. As amostras foram retiradas após 2, 4, 12, 15 e 17 semanas e pesadas. A porcentagem de perda de massa foi determinada segundo a Equação X.

$$\text{Weight loss (\%)} = \frac{(W_i - W_f)}{W_i} * 100$$

Onde W_i e W_f é o peso inicial e final respectivamente.

CAPÍTULO 4 – RESULTADOS

Artigo I

PBAT/TPS composite films reinforced with starch nanoparticles produced by ultrasound

Authors names:

Normane Mirele Chaves da Silva¹, Paulo Romano Cruz Correia², Janice Izabel Druzian², Farayde Matta Fakhouri³, Rosana Lopes Lima Fialho¹, Elaine Christine Magalhães Cabral de Albuquerque¹

Author affiliations:

¹Program in Industrial Engineering, Federal University of Bahia, Salvador, Bahia, Brazil.

(Silva: normanemirele@gmail.com; Fialho: rosanafialho@ufba.br; Cabral Albuquerque: elainecmca@ufba.br)

²Department of Bromatological Analysis, College of Pharmacy, Federal University of Bahia, Brazil.

(Correia: paulo.romano85@hotmail.com; Druzian: janicedruzian@hotmail.com)

³Faculty of Engineering, Federal University of Grande Dourados, Brazil.

(Fakhouri: farayde@gmail.com)

*Correspondence to: Department of Chemical Engineering, Federal University of Bahia, Aristides Novis Street, n° 2, Second floor, Federação, Salvador, Bahia, CEP: 40210-630, Brazil.

E-mail: normanemirele@gmail.com

Abstract

The objective of the present work was to study the incorporation of starch nanoparticles (SNP) produced by ultrasound in blends of poly (butylenes adipate-co-terephthalate)-PBAT and thermoplastic starch (TPS). The films were produced by extrusion using varying percentages of SNP (1, 2, 3, 4 and 5% w / w). The SNP were prepared in water without the addition of any chemical reagent. The results revealed that ultrasound treatment results in the formation of SNP less than 100 nm in size and of an amorphous character. Besides lower thermal stability and low gelatinization temperature when compared with cassava starch. Scanning Electron Microscopy (SEM) showed that films presented some starch granules. The relative crystallinity (RC) of films decreases with increasing concentration of SNP. The addition of SNP slightly affected the thermal degradation of the films. The DSC results showed that the addition did not modify the interaction between the different components of the films. Mechanical tests revealed an increase in Young's modulus (36%) and elongation at break (35%) with the incorporation of 1% SNP and this concentration reduced the water vapor permeability (53%) and significantly decreased the water absorption of the films, demonstrating that low concentrations SNP can be used as reinforcement in a polymeric matrix.

Keywords: nanocomposite; nanoparticles; biodegradability; thermoplastic extrusion.

1. Introduction

Severe environmental problems, including the increasing difficulties of waste disposal and the deepening threat of global warming (due to carbon dioxide released during incineration) caused by the non-biodegradability of a number of polymers have raised concerns all over the world [1]. To overcome some of these problems, several studies have focused on the development of biodegradable plastic for the development of sustainable packaging materials made from starches, agro-resources, and co-polyesters [2].

Among the biodegradable polymers made from renewable resources, starch is probably the most renewable naturally biodegradable polymer source because it is versatile, cheap and abundant [3]. It shows compatibility with extrusion processes used in the manufacture of conventional films and in the presence of a plasticizer it produces a material with thermoplastic characteristics, known as thermoplastic starch (TPS) [4], [5]. However, the hydrophilic nature of thermoplastic starches, its fragility and high sensitivity to moisture limit its use as a packaging material. Besides this, the retrogradation and crystallization of the mobile starch chains change its mechanical and barrier properties [6]. As a result, TPS is often blended with other polymers, such as poly(butylene adipate-co-terephthalate) (PBAT), biodegradable aliphatic-aromatic copolyester, which combines biodegradability with other desirable physical properties [7]. However, it is expensive to produce, which limits its use on a wider scale [8]. When starch and PBAT are mixed on the other hand, the cost is lower and its degradability properties are increased. Moreover, the incorporation of other additives, such as a plasticizer, compatibilisers and nanocomposites may also improve mechanical and barrier properties of the films. Nanofibers and nanocrystals (nanowhiskers) of cellulose are among additives/nanomaterials widely used as reinforcement in films of different polymeric matrices [9–11]. Starch nanoparticles can be also used as reinforcement. These may be produced by different methods (acid hydrolysis, mechanical, regeneration and others) [12–14].

Acid hydrolysis has been widely used for the preparation of starch nanoparticles (SNP). However, using this method the recovery yield is relatively low, in addition to generating waste with a negative environmental

impact, which hinders any industrial application of SNP [15]. For these reasons, many researchers have been examining other procedures with physical treatments or a combination of different methods [16]. The ultrasound technique is a new method for producing SNP involving a physical-disintegration process. There is no need to do any chemical treatment or to add any chemical reagent and it is an environmentally friendly approach which is arousing increasing interest [12]. This method has been widely used to produce SNP by many researchers [17–20]. In these SNP has been used as a reinforcing phase in a polymeric matrix to improve the mechanical and barrier properties of films [21]. [22] studied the influence of the addition of SNP produced by gamma radiation into a PBAT/TPS blend based film. These authors reported that the presence of SNP affects the rate of biodegradability and the mechanical properties of the films. It is important highlight that research into the production of biodegradable polymeric films by extrusion with nanoparticles is recent and many approaches are being used.

Thus, the aim of this study was to produce and characterize films by thermoplastic extrusion of PBAT/TPS incorporating with different concentrations (1 – 5%w/w) SNP produced with ultrasound.

2. Material and methods

2.1 Materials

The cassava starch (CS) was kindly donated by Cargil Agrícola S.A. The PBAT with the commercial name of Ecoflex-F was acquired from BASF, and commercial glycerol (Dinâmica, Brasil) was used as a plasticizer. The citric acid (VetecQuímicaFina-LTDA) and the stearic acid (Dinâmica, Brasil) were used as compatibilizer agents.

2.2 Starch Nanoparticles (SNP) production

Starch nanoparticles (SNP) were produced according to the method adapted from [17]. The starch suspension (50 mL) with a solid content of 1.5w/t% was sonicated in a QSonica ultrasound (model Q55, USA) at 50 W for 75 minutes. Then, the colloidal suspension was frozen and dried by freezing (lyophilization).

2.3 Films Production

The blends (films) were processed by the thermoplastic extrusion process using a laboratory twin-screw extruder (model AX16DR, AX Plásticos, Brazil) with a screw diameter (D) of 16mm and length to diameter ratio (L/D) of 40D. Glycerol was used as the plasticizer, and citric and stearic acids as compatibilizers.

The films were prepared according to the method adapted from [23] and following three steps. Initially the glycerol (7.0 w/w %) compatibilizers citric acid (0.6w/w %) and stearic acid (0.3w/w %) with or without SNP was mixed with starch and homogenized. The concentration of SNP used was 1, 2, 3, 4 and 5 w/w% of the matrix.

In the second stage, the PBAT/TPS blends in the ratio 70/30 were prepared. Pellets were obtained by extruding from the mixtures in a twin extruder. The screw speed was 44rpm and the barrel zone temperature profile was set at 80/120/130/130/140/140/140 and 145°C, for zones from 1 to 8, respectively.

In the last stage, the pellets were processed to obtain the final material in the form of films, the same parameters (screw speed and zone temperature) were used, with the inclusion of the former matrix of the films that was kept at 130°C.

The corresponding films were labelled XX/YY/Z, where X is the proportion of PBAT, Y is the proportion of starch in the blend, and Z is the w/w% of SNP. All of the samples were conditioned at a $53 \pm 2\%$ relative humidity and $25 \pm 2^\circ\text{C}$ before the analysis.

2.4 Starch nanoparticles (SNP) and polymeric films characterization

2.4.1 Mean diameter, polydispersity index and SNP zeta potential

The mean diameter and size distribution of colloidal suspension were determined by dynamic light scattering using a Zetasize Nano-ZS equipment (Malvern Instruments, United Kingdom). The reported values are the average of the 3 (three) measures.

2.4.2 Morphology

The morphology of the SNP was evaluated using the transmission electron microscopy (TEM) through the negative contrast technique, carried out in a 120kV Tecnai G2-12 Spirit (FEI, Holland) Transmission Electron Microscope. The suspension was deposited on a carbon coated grid and after around 2 minutes the excess liquid was absorbed with filter paper specifically designed for drying. One drop of 2% uranyl acetate was deposited over the grid and after removing the excess dye, the resultant thin film was exposed for drying for later visualization.

The morphological characteristics of the surfaces of films were analyzed with the scanning electron microscopy (SEM) in a Quanta 200 model microscope (FEI, Holland). All samples were metalized by deposition of a thin layer of gold in a Quorum 150R sputter. A 5Kv tension was used to avoid film degradation.

2.4.3 Crystallinity (XRD)

The CS, SNP and film analyses were carried out using a Rigaku, model Miniflex X-Ray Diffractometer (Japan), with a pace of 4°/min (SNP) or 2°/min (films) and copper radiation $\lambda = 1,5433 \text{ \AA}$, operating with 40 kV and a flow of 30 mA, scanning between 5°C and 40°C. The relative crystallinity (RC) of the films was quantitatively calculated following the method of Nara & Komiya (1983), according to Equation (1).

$$RC(\%) = \frac{Ac}{Aa+Ac} \quad (1)$$

Where Ac is the crystalline area, and Aa is the amorphous area on the X-ray diffractogram.

2.4.4 Thermal analysis

The Thermogravimetric Analysis (TGA) was made in a Perkin Elmer thermal analyzer, STA 6000 model (USA), assisted by Pyris Series software. In the tests for the CS, SNP and films of about 8 mg in an inert nitrogen atmosphere of 30mL/min were used, with a heat rate of 10°C/min, at a temperature interval of 25 to 600°C.

For the Differential Scanning Calorimetry (DSC) a TA Instruments (USA) calorimeter, TA 2010 model (USA), was used. Approximately 10mg of pre-conditioned samples (60%UR, 25°C) were hermetically sealed in an aluminum crucible to prevent water evaporation during the scan. The CS and SNP samples were heated from 20 to 200°C and the sample films were heated from -40 to 200°C all at a rate of 10°C/min.

2.4.5 Film Thickness

The film thickness was set using a Digimess (Brazil) flat tip digital micrometer (from 0-25mm, with 0.001mm resolution) and set by the average of 10 random measures in different parts of an equal sample.

2.4.5 Water vapor permeability (WVP)

The permeability rate of the water steam and the permeability of the films were carried out by using a modified E96-95 ASTM Standard method (ASTM, 1995). The change in the weight of the cell was plotted as a function of time and the slope of each line was calculated by linear regression. The water vapor transmission rate (WVTR, g h⁻¹ m⁻²) was calculated from the slope (g/s) and the cell area (m²). WVP (gmsPa⁻¹) was determined using Equation (2).

$$WVP = \frac{WVPT \cdot x \cdot S^{-1}}{R1 - R2} \quad (2)$$

Where WVP is permeability rate of the water steam, x is the film thickness, S is saturation pressure of water steam in work temperature, R1 and R2 are the relative humidities of the air in each of the faces of the sample, G is the mass variation, t is the time, Ap is the permeation area and S, a constant (2329.69 Pa).

2.4.6 Apparent Opacity

This test was carried out in FEMTO model 700 PLUS (Brazil) spectrophotometer according to [25]. The films were cut into squares and

adhered to the inner wall of the bucket in such a way as to be positioned perpendicular to the light beam. The visibly light band was scanned, at 600 nm for each film and the opacity was calculated according to Equation (3).

$$\text{Opacity} = \frac{A_{600}}{T} \quad (3)$$

Where A_{600} is the absorption at 600 nm and T is the thickness of the film in mm. The analyses were carried out in triplicate.

2.4.7 Water absorption measurement

The samples were cut into pieces of 2 cm × 2 cm stored at 55%RH for 7 days before testing, and then dried in the oven at 105°C for 24 h. These samples were weighed immediately after being removed from the oven. The water absorption was calculated using the following Equation (4) [26–28].

$$\text{Water absorption (\%)} = \frac{(W_1 - W_2)}{W_2} \quad (4)$$

Where W_1 is the weight of sample before drying and W_2 is the weight of sample after drying. All measurements were performed in triplicate.

2.4.8 Mechanical Properties

The films were characterized through traction tests, according to the ASTM Standard method D882-02 (ASTM, 2002). Rectangular proof bodies (with 25 mm width and 190 mm length) were acquired and put into a test machine from Emic, model DL 2000 (Brazil), with charge cell of 500N, at ambient temperature, characterizing the rupture properties and elasticity module.

2.5 Statistical analysis

The data were analyzed using ASSISTAT software, version 7.7 (Brazil), with the analysis of variance (ANOVA) and Tukey's test at a 5% significance level.

3. Results and discussions

3.1 SNP mean diameter, size distribution and zeta potential of SNP

The SNP demonstrated a bimodal distribution with mean diameter ($D_{[4,3]}$) of approximately 77.51 ± 0.77 nm (93.1% of the major population). [17] obtained starch nanoparticles produced by ultrasound (75 minutes at 136W) with size distribution ranging from 30 to 100 nm. The mean diameter of the nanoparticles plays an important role in the physical and chemical properties and therefore in their industrial application [29].

The polydispersity index (PDI) values varied between 0.2-0.5. PDI values smaller than 0.5 indicate a relative homogenous dispersion [30]. [20] produced SNP from *Araucaria angustifolia* by acid hydrolysis and by ultrasound. They obtained polydispersity index values of 0.380 for nanoparticles produced by ultrasound.

The zeta-potential of the SNP was slightly negative (-8.67mV). This result is consistent with those obtained by [31] who observed zeta-potential of -3mV for waxy maize using the same technique. The negative surface charges of the starch due to hydroxyl groups present in its structure tend to ionize in water and this may be affected by the sonication [32]. High zeta-potential value or its magnitude (negative or positive absolute value) is important as physical stability is an indicator of a colloidal dispersion because great repulsive forces tend to discourage aggregation of the nanoparticles [29]. In this work, the zeta-potential values were between -10mV and 0mV, and they are considered approximately neutral particles with a tendency for aggregation in water. However, SNP were incorporated into PBAT/Starch mixture in powder form and not in aqueous medium to be processed by extrusion. As a result, the nanoparticles instability does not affect the processing of the film.

3.2 Morphology

Figure 1 shows the photomicrography of the SNP. It can be observed that the nanoparticles have a roughly spherical morphology and diameters which are smaller than 100 nm. Figure 1 confirms the particle size distribution pattern observed by QELS analysis (major population with mean diameter of 77.51 ± 0.77 nm).

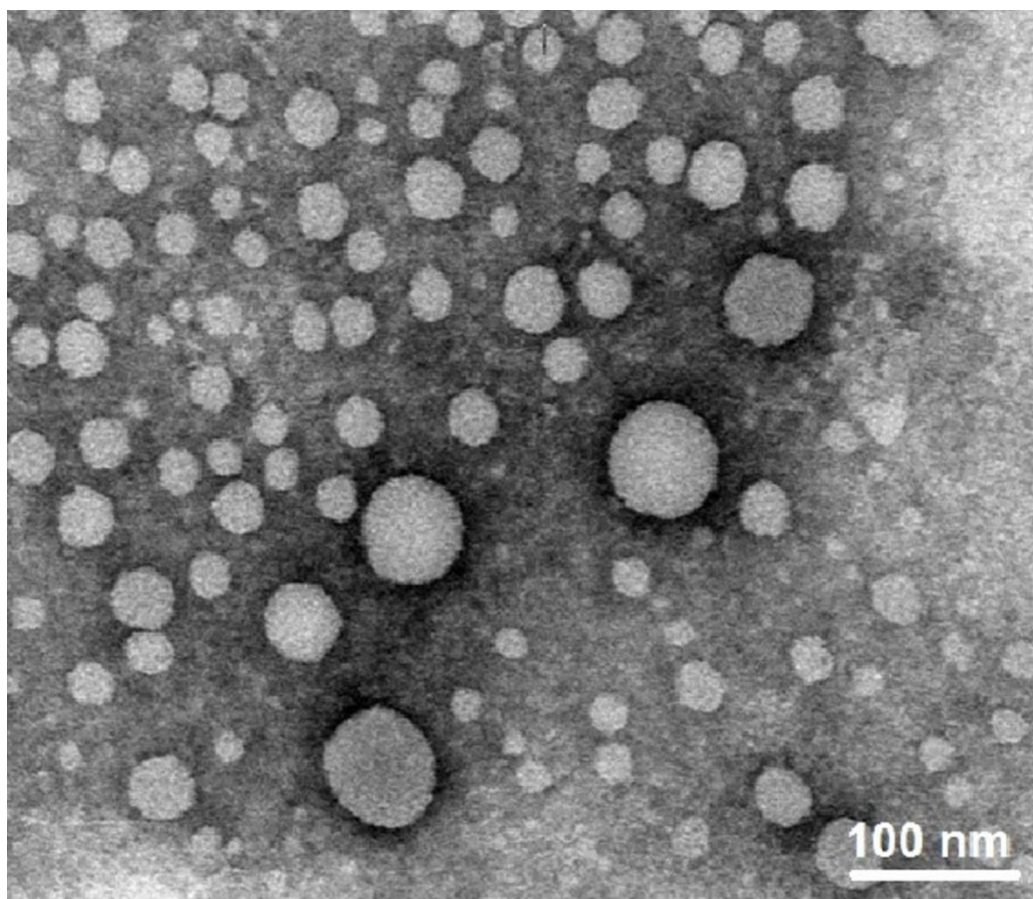


Figure 1. SNP images obtained by transmission electronic microscope (TEM). Magnification 1000x.

Figure 2 shows the scanning electronic microscopy (SEM) images of the surface of the films. The PBAT film (Figure 2a) micrograph shows a homogenously and smooth structure, with the absence of pores and without major defects. In the morphology of the surface of the PBAT/TPS film (Figure 2b), a smooth surface can also be seen. However, it is possible to see starch granules that were not completely ruptured during the extrusion process, probably the temperature and the time used were not enough for break all the

granules. Despite the starch granules, no cracks in the polymer matrix were found. The same film surface behavior has also been reported by other authors for PBAT/TPS blends for PBAT/TPS blends in a ratio of 70:30 [22], [33], [34].

The addition of SNP to PBAT/TPS blends (Figures 2c, 2d, 2e, 2f and 2g) did not affect the film surface.

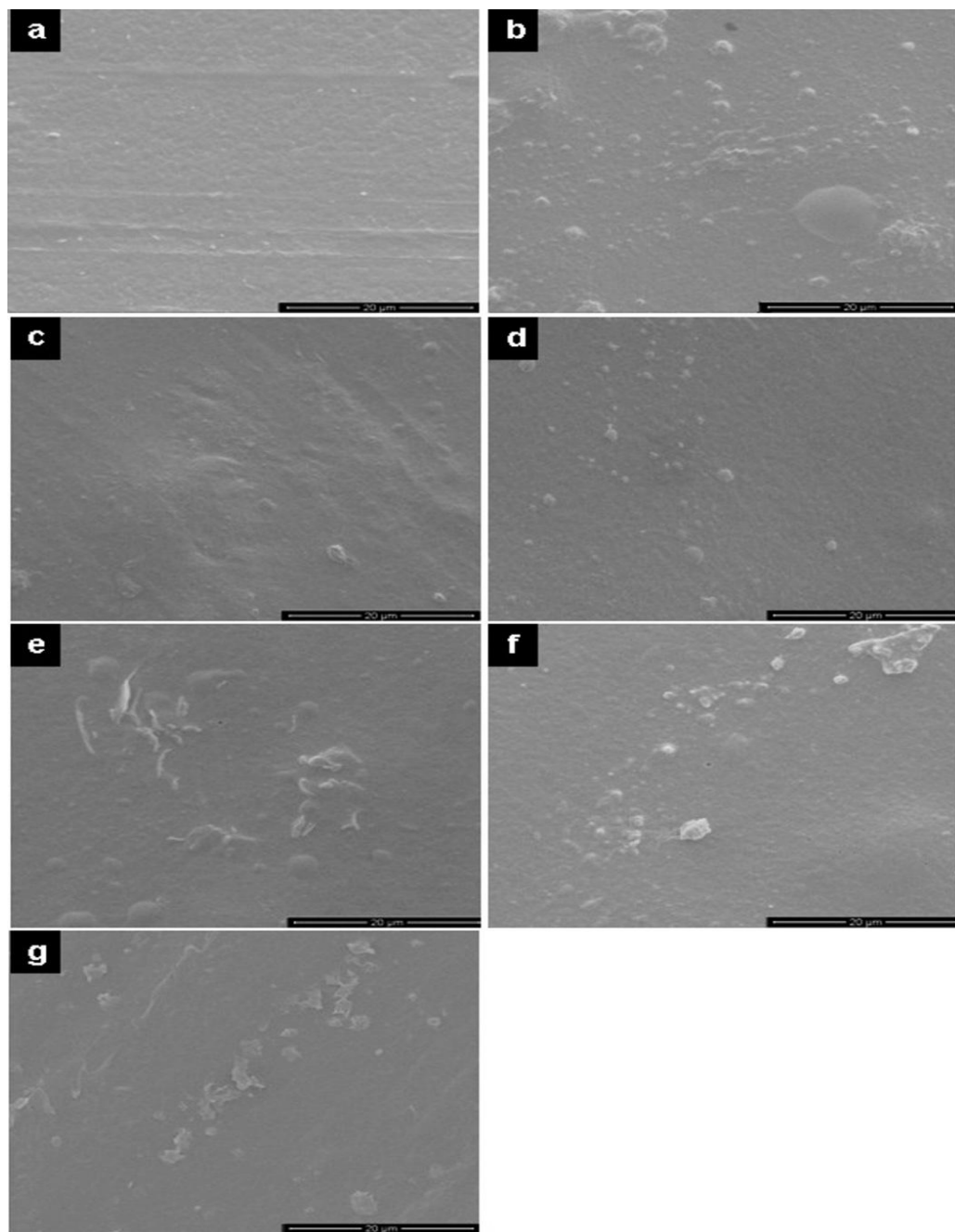


Figure 2. SEM of the surface of the films. PBAT (a), PBAT/TPS (b), 70/30/1% (c), 70/30/2% (d), 70/30/3% (e), 70/30/4% (f) and 70/30/5% (g). Magnification 5000x.

3.3 Crystallinity –XRD

The X-ray diffraction (XRD) patterns recorded for CS, SNP and films are shown in Figure 3 and Figure 4, respectively. The starch granule (that presents a certain degree of molecular organization) is partially crystalline and has a degree of crystallinity ranging from 20% to 45%. The cassava starch has C-type crystallinity (with characteristics of type A and B), and diffraction peaks in $2\theta = 15,3^\circ; 17,3^\circ; 18,3^\circ; 22,0^\circ; 23,5^\circ$ [35].

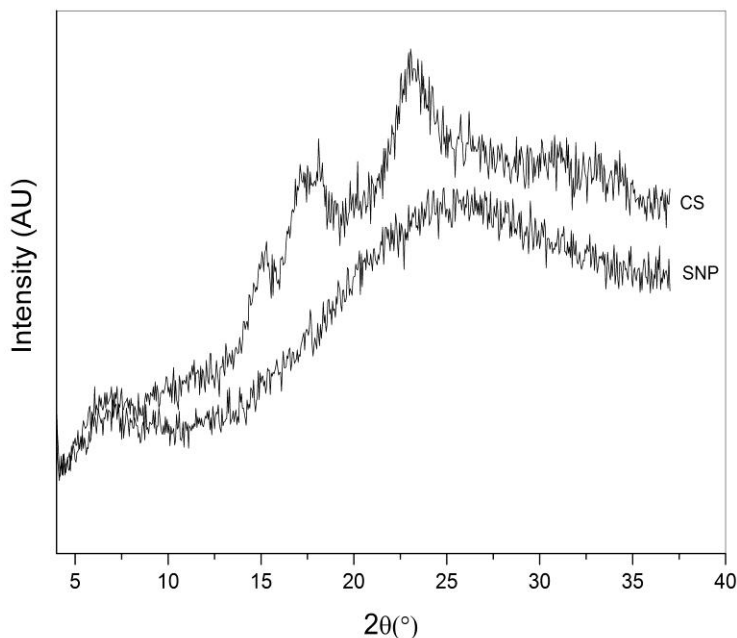


Figure 3. X-ray diffraction patterns for cassava starch (CS) and starch nanoparticles (SNP).

It was also observed that cassava starch has more intense and straight peaks corresponding both to A-type crystallinity ($2\theta \sim 15^\circ$) and B-type crystallinity ($2\theta \sim 17^\circ, 18^\circ$ and 23°), characterizing C-type crystallinity. Starches are classified A-, B-, or C-type, depending on the type of crystalline structures present in your granules. In A-type starch, double helices of chains are densely packed. The B-type crystals with a pseudo-hexagonal system are formed by rather loosely arranged double helices. The C-type is considered a mixture of A and B forms. The relative crystallinity for the C-type starch was 28%.

Analyzing the X-ray diffraction pattern of SNP (Figure 3), it can be seen that the ultrasonication process influenced the crystalline structure of the native starch. The cassava starch processing resulted in a serious disruption of the crystalline structure of clustered amylopectin, leading to nanoparticles with low crystallinity or an amorphous character. This corroborates other research results reported in the literature [17-20].

The X-ray diffraction pattern of the films with and without SNP are shown in Figure 4. All the X-ray diffraction patterns showed peaks at $2\theta = 17.5^\circ$, 20.5° and 23.2° , attributed mainly to PBAT [36], [37].

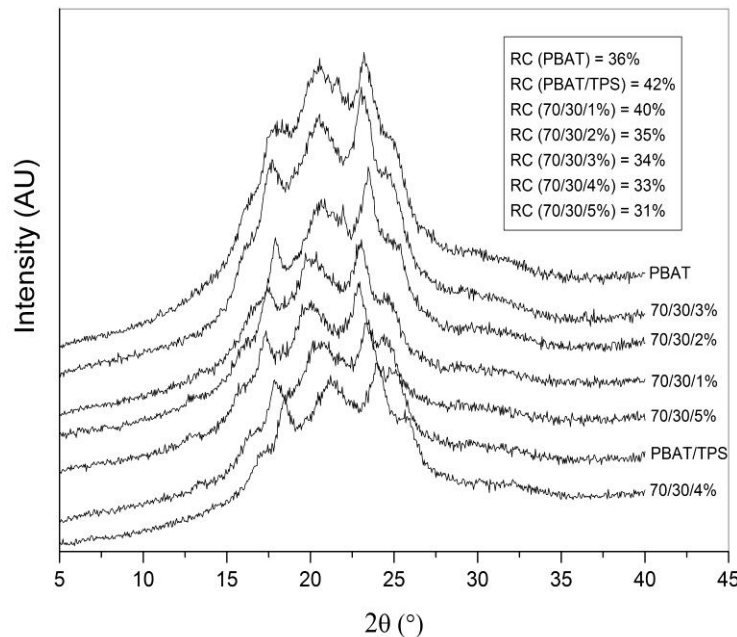


Figure 4. X-ray diffraction patterns and relative crystallinity (RC) of the films.

The level of the relative crystallinity of the films based on the peak intensity ranged from 32% (5% of SNP) to 42% (PBAT/TPS). The addition of starch to the PBAT matrix increased the crystallinity, suggesting amylose recrystallization during the extrusion process [38]. The crystallinity associated to the recrystallization of the amylose which occurs may be because during the extrusion process an amylose (amorphous portion of the native starch) can be

crystallized and this structural change can increase the degree of crystallinity [36–38].

The PBAT/TPS/SNP films showed a decrease in the degree of crystallinity when compared to PBAT/TPS films. This may be associated with the amorphous character of the nanoparticles (as shown in Figure 3).

3.4 Thermal Analysis

The thermal stability of CS and SNP are shown in Figure 5. Thermogravimetric (TG) curves show a two step degradation processes. For starch, there is a mass decrease in the initial stage (60–118°C) corresponding to water evaporation. In the second stage (280–356°C), a mass loss of 77.4% corresponding to thermal decomposition of the sample can be seen. For SNP, there is an initial mass loss of 8.97% (40–93°C) followed by second stage of mass loss (269–352°C) corresponding to 76.8%.

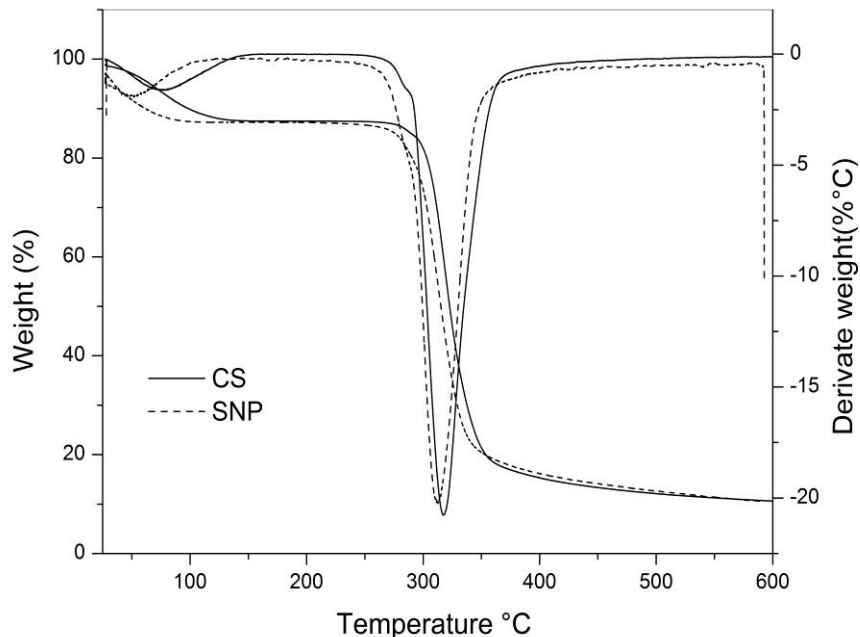


Figure 55. Thermogravimetric analysis (TG) and derivative thermogravimetric (DTG) curves cassava starch (CS) and starch nanoparticles (SNP).

It can be also observed from Figure 5 that SNP began to lose weight at a temperature lower than that of native starch. The lower thermal stability of this material is related to a high number of hydroxyl groups on their surface it is through which thermal degradation start [42], [43].

The TG curves of the films are shown in Figure 6. The PBAT film presents a single degradation process with a initial degradation temperature of 352°C and final degradation peak of 436.85°C, similar to those obtained in the literature [33], [34].

In case of PBAT/TPS films and PBAT/TPS with SNP the thermogram shows two step degradation processes. The initial step degradation at 280°C corresponds to the water loss, step at 345°C corresponds to the starch and glycerol decomposition [44]. The maximum degradation of PBAT was noticed at around 430°C, which was marginally reduced to 400°C in PBAT/TPS and PBAT/TPS/SNP biodegradable blends. This is probably due to the hydrophilic nature of TPS and lower thermal stability of the SNP, as shown in Figure 5.

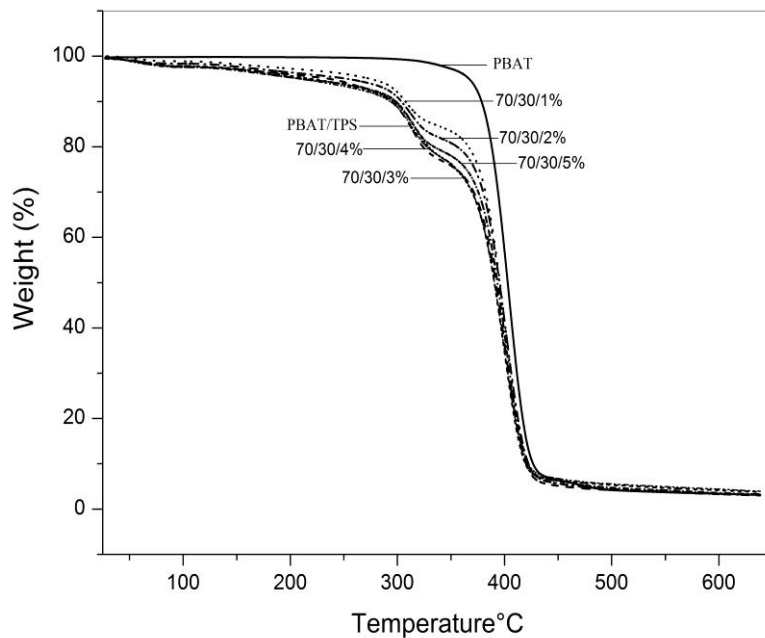


Figure 6. Thermogravimetric analysis of the films.

3.5 Differential Scanning Calorimeter-DSC

The curves obtained through the analysis by DSC of CS, SNP and the films are presented in Figures 7 and 8 respectively.

In the DSC analysis of starch and SNP, the presence of only one endothermic event in each one of the curves (0–200°C) can be seen. For SNP, the event occurred at 43.58°C and for CS it occurred at 64.50°C, probably associated to gelatinization temperature. SNP presented a lower gelatinization temperature, due to its amorphous character (Figure 3), as gelatinization tends to occur in the amorphous regions and as a result hydrogen bonding is weakened in this region.

There is no detailed description about the gelatinization temperature of starch nanoparticles produced by ultrasound in the literature. [45] claims that gelatinization related to SNP can be affected by experimental conditions of ultrasonication, starch type and composition. [46] and [47] showed that gelatinization temperature of corn starch nanoparticles, produced using the same technique, was between 66.44°C and 78.39°C.

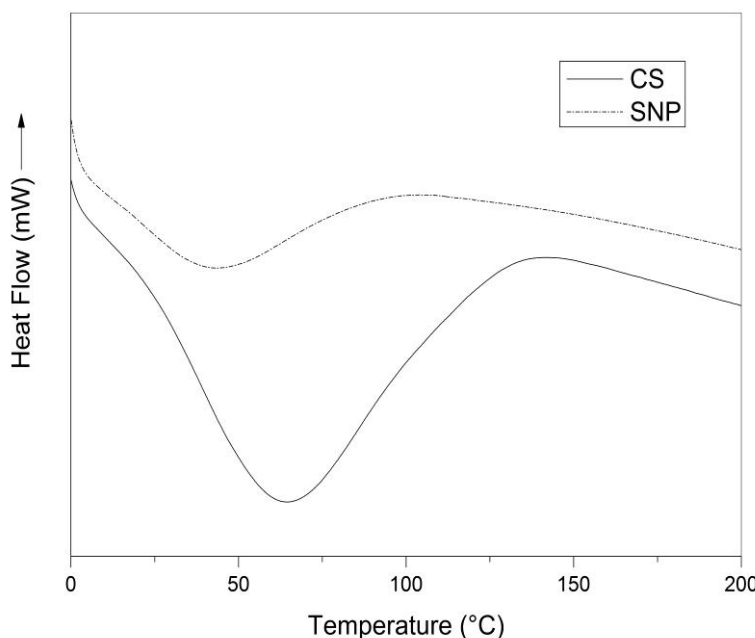


Figure 7. Differential thermal analysis of cassava starch (CS) and starch nanoparticles (SNP).

DSC curves of films are shown in Figure 8. The PBAT film presents a glass transition temperature (T_g) of around -33.31°C . Similar results were obtained by other authors [34], [48], [49]. The DSC curves had two additional peaks related to melting temperatures, T_{m1} and T_{m2} , 53°C and 130°C , respectively [50]. These two endothermic events are related to the two segments that make up the chemical structure of PBAT, which are butylene terephthalate (BT) and butylene adipate (BA) segment. The first (T_{m1}) refers to the presence of a soft crystal lattice containing mainly butylene adipate segment and the second (T_{m2}) to the fusion of butylene terephthalate crystals [22].

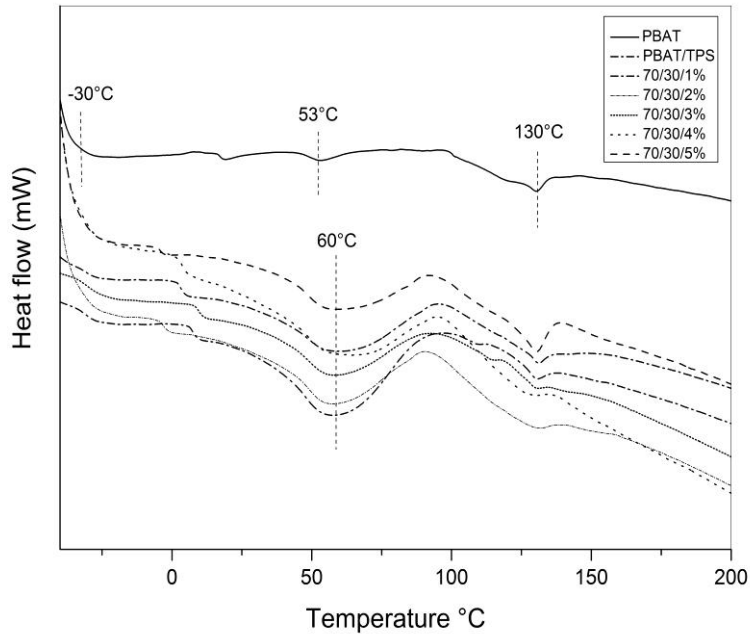


Figure 8. Differential thermal analysis for films.

All the films, PBAT/TPS and PBAT/TPS/SNP, had similar profiles (T_g and T_{m2}) to PBAT film. However, a displacement peak in T_{m1} towards higher temperatures (around 60°C) was observed when compared to the PBAT film. This indicates moderate interaction between the PBAT matrix and TPS [34].

3.6 Thickness, Water vapor permeability (WVP) and opacity

In Table 1 the results of the thickness, WVP and opacity of the films are presented. It can be observed that the films were not significantly thickness ($p>0.05$).

Table 1 - Values of thickness, water vapor permeability (WVP) and opacity of the films.

Sample	Thickness (mm)	WVP (10^{-8} ($\text{g}^{-1} \text{Pa s m}$)	Opacity (%)
PBAT	$0.0913 \pm 0.0011^{\text{a}}$	$7.55 \pm 9.87 \times 10^{-10\text{b}}$	$0.59 \pm 0.0001^{\text{g}}$
PBAT/TPS	$0.1085 \pm 0.0041^{\text{a}}$	$9.89 \pm 5.52 \times 10^{-11\text{a}}$	$0.74 \pm 0.0013^{\text{d}}$
70/30/ 1%	$0.0769 \pm 0.0057^{\text{a}}$	$3.50 \pm 5.83 \times 10^{-10\text{c}}$	$1.09 \pm 0.0032^{\text{b}}$
70/30/ 2%	$0.1094 \pm 0.0044^{\text{a}}$	$4.09 \pm 2.17 \times 10^{-10\text{c}}$	$0.82 \pm 0.0056^{\text{e}}$
70/30/ 3%	$0.0737 \pm 0.0005^{\text{a}}$	$3.32 \pm 7.64 \times 10^{-10\text{c}}$	$0.78 \pm 0.0007^{\text{c}}$
70/30/ /4%	$0.0740 \pm 0.0005^{\text{a}}$	$3.66 \pm 1.17 \times 10^{-9\text{c}}$	$1.19 \pm 0.0023^{\text{a}}$
70/30/ 5%	$0.0833 \pm 0.0131^{\text{a}}$	$4.02 \pm 2.76 \times 10^{-10\text{c}}$	$0.75 \pm 0.0011^{\text{f}}$

Values with different letters in the same column are significantly different ($p<0.05$).

The water vapor barrier properties of a polymer are very important for estimating and predicting the shelf-life of a product-package. Food packaging barrier requirements are related to the product characteristics and the intended end-use application. Water vapor is crucial as it alters the sensory, physico-chemical and microbiological characteristics of food products. Depending on its end-use application, food packaging film must have the lowest WVP possible [51]

The incorporation of TPS into the PBAT matrix increased the WVP of the films ($p<0.05$) significantly. This probably occurred due to the hydrophilic nature of the starch, favoring the intermolecular hydrogen bonding which can increase the water vapor diffusion through the film.

The WVP of all the films with SNP decreased significantly ($p<0.05$) when compared to those of the PBAT films and PBAT/TPS. It was observed that films with SNP (1 w/w %) showed an approximate 53% WVP reduction because the starch nanoparticles tend to increase the compactness of the films. The presence of SNP probably made the path for water molecules to pass through more tortuous [25] .

As regards the opacity results, all the films presented significant differences between them ($p<0.05$), the PBAT film showed the lowest value (0.59) and the film with SNP (4w/w %) the highest value (1.19). The opacity of a film indicates the amount of light that gets through it. Photo sensitive food needs to be protected with high-opacity packaging [54].

3.7 Water absorption measurement

The water absorption of the films after storage at 55%RH for 7 days is shown in Figure 9. The water absorption of PBAT film was 3.29%, the PBAT is a hydrophobic polymer, therefore presents low water absorption [53]. The PBAT/TPS films presented larger water absorption capacity (4.61%) when compared to PBAT films, with a significant difference between them ($p<0.05$). This increase can be attributed to the hydrophilic character of starch [54].

For the films with SNP the water absorption decreased when compared to PBAT and PBAT/TPS films with a significant difference ($p<0.05$), the values obtained were 2.55%, 2.58%, 2.99%, 2.79% and 2.78% for samples with 1-5 w/w% of the SNP respectively. These results could be explained by the fact that the nanoparticles improve the homogeneity and compactness of the polymeric structure reducing the penetration of water and consequently your absorption.

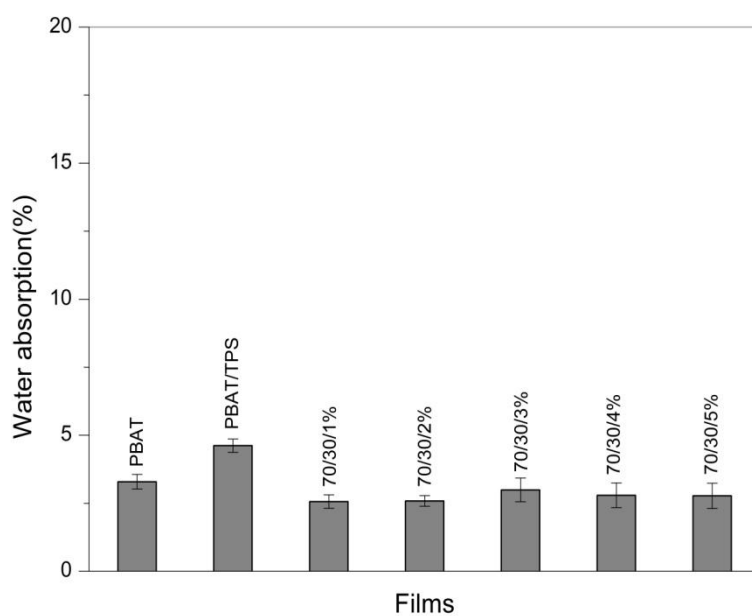


Figure 9. Water absorption of the films.

3.8 Mechanical Properties

In Table 2 the results to Young's modulus (E), tensile strength (TS) and elongation-at-break (Eb) of the films are presented. As can be seen the Young's modulus of the PBAT films was 67MPa, elongation-at-break 214% and tensile strength (TS) of 9.33MPa. The incorporation of starch in the films (70/30 film) resulted in decreasing values of E (~ 17%), TS (~21%) and Eb (22%). The presence of some starch grains that were not completely ruptured during the extrusion process of the films (Figure 2b) explains such behavior. Starch granules can tease fissures that do not favor the interaction between the carbonyl group of the PBAT matrix and the starch [48].

Table 1 - Mechanical properties of PBAT, PBAT/TPS and PBAT/TPS/SNP films.

Sample	E(MPa)	TS (MPa)	Eb (%)
PBAT	67.00 \pm 1.63 ^{cd}	9.33 \pm 0.47 ^{bc}	214.00 \pm 2.94 ^{bcd}
PBAT/TPS	56.00 \pm 0.81 ^d	7.33 \pm 0.47 ^c	168.33 \pm 4.64 ^d
70/30/ 1%	76.66 \pm 2.05 ^{bc}	9.33 \pm 0.47 ^{bc}	227.33 \pm 1.24 ^a
70/30/ 2%	80.00 \pm 1.63 ^{ab}	11.24 \pm 0.47 ^{ab}	221.66 \pm 4.92 ^{ab}
70/30/ 3%	81.33 \pm 4.02 ^{ab}	11.33 \pm 0.81 ^{ab}	217.00 \pm 0.94 ^{ab}
70/30/ 4%	86.66 \pm 1.24 ^{ab}	11.00 \pm 0.85 ^{ab}	210.00 \pm 1.24 ^{bc}
70/30/ 5%	87.66 \pm 7.31 ^{ab}	11.33 \pm 0.94 ^{ab}	202.33 \pm 4.92 ^c

*Values with different letters in the same column are significantly different ($p<0.05$).

The addition of 1% of SNP leads to a significant increase ($p<0.05$) of the E (36%) and Eb (35%) of the films, when compared to the PBAT/TPS film. The addition of 2-5 w/w% SNP did not improve the Young's modulus parameter significantly ($p>0.05$). The Eb behavior for PBAT/TPS/ (1-3 w/w %) SNP films are similar with a better elongation effect when compared to the PBAT/TPS films. Such behavior can be attributed to interactions among the carbonyl groups of PBAT and the hydroxyl groups of the SNP and starch grains contributing to obtain a more homogeneous film. The nanoparticles can fill the voids improving the plasticization of the film. [22] investigated the effect of 0.6% of SNP produced by Gamma radiation on a PBAT/TPS blend. The authors concluded that the incorporation of SNP in the polymer matrix improves the E and Eb of the composite.

However, it was observed that films with SNP ($\geq 4\text{w/w \%}$) resulted in reduced values ($p<0.05$) of E_b . In this work, we found that a high concentration of SNP can produce a rigid hydrogen bond network between SNP and starch, and this weakens the stress distribution, which hinders the elongation of the films [55].

Analyzing the behavior of the tensile strength for the PBAT/TPS films, it can be seen that the incorporation of 1% of SNP led to a slight increase in the TS, but this was not significant ($p>0.05$). However, the incorporation of 2-5 wt% SNP in the films resulted in significantly ($p<0.05$) improved values. [25] claim that the interaction between TPS and SNP is favored due to their molecular structure and chemical nature, which facilitates the production of homogeneous films with good mechanical properties.

4. Conclusions

Starch nanoparticles were successfully prepared using the physical method of high-intensity ultrasonication without any chemical additives. XRD analysis showed the amorphous character nanoparticles. The thermal analysis showed that the SNP are more thermally unstable and have a lower gelatinization temperature when compared to starch.

The incorporation of SNP did not modify the morphology of the PBAT/TPS films. However, decreased relative crystallinity occurred with the increase in the SNP concentration in the films.

The TGA showed that the SNP induced a displacement of the degradation temperature of the first event. DSC analysis revealed that the SNP did not cause any change in the T_g and T_m films. The opacity values differed in all films.

With the addition of starch to PBAT matrix, all the tensile parameters exhibit slight decreases and an increase in the WVP of the films. Incorporation of only 1% SNP in a PBAT/TPS matrix produced films with better properties (E , E_b , WVP and Water absorption) than PBAT films. As a result, blends of PBAT/TPS/SNP are an interesting option for developing environmentally friendly and energy saving packaging materials at a low cost.

Acknowledgements

The authors thank to the Engineering and Polymerization Laboratory (Engepol) at the Rio de Janeiro Federal University-UFRJ and Gonçalo Muniz Research Center FIOCRUZ – Salvador - BA for their assistance in the analysis.

Conflicts of Interest: The author(s) declare(s) that there is no conflict of interest regarding the publication of this paper.

References

- [1] G. E. Luckachan and C. K. S. Pillai, "Biodegradable Polymers- A Review on Recent Trends and Emerging Perspectives," *Journal of Polymers and the Environment*, vol. 19, no. 3, pp. 637–676, 2011.
- [2] C. M. O. Müller, J. B. Laurindo, and F. Yamashita, "Composites of thermoplastic starch and nanoclays produced by extrusion and thermopressing," *Carbohydrate Polymers*, vol. 89, no. 2, pp. 504–510, 2012.
- [3] N. R. Savadekar and S. T. Mhaske, "Synthesis of nano cellulose fibers and effect on thermoplastics starch based films," *Carbohydrate Polymers*, vol. 89, no. 1, pp. 146–151, 2012.
- [4] P. Sarazin, G. Li, W. J. Orts, and B. D. Favis, "Binary and ternary blends of polylactide, polycaprolactone and thermoplastic starch," *Polymer*, vol. 49, no. 2, pp. 599–609, 2008.
- [5] M. Thunwall, V. Kuthanová, A. Boldizar, and M. Rigdahl, "Film blowing of thermoplastic starch," *Carbohydrate Polymers*, vol. 71, no. 4, pp. 583–590, 2008.
- [6] H. Angellier, S. Molina-Boisseau, P. Dole, and A. Dufresne, "Thermoplastic starch-waxy maize starch nanocrystals nanocomposites.," *Biomacromolecules*, vol. 7, pp. 531–539, 2006.
- [7] J. B. Olivato, C. M. Oliveira Mueller, F. Yamashita, M. V. Eiras Grossmann, and M. M. Nobrega, "Study of the Compatibilizer Effect in the Properties of Starch/Polyester Blends," *Polimeros-Ciencia E Tecnologia*, vol. 23, no. 3, pp. 346–351, 2013.
- [8] A. D. Marinho, C. A. B. Pereira, M. B. C. Vitorino, A. S. Silva, L. H.

- Carvalho, and E. L. Canedo, "Degradation and recovery in poly (butylene adipate- co -terephthalate)/ thermoplastic starch blends," vol. 58, pp. 166–172, 2017.
- [9] D. Chen, D. Lawton, M. R. Thompson, and Q. Liu, "Biocomposites reinforced with cellulose nanocrystals derived from potato peel waste," *Carbohydrate Polymers*, vol. 90, no. 1, pp. 709–716, 2012.
- [10] A.-L. Goffin, J.-M. Raquez, E. Duquesne, G. Siqueira, Y. Habibi, A. Dufresne, and P. Dubois, "From Interfacial Ring-Opening Polymerization to Melt Processing of Cellulose Nanowhisker-Filled Polylactide-Based Nanocomposites," *Biomacromolecules*, vol. 12, no. 7, pp. 2456–2465, 2011.
- [11] H.-Y. Yu, Z.-Y. Qin, Y.-N. Liu, L. Chen, N. Liu, and Z. Zhou, "Simultaneous improvement of mechanical properties and thermal stability of bacterial polyester by cellulose nanocrystals," *Carbohydrate Polymers*, vol. 89, no. 3, pp. 971–978, 2012.
- [12] S. Bel Haaj, W. Thielemans, A. Magnin, and S. Boufi, "Starch nanocrystals and starch nanoparticles from waxy maize as nanoreinforcement: A comparative study," *Carbohydrate Polymers*, vol. 143, pp. 310–317, 2016.
- [13] Y. Chang, X. Yan, Q. Wang, L. Ren, J. Tong, and J. Zhou, "High efficiency and low cost preparation of size controlled starch nanoparticles through ultrasonic treatment and precipitation," *Food Chemistry*, vol. 227, pp. 369–375, 2017.
- [14] Y. Qin, C. Liu, S. Jiang, L. Xiong, and Q. Sun, "Characterization of starch nanoparticles prepared by nanoprecipitation: Influence of amylose content and starch type," *Industrial Crops & Products*, vol. 87, pp. 182–190, 2016.
- [15] X. Ma, R. Jian, P. R. Chang, and J. Yu, "Fabrication and Characterization of Citric Acid-Modified Starch Nanoparticles/Plasticized-Starch Composites," *Biomacromolecules*, vol. 9, no. 11, pp. 3314–3320, Nov. 2008.
- [16] H. Y. Kim, S. S. Park, and S. T. Lim, "Preparation, characterization and utilization of starch nanoparticles," *Colloids and Surfaces B: Biointerfaces*,

- vol. 126, pp. 607–620, 2015.
- [17] S. Bel Haaj, A. Magnin, C. Pétrier, and S. Boufi, “Starch nanoparticles formation via high power ultrasonication,” *Carbohydrate Polymers*, vol. 92, no. 2, pp. 1625–1632, 2013.
 - [18] H. Y. Kim, D. J. Park, J. Y. Kim, and S. T. Lim, “Preparation of crystalline starch nanoparticles using cold acid hydrolysis and ultrasonication,” *Carbohydrate Polymers*, vol. 98, no. 1, pp. 295–301, 2013.
 - [19] Q. Sun, H. Fan, and L. Xiong, “Preparation and characterization of starch nanoparticles through ultrasonic-assisted oxidation methods,” *Carbohydrate Polymers*, vol. 106, no. 1, pp. 359–364, 2014.
 - [20] P. M. Gonçalves, C. P. Z. Noreña, N. P. da Silveira, and A. Brandelli, “Characterization of starch nanoparticles obtained from Araucaria angustifolia seeds by acid hydrolysis and ultrasound,” *LWT - Food Science and Technology*, vol. 58, no. 1, pp. 21–27, 2014.
 - [21] D. Le Corre and H. Angellier-Coussy, “Preparation and application of starch nanoparticles for nanocomposites: A review,” *Reactive and Functional Polymers*, vol. 85, pp. 97–120, 2014.
 - [22] P. G. Seligra, L. E. Moura, L. Famá, J. I. Druzian, and S. Goyanes, “Influence of Incorporation of Starch Nanoparticles in PBAT/TPS Composites Films,” *Polymer International*, no. April, 2016.
 - [23] J. B. Silva, J. I. Druzian, F. V. Pereira, C. S. Miranda, N. M. José, R. E. S. Bretas, D. C. Horácio, “Processo de preparação de blendas poliméricas ambientalmente degradáveis reforçadas com nanocristais de celulose (nanocelulose) para produção de filmes flexíveis por extrusão,” BR Patent INPI 011120000389, BR102012014512-0. 2012.
 - [24] S. Nara and T. Komiya, “Studies on the Relationship Between Water-saturated State and Crystallinity by the Diffraction Method for Moistened Potato Starch,” *Starch - Stärke*, vol. 35, no. 12, pp. 407–410, 1983.
 - [25] A. M. Shi, L. J. Wang, D. Li, and B. Adhikari, “Characterization of starch films containing starch nanoparticles Part 1: Physical and mechanical properties,” *Carbohydrate Polymers*, vol. 96, no. 2, pp. 593–601, 2013.
 - [26] M. F. Huang, J. G. Yu, and X. F. Ma, “Studies on the properties of Montmorillonite-reinforced thermoplastic starch composites,” *Polymer*,

- vol. 45, no. 20, pp. 7017–7023, 2004.
- [27] X. F. Ma, J. G. Yu, and N. Wang, “Fly ash-reinforced thermoplastic starch composites,” *Carbohydrate Polymers*, vol. 67, no. 1, pp. 32–39, 2007.
 - [28] K. Kaewtatip and J. Thongmee, “Effect of kraft lignin and esterified lignin on the properties of thermoplastic starch,” *Materials and Design*, vol. 49, pp. 701–704, 2013.
 - [29] S. Rezende, S. Stanis̄uaski, L. De Lucca, and A. Raffin, “Revisão,” vol. 26, no. 5, pp. 726–737, 2003.
 - [30] M. R. Avadi, A. M. M. Sadeghi, N. Mohammadpour, S. Abedin, F. Atyabi, R. Dinarvand, and M. Rafiee-Tehrani, “Preparation and characterization of insulin nanoparticles using chitosan and Arabic gum with ionic gelation method,” *Nanomedicine: Nanotechnology, Biology, and Medicine*, vol. 6, no. 1, pp. 58–63, 2010.
 - [31] S. B. Haaj, A. Magnin, and S. Boufi, “Starch nanoparticles produced via ultrasonication as a sustainable stabilizer in Pickering emulsion polymerization,” *RSC Adv*, vol. 4, no. 80, pp. 42638–42646, Sep. 2014.
 - [32] D. Liu, Q. Wu, H. Chen, and P. R. Chang, “Transitional properties of starch colloid with particle size reduction from micro- to nanometer,” *Journal of Colloid and Interface Science*, vol. 339, no. 1, pp. 117–124, 2009.
 - [33] J. B. Olivato, J. Marini, E. Pollet, F. Yamashita, M. V. E. Grossmann, and L. Avérous, “Elaboration, morphology and properties of starch/polyester nano-biocomposites based on sepiolite clay,” *Carbohydrate Polymers*, vol. 118, pp. 250–256, 2015.
 - [34] S. K. Nayak, “Biodegradable PBAT/Starch Nanocomposites,” *Polymer-Plastics Technology and Engineering*, vol. 49, no. 14, pp. 1406–1418, 2010.
 - [35] J. J. G. Van Soest and J. F. G. Vliegenthart, “Crystallinity in starch plastics: Consequences for material properties,” *Trends in Biotechnology*, vol. 15, no. 6, pp. 208–213, 1997.
 - [36] E. Cranston, J. Kawada, S. Raymond, F. G. Morin, and R. H. Marchessault, “Cocrystallization model for synthetic biodegradable poly(butylene adipate-co-butylene terephthalate),” *Biomacromolecules*,

- vol. 4, no. 4, pp. 995–999, 2003.
- [37] J.-M. Raquez, Y. Nabar, R. Narayan, and P. Dubois, “In situ compatibilization of maleated thermoplastic starch/polyester melt-blends by reactive extrusion,” *Polymer Engineering & Science*, vol. 48, no. 9, pp. 1747–1754, Sep. 2008.
- [38] R. A. L. Santos, C. M. O. Muller, M. V. E. Grossmann, S. Mali, and F. Yamashita, “Starch/Poly(Butylene Adipate–Co-Terephthalate)/Montmorillonite Films Produced By Blow Extrusion,” *Química Nova*, vol. 37, no. 6, pp. 937–942, 2014.
- [39] A. Buléon, P. Colonna, V. Planchot, and S. Ball, “Starch granules: Structure and biosynthesis,” *International Journal of Biological Macromolecules*, vol. 23, no. 2, pp. 85–112, 1998.
- [40] R. Parker and S. G. Ring, “Aspects of the Physical Chemistry of Starch,” *Journal of Cereal Science*, vol. 34, no. 1, pp. 1–17, Jul. 2001.
- [41] E. Corradini, C. Lotti, E. S. De Medeiros, A. J. F. Carvalho, A. a. S. Curvelo, and L. H. C. Mattoso, “Estudo comparativo de amidos termoplásticos derivados do milho com diferentes teores de amilose,” *Polímeros*, vol. 15, pp. 268–273, 2005.
- [42] N. L. García, M. Lamanna, N. D’Accorso, A. Dufresne, M. Aranguren, and S. Goyanes, “Biodegradable materials from grafting of modified PLA onto starch nanocrystals,” *Polymer Degradation and Stability*, vol. 97, no. 10, pp. 2021–2026, 2012.
- [43] M. Lamanna, N. J. Morales, N. L. Garcia, and S. Goyanes, “Development and characterization of starch nanoparticles by gamma radiation: Potential application as starch matrix filler,” *Carbohydrate Polymers*, vol. 97, no. 1, pp. 90–97, 2013.
- [44] N. L. García, L. Famá, A. Dufresne, M. Aranguren, and S. Goyanes, “A comparison between the physico-chemical properties of tuber and cereal starches,” *Food Research International*, vol. 42, no. 8, pp. 976–982, 2009.
- [45] F. Zhu, “Impact of ultrasound on structure, physicochemical properties, modifications, and applications of starch,” *Trends in Food Science and Technology*, vol. 43, no. 1, pp. 1–17, 2015.
- [46] A. R. Jambrak, Z. Herceg, D. Subaric, J. Babic, M. Brncic, S. R. Brncic, T.

- Bosiljkov, D. Cvek, B. Tripalo, and J. Gelo, "Ultrasound effect on physical properties of corn starch," *Carbohydrate Polymers*, vol. 79, no. 1, pp. 91–100, 2010.
- [47] J. Huang, H. A. Schols, J. J. G. van Soest, Z. Jin, E. Sulmann, and A. G. J. Voragen, "Physicochemical properties and amylopectin chain profiles of cowpea, chickpea and yellow pea starches," *Food Chemistry*, vol. 101, no. 4, pp. 1338–1345, 2007.
- [48] S. Mohanty and S. K. Nayak, "Starch based biodegradable PBAT nanocomposites: Effect of starch modification on mechanical, thermal, morphological and biodegradability behavior," *International Journal of Plastics Technology*, vol. 13, no. 2, pp. 163–185, 2010.
- [49] M. Kumar, S. Mohanty, S. K. Nayak, and M. Rahail Parvaiz, "Effect of glycidyl methacrylate (GMA) on the thermal, mechanical and morphological property of biodegradable PLA/PBAT blend and its nanocomposites," *Bioresource Technology*, vol. 101, no. 21, pp. 8406–8415, 2010.
- [50] R. Al-Ittry, K. Lamnawar, A. Maazouz, N. Billon, and C. Combeaud, "Effect of the simultaneous biaxial stretching on the structural and mechanical properties of PLA, PBAT and their blends at rubbery state," *European Polymer Journal*, vol. 68, pp. 288–301, 2015.
- [51] I. F. E. Silva, F. Yamashita, C. M. O. Müller, S. Mali, J. B. Olivato, A. P. Bilck, and M. V. E. Grossmann, "How reactive extrusion with adipic acid improves the mechanical and barrier properties of starch/poly (butylene adipate-co-terephthalate) films," *International Journal of Food Science & Technology*, vol. 48, no. 8, pp. 1762–1769, Aug. 2013.
- [52] X. Li, C. Qiu, N. Ji, C. Sun, L. Xiong, and Q. Sun, "Mechanical, barrier and morphological properties of starch nanocrystals-reinforced pea starch films," *Carbohydrate Polymers*, vol. 121, pp. 155–162, 2015.
- [53] R. P. H. Blandelero, M. V. Grossmann, and F. Yamashita, "Films of starch and poly(butylene adipate co-terephthalate) added of soybean oil (SO) and Tween 80," *Carbohydrate Polymers*, vol. 90, no. 4, pp. 1452–1460, 2012.
- [54] H. ming Chen, Q. Huang, X. Fu, and F. xing Luo, "Ultrasonic effect on the

- octenyl succinate starch synthesis and substitution patterns in starch granules," *Food Hydrocolloids*, vol. 35, pp. 636–643, 2014.
- [55] S. Jiang, C. Liu, X. Wang, L. Xiong, and Q. Sun, "LWT - Food Science and Technology Physicochemical properties of starch nanocomposite films enhanced by self-assembled potato starch nanoparticles," *LWT - Food Science and Technology*, vol. 69, pp. 251–257, 2016.

Artigo II

Starch/recycled gelatin composite films produced by extrusion: physical and mechanical properties

Normane Mirele Chaves da Silva^{a*}, Farayde Matta Fakhouri^b, Rosana Lopes Lima Fialho ^a, Elaine Christine de Magalhães Cabral Albuquerque ^a

^aProgram in Industrial Engineering, Federal University of Bahia, Salvador, Bahia, Brazil.

(Silva: normanechaves@yahoo.com; Fialho: rosanafialho@ufba.br; Cabral Albuquerque: elainecmca@ufba.br)

^bFaculty of Engineering, Federal University of Grande Dourados, Brazil.
(Fakhouri: farayde@gmail.com)

* Corresponding author at: Program in Industrial Engineering, Federal University of Bahia, Salvador, Bahia, Brazil. Tel. +55 77 99115 4916. E-mail address: normanemirele@gmail.com

Abstract

The objective of this work was to study physical and mechanical properties of composite films based on blends of starch and recycled gelatin plasticized with glycerol (20% wt). The films were produced by extrusion using varying percentages of recycled gelatin (2.5%, 5%, 7.5%, 10%, 12.5% and 15%). The morphology results revealed the good compatibility between both polymers (starch and recycled gelatin) to form the film matrix. The crystallinity analysis showed that the extrusion process eliminated crystalline zones of the granules and produced semi-crystalline profile films. The thermal analysis showed increased thermal and glass temperature (T_g) stability with increasing recycled gelatin concentration. The incorporation of recycled gelatin significantly increased the mechanical strength and solubility in water of the films. Besides this, it accelerated the biodegradation process.

Keywords: gelatin; extrusion; biodegradability; mechanical properties.

Chemical compounds studied in this article

Glycerol (PubChem CID: 753)

Abbreviations used

ANOVA, analysis of variance; DSC, differential scanning calorimetry; TG, thermogravimetry; DTG, derivative thermogravimetry; SEM, scanning electron microscopy; DRX, x-ray diffraction.

1. Introduction

Petroleum-derived plastics have been traditionally used as packaging materials due to their low cost, good mechanical and barrier properties and their thermo-processing ability. However, issues related to sustainability, dwindling energy reserves and variations in oil prices are challenges to conventionally plastic packaging. An interesting alternative to replace conventional plastics are natural biopolymers which have the advantages of being renewable in many cases as they are biodegradable or compostable in nature.^{1,2}

Biodegradable films can be produced from protein, polysaccharides, lipids or a combination of these components.^{3,4} Starch it is one of the biopolymers with the greatest potential to produce biodegradable materials due to its versatility, cheap price and abundance.^{5,6} However, starch films present some drawbacks due to their great sensitivity to water which can affect the mechanical properties and barrier capacity of such films.⁷ However, there are various ways that these problems can be overcome. Among them, the formation of blends with other natural polymers, such as proteins (gelatin), has been shown to enhance their mechanical behavior.⁸

Gelatin is a protein of animal origin, obtained by the thermal desnaturation or physicochemical degradation of collagen. It is well-known for its good film forming properties with good mechanical properties.^{9,10} Brazil is a great producer and exporter of gelatin and collagen with a production of almost 20 thousand tons per year.¹¹ However, due to the production process, the desired characteristics (bloom and viscosity) required by industry, that material present high cost when compared to others hydrocolloids, for example, cassava starch. One way of reducing the cost of gelatin-based films as well as contributing to the elimination of waste would be the use of recycled gelatin, which is food industry waste, a gelatin which has already been processed. Gelatin-based films have good mechanical resistance and high elasticity. However, they are also sensitive to environmental conditions, such as relative humidity.¹²

Blends of gelatin with starch have attracted much attention and many studies have recently been published.^{3,5,8,13-15} However, in these works a casting method is used to produce films and this method generally presents a

low production scale which hinders industrial application. Extrusion is a more viable alternative for the production of biodegradable blends as it is a continuous process that combines shear forces, high pressure and high temperature in a short time.¹⁶ Therefore, the production of biodegradable films from carbohydrates and proteins is an alternative because it can add value to low cost raw materials.

The objective of this study was to evaluate physical and mechanical properties of starch/ recycled gelatin films produced by extrusion.

2. Materials and methods

2.1 Materials

Commercial cassava starch (amylose content: 29.6 \pm 0.6%; solubility index: 0.326 \pm 0.06%; pH: 5.38 \pm 0.04; acidity: 1.03 \pm 0.01%; moisture content: 13.01 \pm 0.09%; ash content: 0.13 \pm 0.01) was acquired from Yoki (Brazil). Recycled gelatin (bovine origin; 218.45 Bloom value; protein content 69.26 \pm 1.66%; moisture content: 12.33 \pm 0.03%; ash content: 1.3 \pm 0.01%; purity < 90%) provided by the State University of Campinas (Unicamp-Brazil) was used and a commercial glycerol (Dinâmica, Brazil) was used as a plasticizer.

2.2 Films production

The films were obtained using a single screw extruder (model EL-25, BGM, São Paulo-Brazil) located in the Department of Science and Food Technology at the State University of Londrina.

The films were prepared in two stages: in the first stage the starch, recycled gelatin and plasticizer were mixed manually to production of pellets by extrusion; in the second step the pellets were extruded to produce the films, engaging a specific matrix with the extruder. The extruder consisted of the following components: a screw with a diameter of 25 mm, 4 heating zones, an internal air system to blow the balloons and an external ring of air for cooling the samples. The screw speed was 30 rpm and the zone temperature set between 90 and 120 °C in the four heating zones.⁵ These parameters were used for two stages.

Films were produced by varying the percentage of gelatin in relation to the quantity of starch (100 wt %), while the glycerol percentage was 20% wt. The films were designated as follows: 2.5GEL (2.5% gelatin), 5GEL (5% gelatin), 7.5GEL (7.5% gelatin), 10GEL (10% gelatin), 12.5GEL (12.5% gelatin) and 15GEL (15% gelatin). The films obtained were conditioned for 48h at 25 °C and 50% humidity prior to the tests.

2.3 Analysis

2.3.1 Thickness of the films

Film thickness was measured using a Digimess flat tip digital micrometer (from 0-25 mm, with 0.001 mm resolution) and set to the average of 10 random measures in different parts of an equal sample.

2.3.2 Morphology

The morphological characteristics of the internal structures of the films were analyzed with the scanning electron microscopy (SEM) in a microscope (model VEGA 3LMU - Tescan, Holland). To investigate the cross-sections a cryoscopic cut were made using liquid nitrogen. All samples were covered with a thin layer of gold in a Quorum 150R sputter. A 5kV tension was used to avoid film degradation. The morphology of the cassava starch was evaluated using the transmission electron microscopy (TEM) through the negative contrast technique, carried out in a 120kV (model Tecnai G2-12 Spirit - FEI, Holland) Transmission Electron Microscope.

2.3.3 X-ray diffraction (XRD)

The XRD patterns were collected using a Shimadzu X-ray diffractometer (model XRD-6100 - Japan), operating at 40 kV and 30 A, scan range: 2θ, from 5 ° and 30 °, with a rate of 0.1°/min and copper radiation $\lambda = 1.5433 \text{ \AA}$. The relative crystallinity (RC) of the films was quantitatively calculated following the method of ¹⁷ in triplicate, according to Equation (1).

$$RC (\%) = A_c / (A_a + A_c) \quad (1)$$

Where A_c is the crystalline area, and A_a is the amorphous area on the X-ray diffractogram.

2.3.4 Thermal analysis

Thermogravimetric analysis (TGA) was performed using a Perkin Elmer thermal analyzer (model STA 6000 - USA), assisted by Pyris Series software. A sample of about 8 mg in an inert nitrogen atmosphere of 30 mL/min was used, with a heat rate of 10 °C/min, in a temperature interval of 25 to 600 °C.

For the Differential Scanning Calorimetry (DSC) a TA Instruments calorimeter (model TA 2010 - USA), was used. The samples were pre-conditioned at 25 °C and 60% relative humidity. All measurements were performed in an inert atmosphere of ultra-dry nitrogen gas. Tests were performed from 20 °C up to 250 °C, using a heating rate of 10 °C/min and atmospheric air as the material reference.

2.3.5 Water and acid solubility

The solubility of the films to water was evaluated according to the method of ¹⁸ and ¹⁹. Three film samples were dried at 105 °C for 24h in an air circulation oven (Tecnal-E-394/2, Brazil). Each dried sample was immersed in distilled water maintained under slow agitation for 24 h in a shaker (TE-424-Brazil). The film samples were then removed from the solutions and re-dried at 105 °C for 24 h.

The solubility of the films in acid was tested as described for water. However, after determining their initial dry weight, the samples were immersed in a recipient containing hydrochloric acid (1 mol M/L) without agitation.

Solubility was expressed as percentage of film using Equation 2:

$$\text{Solubility(%)} = \frac{(W_i - W_f)}{W_i} * 100 \quad (2)$$

Where W_i is the initial mass of the sample before immersion and W_f is the weight of the dry sample after immersion. All final determinations were recorded as the mean of three measurements

2.3.6 Mechanical properties

The mechanical behavior was analyzed following the standard method.²⁰ Rectangular proof bodies (with 25 mm width and 190 mm length) were cut with metal scissors and put into a test machine from Emic (model DL 2000 - Brazil), with load cell of 500N and crosshead speed of 5 mm/s, at ambient temperature, characterizing the mechanical properties of films (tensile strength, elongation at break and elastic modulus).

2.3.7 Biodegradation of the films in vegetable compost

The samples were cut into pieces of 2 cm × 2 cm. The vegetable compost, which was used as soil, was prepared by mixing equal parts of fertile soil with low clay content, dry beach sand and sieved (40 mesh), and manure dry horse in the sun for 2 days²¹ and was poured into plastic trays up to a thickness of about 8 cm. Samples were buried below 5 cm of soil, and the plastic trays were kept under ambient temperature (25 °C) and humidity conditions (~30%). The samples were removed every two weeks and the percentage weight loss was determined using the following Equation 3:

$$\text{Weight loss (\%)} = (W_i - W_f)W_i * 100 \quad (3)$$

Where W_i is initial and W_f is final weight. All final determinations were recorded as the mean of three measurements.

2.4 Statistical analysis

The data were analyzed using ASSISTAT software, version 7.7 (Brazil), with the analysis of variance (ANOVA) and Tukey's test at a 5% significance level.

3. Results and discussion

3.1 Film morphology

Figure 1a shows the micrographs corresponding to the surfaces of every studied composite film. It can be seen that all the films presented surface

roughness and that as the gelatin percentage increases, this roughness was more evident. Despite the surface roughness, no cracks in the polymer matrix were found.

The cassava starch micrograph, of the fracture of the film containing 2.5% and 12.5% recycled gelatin are presented in the Figure 1b (a), Figure 1b (b) and Figure 1b (c) respectively. It is possible to observe the presence of non-gelatinized starch granules (indicated by arrows) in the samples with a lower percentage of gelatin. This is probably due to the fact that the samples with lower gelatin concentrations were extruded continuously and faster, which did not allow complete starch granule gelatinization and the rupture of crystalline zones. Furthermore, it was observed that with increased gelatin concentrations starch granules were gradually eliminated, indicating that the extrusion process was enough to eliminate the crystalline zones of the granules (Figure 1b). Thus, those results demonstrate that it was possible to produce blown films through the processing conditions studied in this work. Furthermore, SEM analysis of the films showed no phase separation in the films. The compatibility between gelatin and starch can be affected by various parameters, such as processing time, temperature, pH value and solid concentration.¹⁵

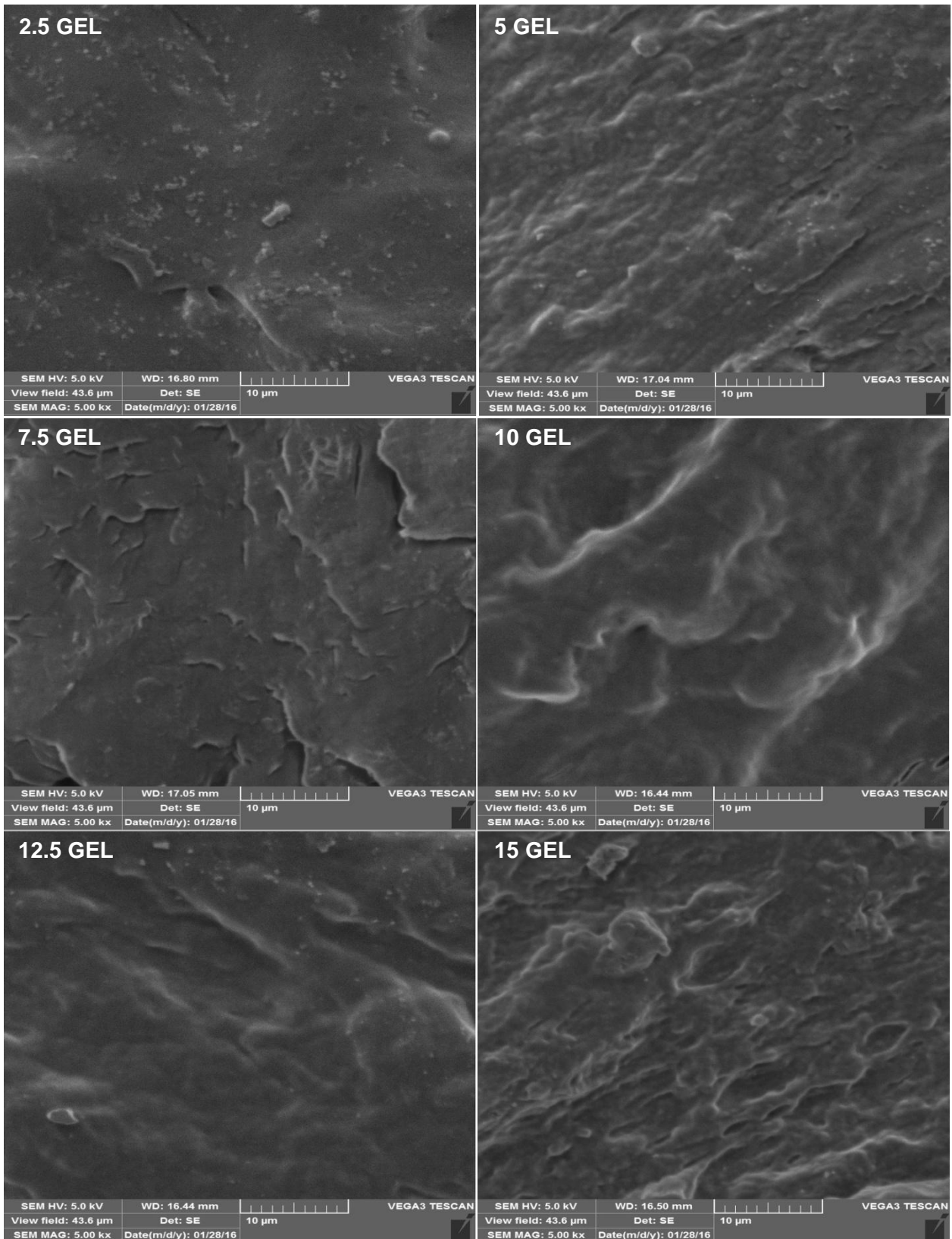


Fig. 1a - SEM features of the surface of the composite films.

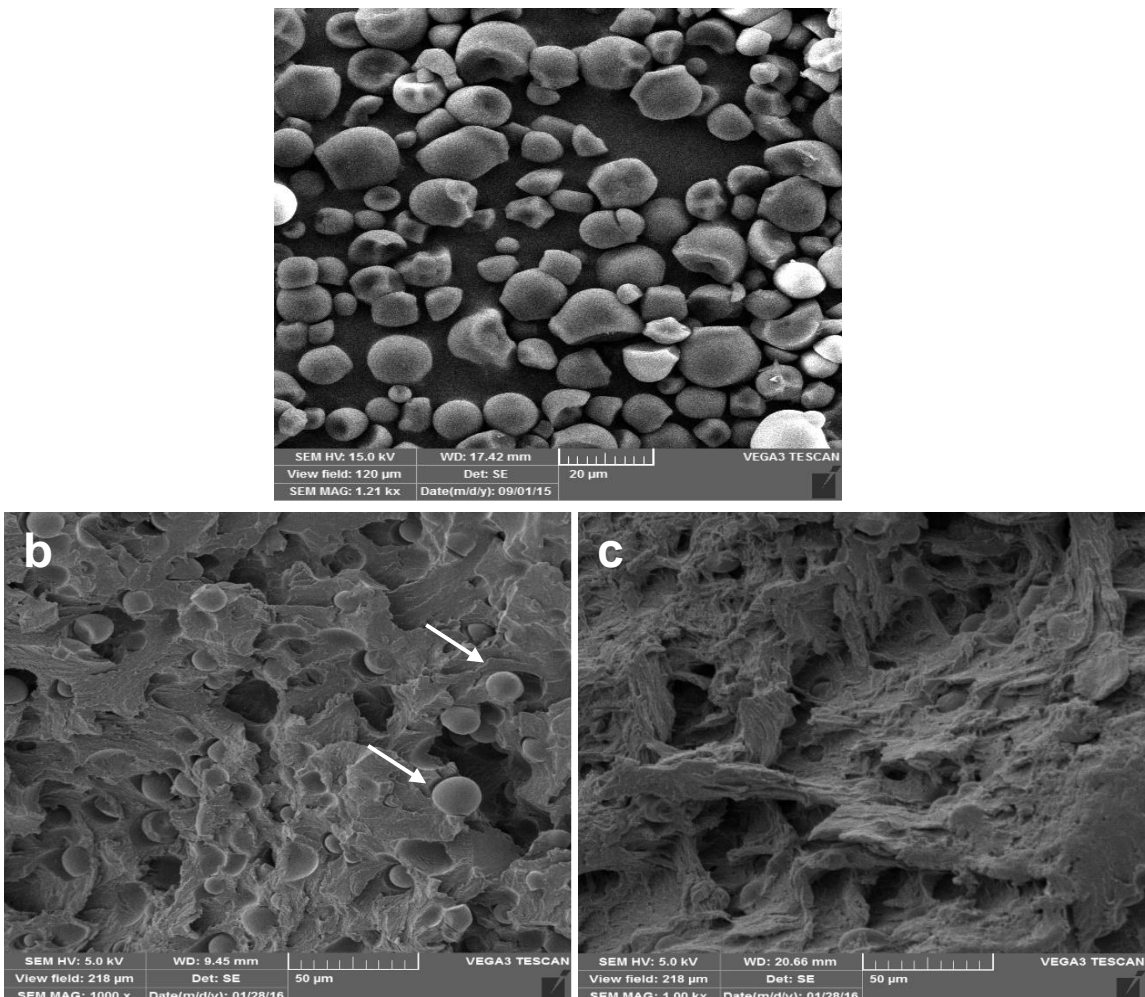


Fig. 1b - Micrograph of native cassava starch (a) and SEM features of cross section of the composite films containing 2.5% (b) and 12.5% (c) of recycled gelatin.

3.2 Crystallinity

X-ray diffractograms (XRD) of starch, recycled gelatin and composite films are shown in Figure 2. The gelatin presented an X-ray diffraction with low crystallinity or an amorphous character, with only one peak intensity located in region at $2\theta = 25^\circ$. This characteristic peak is usually associated to the triple-helical structure of the collagen and gelatin.^{22,23}

The crystallinity of starches is related with the packing of the amylopectin double helices, and the content of amylose mainly dispersed in the amorphous region of starches.²⁴ Depending on the type of crystalline structures

present in the granules, starches are called A-, B-, or C-type. In A-type starch, the structure is highly condensed and crystalline. The B-type crystals with a hexagonal system are formed by rather loosely arranged double helices. The C-type is considered a mixture of A and B types.²⁵ In this study, X-ray diffractograms of the starch presented more intense patterns in $2\theta = 14^\circ$; 16° ; 17° and 22° . Some less intense patterns can be observed in region de 2θ next 12° (~ 10 , 5°). Therefore, presenting A-type and B-type patterns, which can be classified as C-type.²⁶

The films presented an X-ray diffraction pattern characteristic of a partially crystalline material (broad peaks and low intensity) with four main diffraction peaks in region of $2\theta = 12^\circ$, 17° , 19° and 22° . That result indicates that extrusion process conditions were efficient because the films presented low crystallinity when compared to starch, since the relative crystallinity for the starch was $28\% \pm 0.03\%$ while of the films were of $12\% \pm 0.05\%$, $11\% \pm 0.03\%$, $10\% \pm 0.02\%$, $12\% \pm 0.05\%$, $12\% \pm 0.06\%$ and $10\% \pm 0.01\%$ for samples 2.5GEL, 5GEL, 7.5GEL, 10GEL, 12.5GEL and 15 GEL respectively, this result is related the plasticization process (extrusion) which leads to a disorganization of starch structure, which cause the crystallinity decreases in relation to the native starch. However, this same result indicates of the presence remaining crystalline starch granules within the films (high concentrations of gelatin) samples post extrusion, which corroborates the microscopic images (Figures 1a and 1b). Besides this, pure gelatin exhibits a pattern located at $2\theta = 25^\circ$ (a typical XRD pattern) which can be also seen in films containing 10, 12.5 and 15% of gelatin (higher concentrations).

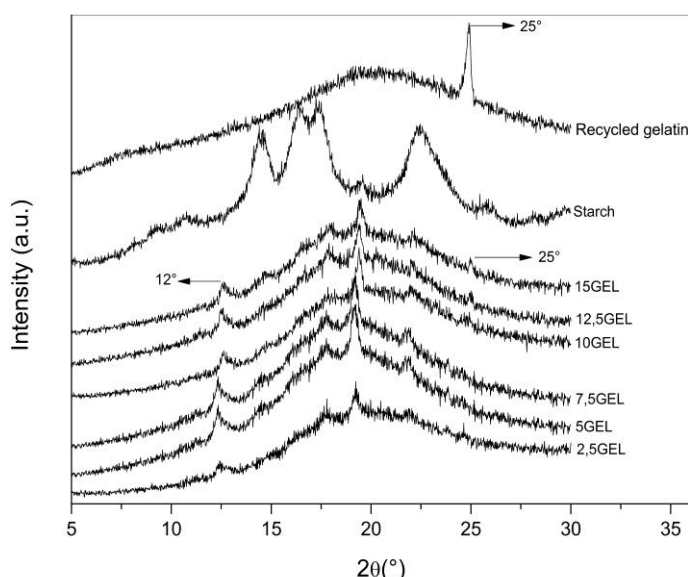


Fig. 1. X-ray diffractograms for starch, recycled gelatin and composite films.

3.3 Thermal analysis

3.3.1 Thermogravimetric Analysis (TGA)

Figure 3 shows the thermograms obtained for the starch, recycled gelatin and composite films. Thermograms curves of the starch and gelatin provide evidence of the two step degradation processes. For the starch, in the first stage initial mass decreases in the range 60 – 118 °C (2%) related to the evaporation of water. In the second stage (270 – 346 °C) the major thermal decomposition of the sample occurs (mass loss of 82.4%). In the recycled gelatin curve, the first stage starts in the range 50 – 145 °C with a loss of mass of 12.1%, due mainly to the loss of water.

In the second stage, between 240 °C and 397 °C (loss of mass of 66.05%), the loss is attributed to the thermal decomposition. This phenomenon occurs in stages, protein chain breakage and peptide bonds rupture are preliminary stages for decomposition of gelatin. The loss of mass occurs due to the decomposition of amino acids fragments of easy degradation and the elimination of amino acids of difficult degradation, mainly glycine.^{14,23,28} By analyzing the thermal behavior of the films a small mass loss in the region of 100 °C can be seen probably caused by the loss of water molecules. Nevertheless, the first event only occurred around 140 °C.

The second event shows that temperatures where the largest mass loss occurred varied between next to 345 °C (2.5 GEL) with a weight loss around 77% and next to 369 °C (15 GEL) which showed a mass loss 70%. This seems to indicate that increasing the gelatin concentration in the films caused an increase in the thermal stability of the films. This behavior is probably due to the higher thermal stability of gelatin when compared to starch. The starch/gelatin blend presents high thermal stability due to probably the increasing dissociation energy owing to many interactions occurring between the polymer blend constituents.²⁵ In the Table 1 are shown the temperatures

(second stage) where the largest mass loss occurred of the films. It can be observed that the initial temperature of the mass loss is very similar. However, the temperatures of maximum thermal degradation increase in the samples with high gelatin concentration. This result indicates that the recycling process which gelatin was subjected did not interfere in the thermal stability.

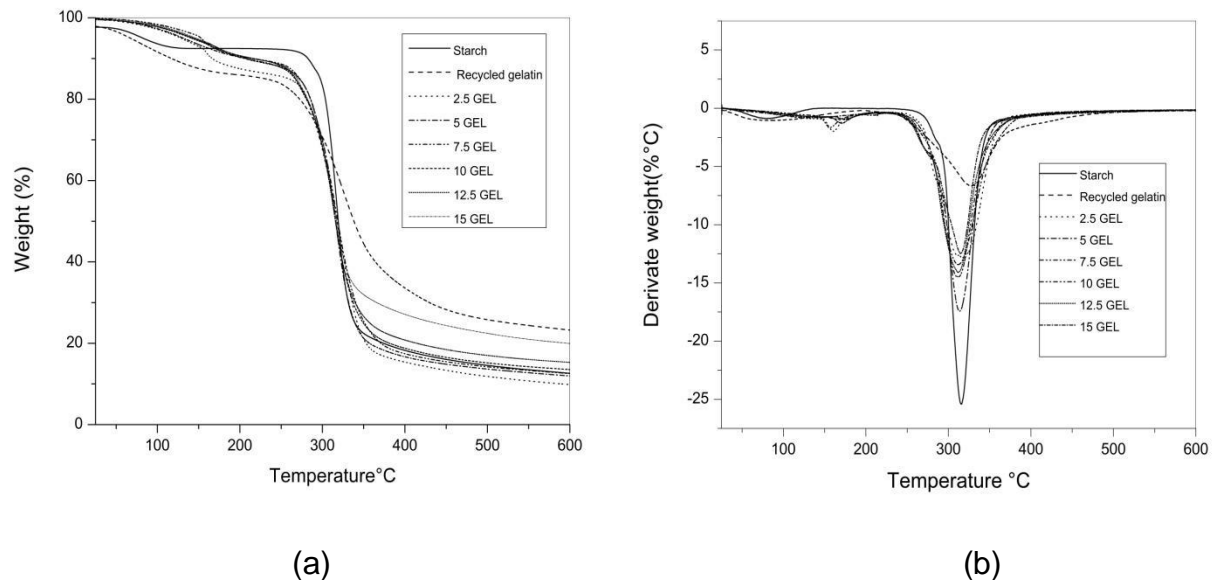


Fig. 2. Thermogravimetric (TG) (a) and derivative TG (DTG) (b) of starch, recycled gelatin and composite films.

Table 1 - Thermal Stability of films.

Sample	Second stage	
		T _{onset} – T _{offset} (°C)
2.5 GEL		250.01 – 346.03
5 GEL		256.12 – 351.09
7.5 GEL		258.00 – 353.25
10 GEL		258.15 – 357.32
12.5 GEL		259.67 – 358.53
15 GEL		261.63 – 369.57

3.3.1 Differential scanning calorimetry (DSC)

The DSC curves of starch, recycled gelatin and composite films are presented in Figure 4. For the gelatin, in temperature range of 25 – 250 °C it was not possible observe glass transition temperature (T_g). The glass transition of native gelatin may occur between 217 °C to 0 °C depending on the water content.²⁹ The recycled gelatin, in our work, presented a moisture content of the 13.01% ($\pm 0.09\%$), suggesting that T_g may occur in the region from 50 to 75 °C. However, in that range, another thermal event was identified, which can be attributed to unbound water from gelatin processing, difficulting the identification of glass transition temperature. Besides that, it can be observed one endothermic peak in the region of 120 °C related to thermal unfolding of the gelatin.³⁰ The starch shows one shift (around 64 °C) that is probably associated to the beginning of the gelatinization temperature and the enthalpy of gelatinization of 12.47 J/g.³¹ The enthalpy of gelatinization (ΔH_{gel}), represents the amount of thermal energy involved in the gelatinization process, the high ΔH_{gel} suggests that the double helices (formed by the outer branches of adjacent amylopectin chains) that unravel and melt during gelatinization are strongly associated with the native granule.³² In the films, this peak (around 64°C) is still present but to a lesser extent. This fact can be explained that the extrusion brought about broken of starch granules, consequently, less energy was needed to gelatinize the starch granules.

In general, the DSC curves of the films were similar. Starch-gelatin films exhibit different behavior from pure starch and gelatin suggesting homogeneity between biopolymers as can be seen in the morphology analysis (no phase separation). However, it can be observed that the displacements of the peaks with increase in the concentration of gelatin. The film with 2.5% of gelatin presented one peak (more evident) of around 120 °C, while 15GEL film showed a one peak in 130.55 °C. The displacements shows that the films with higher concentrations of gelatin are more thermally stable, corroborating with the results of the TGA.

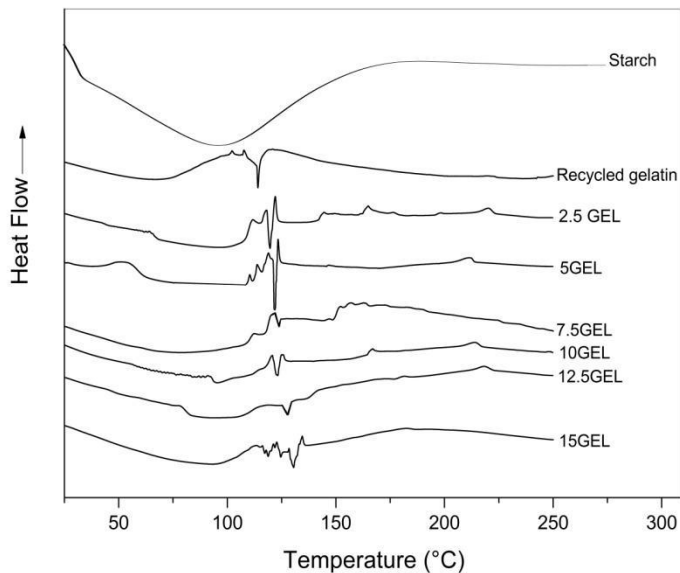


Fig. 3. DSC thermograms of starch, recycled gelatin and composite films.

3.4 Water and acid solubility

Figure 5 shows the water solubility for the different films. The films presented increasing water solubility with increasing gelatin concentration, the film with 2.5% showed the lowest value (9.51%) and the film with 15% showed the highest value (20.31%) with a significant difference between them ($p<0.05$). This can be related to the increased content of hydrophilic groups in the final mass of the films.³³ All the films were 100% soluble in acid solution.

Water solubility is an important property of films depending on its end-use application. Water insolubility may be required to enhance product integrity and water resistance. Furthermore, tolerance to water is related to the chemical structure of the materials.⁵

The polymers that present higher solubility are more susceptible to degradation because components can hydrolyze more easily and consequently become smaller molecules.³⁴ In this work, the films with 15% of gelatin presented higher water solubility and faster degradation (as shown in Figure 8).

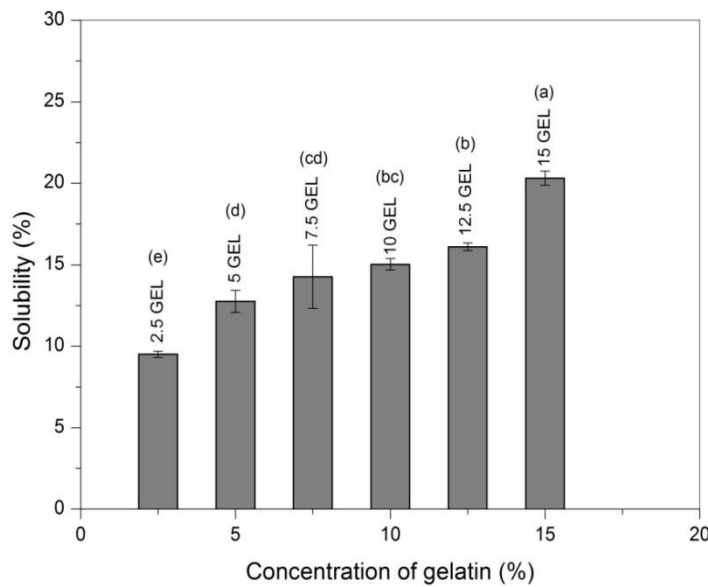


Fig. 4. Water solubility of composites films.

3.5 Mechanical behavior

The values of elongation at break (Eb), tensile strength (TS) and elasticity modulus (EM) were measured and the results are shown in Figure 6.

Elongation at break (Eb) values decreased with increasing concentration of gelatin. The films containing 12.5 and 15% gelatin showed lower elongation at break with a significant difference ($p<0.05$) when compared other films. This can be attributed to the compactness of gelatin, which can reduce the films flexibility and stretchability.³⁵ The same behavior has also been reported by³⁶ and³⁰ who used conventional gelatin in composite films of starch. However, it can be seen that the tensile strength (TS) values increased with increasing concentration of gelatin in the films (Figure 6-b), varying from 7.5 MPa (2.5 GEL) to approximately 14 MPa (15 GEL) with a significant difference between them ($p<0.05$). Such result agreed with SEM micrographs of films, which indicated the production of films with a cohesive matrix and without breaks, which result the tensile strength improvements. This indicates that the gelatin, even when having undergone the process of recycling and reprocessing, still functions as mechanical reinforcement for the starch-based films.

Elastic modulus (EM) values indicated that the increase in the concentration of gelatin resulted in an increasing value of this parameter, with a

significant difference ($p<0.05$) when the concentration increases from 7.5% to 10% of gelatin. This is related to the high mechanical behavior of gelatin, due to the conformation and arrangement of protein chains inducing strong interchain forces close to the collagen structure which improves its mechanical performance.^{8,37} The polysaccharides can form networks with gelatin molecules between anionic domains of the polysaccharides and cationic domains of the gelatin, which strengthen the structure of films.³⁸ Similar results were obtained by other authors in researches with starch and conventional gelatin.^{5,8,14}

The stress–strain curves in Figure 7 clearly show that the all films became less flexible and stiffer with increased concentrations of gelatin.

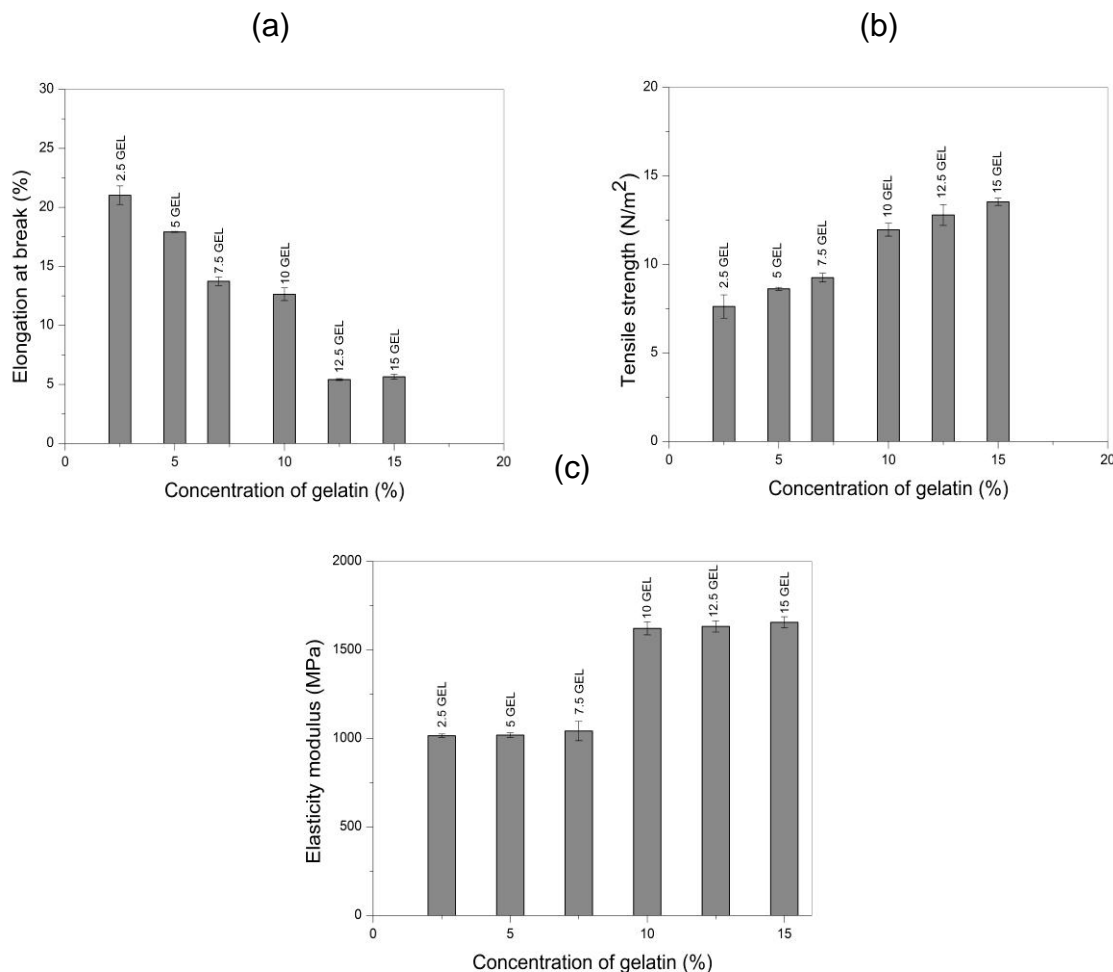


Fig. 5. Effect of gelatin concentration on mechanical properties of the composite films: Elongation at break (a); Tensile strength (b); Elasticity modulus (c).

The stress-strain curves in Figure 7 clearly show that the all films became less flexible and stiffer with increased concentrations of gelatin.

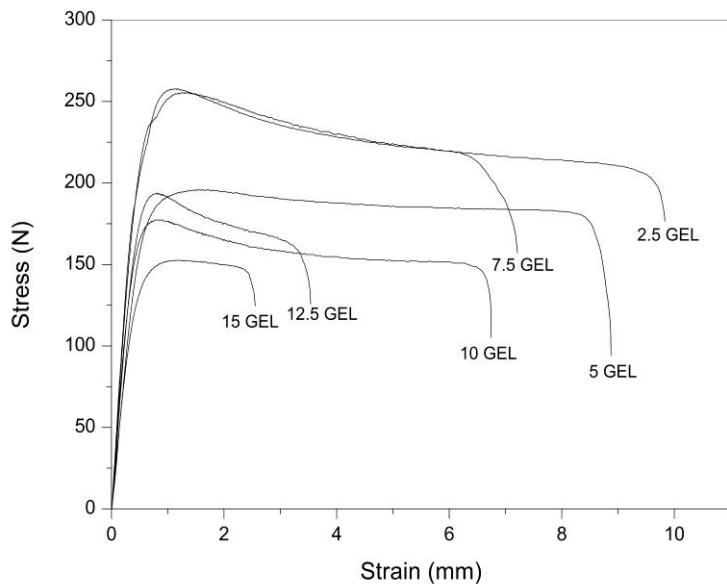


Fig. 6. Stress- strain curves for the composite films.

3.6 Biodegradation of the films in vegetable compost

Figure 8 shows the biodegradation of the films based on weight loss over time. Biodegradation is the degradation of an organic material caused by biological activity, mainly by microorganisms via enzymatic action (Negim et al., 2014). Biodegradation tests showed that the weight loss was dependent on the amount of gelatin present in the polymer matrix. Films with 2.5% gelatin had the lowest weight loss during the period of analysis (25%), whereas the films with 15% gelatin at the end of the 17 weeks showed a weight loss of 50%, indicating that the incorporation of gelatin improved the biodegradability of the films. It can be seen that the decomposition occurs more markedly after 60 days of burial. This is consistent with the results presented for the water solubility test (item 3.5). Due to environmental concerns, the faster the biodegradability of the packaging material, the better.

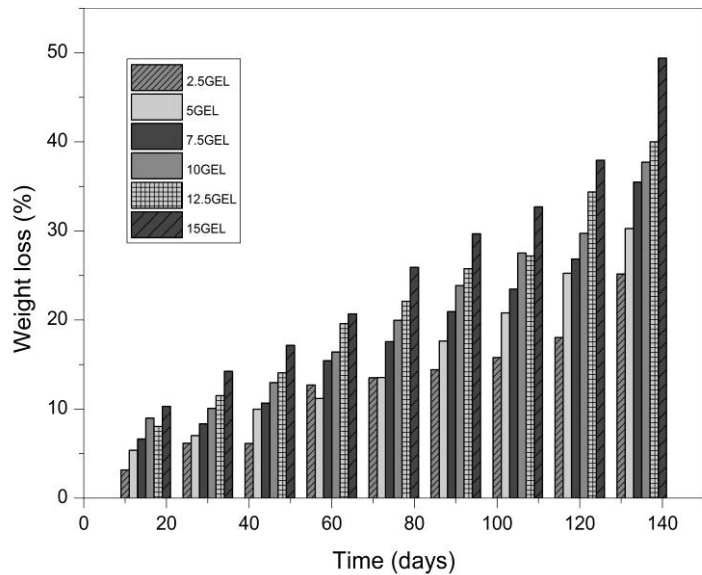


Fig. 7. Evolution of biodisintegration of the composite films buried under solid composting material.

CONCLUSIONS

Composite films made from starch and recycled gelatin plasticized by glycerol were successfully produced by extrusion. The results of DRX and SEM micrographs obtained showed that the extrusion process was enough to eliminate the crystalline zone. Furthermore, the films made from high concentrations of gelatin (15 GEL) showed maximum degrading temperature next to 369 °C and higher water solubility (20.31%). DSC analysis it was possible identify the displacements of the peaks in the films with increase in the concentration of gelatin.

The mechanical properties were affected by increased percentages of recycled gelatin. This indicates that the recycling process that the gelatin has undergone does not interfere with its reinforcement capacity.

Finally, it is interesting to note that the recycled gelatin accelerated the degradation process of the films, making this material an interesting alternative to produce biodegradable and environmentally friendly packaging materials at low cost.

ACKNOWLEDGEMENTS

The authors would like to express their gratitude to the State University of Londrina for their help to produce the films and the Federal Institute of Bahia - Salvador for their assistance in the analysis and also to Professor Lucia H. Innocentini-Mei, State University of Campinas, for donating the recycled gelatin.

REFERENCES

1. Moreno, O.; Díaz, R.; Atarés, L.; Chiralt, A. *Polym. Int.* **2016**, *65*, 905–914.
2. Nur Hanani, Z. A.; Beatty, E.; Roos, Y. H.; Morris, M. A.; Kerry, J. P. *J. Food Eng.* **2012**, *113*, 606–614.
3. Al-Hassan, A. A.; Norziah, M. H. *Food Hydrocoll.* **2012**, *26*, 108–117.
4. Cao, N.; Fu, Y.; He, J. *Food Hydrocoll.* **2007**, *21*, 1153–1162.
5. Fakhouri, F. M.; Costa, D.; Yamashita, F.; Martelli, S. M.; Jesus, R. C.; Alganer, K.; Collares-Queiroz, F. P.; Innocentini-Mei, L. H. *Carbohydr. Polym.* **2013**, *95*, 681–689.
6. Savadekar, N. R.; Mhaske, S. T. *Carbohydr. Polym.* **2012**, *89*, 146.
7. Cano, A.; Jiménez, A.; Cháfer, M.; Gónzalez, C.; Chiralt, A. *Carbohydr. Polym.* **2014**, *111*, 543–555.
8. Acosta, S.; Jiménez, A.; Cháfer, M.; González-Martínez, C.; Chiralt, A. *Food Hydrocoll.* **2015**, *49*, 135–143.
9. Fakhouri, F. M.; Fontes, L. C. B.; Gonçalves, P. V. D. M.; Milanez, C. R.; Steel, C. J.; Collares-Queiroz, F. P. *Ciênc. Tecnol. Aliment.* **2007**, *27*, 369-375.
10. Nur Hanani, Z. A.; Roos, Y. H.; Kerry, J. P. *Food Hydrocoll.* **2012**, *29*, 144–151.
11. Gelita. <https://www.gelita.com/en> (acessed Dec 14, 2017).

12. Coronado Jorge, M. F.; Alexandre, E. M. C.; Caicedo Flaker, C. H.; Bittante, A. M. Q. B.; Sobral, P. J. D. A. *Int. J. Polym. Sci.* **2015**, *2015*, 1–9.
13. Liu, X. X.; Wang, Y. F.; Zhang, N. Z.; Shanks, R. A.; Liu, H. S.; Tong, Z.; Chen, L.; Yu, L. *Chin. J. Polym. Sci. (English Edition)* **2014**, *32*, 108–114.
14. Soliman, E. A.; Furuta, M. *Food Nutr. Sc.* **2014**, *5*, 1040–1055.
15. Zhang, N.; Liu, X.; Yu, L.; Shanks, R.; Petinaks, E.; Liu, H. *Carbohydr. Polym.* **2013**, *95*, 649.
16. Vargas-Solórzano, J. W.; Carvalho, C. W. P.; Takeiti, C. Y.; Ascheri, J. L. R.; Queiroz, V. A. V. *Food Res. Int.* **2014**, *55*, 37–44.
17. Nara, S.; Komiya, T. *Starch - Stärke* **1983**, *35*, 407–410.
18. Gontard, N.; Guilbert, S.; Cuq, J. L. *J. Food Sci.* **1993**, *58*, 206–211.
19. Fakhouri, F. M.; Martelli, S. M.; Caon, T.; Velasco, J. I.; Mei, L. H. I. *Postharvest Biol. Tec.* **2015**, *109*, 57–64.
20. American Society for Testing and Materials (ASTM). *ASTM (Am. Soc. Test. Mater.) Data Ser.* **2003**.
21. American Society for Testing and Materials (ASTM). *ASTM (Am. Soc. Test. Mater.) Data Ser.* **2009**.
22. Yakimets, I.; Wellner, N.; Smith, A. C.; Wilson, R. H.; Farhat, I.; Mitchell, J. *Polymer* **2005**, *46*, 12577–12585.
23. Peña, C.; de la Caba, K.; Eceiza, A.; Ruseckaite, R.; Mondragon, I. *Bioresour. Technol.* **2010**, *101*, 6836–6842.
24. Hoover, R. *Carbohydr. Polym.* **2001**, *45*, 253–267.
25. Van Soest, J. J. G.; Vliegenthart, J. F. G. *Trends Biotechnol.* **1997**, *15*, 208–213.

26. Cai, J.; Cai, C.; Mana, J.; Zhoub, W.; Wei, C. *Carbohydr. Polym.* **2014**, *101*, 289–300.
27. Arvanitoyannis, I.; Psomiadou, E.; Nakayama, A.; Aiba, S.; Yamamoto, N. *Food Chem.* **1997**, *60*, 593–604.
28. Cyras, V. P.; M. C. T. Zenklusen, Vazquez, A. *J. Appl. Poly. Sci.* **2006**, *101*, 4313–4319
29. Apostolov, A. A.; Fakirov, S.; Vassileva, E.; Patil, R. D.; Mark, J. E. *J. Appl. Poly. Sci.* **1999**, *71*, 465–470.
30. Rahman, M. S.; Al-Saidi, G.; Guizani, N.; Abdullah, A. *Therm. Acta* **2010**, *509*, 111–119.
31. Singh, N.; Singh, J.; Kaur, L.; Sodhi, N. S.; Gill, B. S. *Food Chem.* **2003**, *81*, 219–231.
32. Marcon, M. J. A.; Kurtza, D. J.; Raguzzoni, J. C.; Delgadillo, I.; Maraschin, M.; Soldid, V.; Reginatto, V.; Amante, E. R. *Starch/Stärke, Weinheim.* **2009**, *61*, 12, 716–726.
33. Fakhouri, F. M.; Martelli, S. M.; Canhadas Bertan, L.; Yamashita, F.; Innocentini Mei, L. H.; Collares Queiroz, F. P. *LWT-- Food Sci. Technol.* **2012**, *49*, 149–154.
34. Sifuentes-Nieves, I.; Rendón-Villalobos, R.; Jiménez-Aparicio, A.; Camacho-Díaz, B. H.; Gutiérrez López, G. F.; Solorza-Feria, J. *Int. J. Polym. Sci.* **2015**, *2015*, 1–8.
35. Veiga-Santos, P.; Oliveira, L. M.; Cereda, M. P.; Scamparini, A. R. P. *Food Che.* **2007**, *103*, 255–262.
36. Tongdeesoontorn, W.; Mauer, L. J.; Wongruong, S.; Sriburi, P.; Rachtanapun, P. *Int. J. Polymer Mater.* **2012**, *61*, 778–792.
37. Chambi, H.; Grosso, C. *Food Res. Int.* **2006**, *39*, 458–466.

38. Fonkwe, L. G.; Narsimhan, G.; Cha, A. S. *Food Hydrocoll.* **2003**, *17*, 871–883.
39. Negim, E.; Rakhmetullayeva, R.; Yeligbayeva, G.; Urkimbaeva, P.; Primzharova, S.; Kaldybekov, D.; Khatib, J.; Mun, G.; W., C. *Int. J. Basic App. Sci.* **2014**, *3*, 263-273.

CAPÍTULO 5 – CONCLUSÕES FINAIS E SUGESTÃO PARA TRABALHOS FUTUROS

Com base nos resultados obtidos e apresentados nesta tese, pode-se concluir que foi possível produzir, via extrusão, filmes de PBAT/amido reforçado com nanopartículas de amido e filmes de amido reforçados com gelatina reciclada.

Os filmes com 1% de SNP na sua composição apresentaram redução da permeabilidade ao vapor de água e as propriedades mecânicas avaliadas foram significativamente melhoradas ($p<0,05$), apresentando um aumento no módulo de elasticidade de aproximadamente 20% em relação ao filme de PBAT puro, sendo, portanto, adequado para utilização como embalagens alimentícias. Para os filmes reforçados com outras concentrações de nanopartículas (2 - 5% m/m), não houve diferença estatística ($p<0,05$) nas propriedades mecânicas e de permeabilidade ao vapor quando comparados ao filme PBAT/AMIDO 70/30.

Os filmes de amido e gelatina reciclada foram produzidos com sucesso pelo processo de extrusão-sopro. No entanto, as características físico-químicas, visuais e mecânicas foram diferentes dos filmes de PBAT/amido, mostrando-se inadequados para utilização como filmes alimentícios. As matrizes amido/gelatina apresentaram excelentes propriedades mecânicas, sugerindo aplicação na área de embalagens ou descartáveis. Os filmes que foram produzidos com maiores concentrações de gelatina reciclada apresentaram maior estabilidade térmica e solubilidade em água. Por fim, a análise de biodegradação dos filmes a base amido/gelatina reciclada, a concentração de 15% (m/m), mostrou perda de massa total de 50 % após 17 semanas.

Esse resultado demonstra à potencialidade da utilização de polímeros a base de amido na produção de embalagens ou filmes alimentícios com curto tempo de degradação (menor que 30 dias).

Como sugestões para novos trabalhos, pode-se avaliar a aplicação dos filmes de amido e gelatina como matéria-prima para a produção de materiais

rígidos (pratos, copos e talheres). Além disso, estudar a incorporação de nanopartículas de amido contendo moléculas antioxidantes, como a curcumina (ou de outros ativos), aos filmes de PBAT/ amido, e avaliar o filme no recobrimento de embalagens alimentícia de contato direto com o alimento. Durante o desenvolvimento dessa pesquisa, foi possível produzir nanopartículas de amido com curcumina (Apêndice A e B), entretanto, as análises da aplicação nos filmes de PBAT /amido em contato direto com o alimento precisam ser explorados.

CAPÍTULO 6 – REFERÊNCIAS BIBLIOGRÁFICAS

- Acosta, S., Jiménez, A., Cháfer, M., González-Martínez, C., & Chiralt, A. (2015). Physical properties and stability of starch-gelatin based films as affected by the addition of esters of fatty acids. *Food Hydrocolloids*, 49, 135–143.
- Akrami, M., Ghasemi, I., Azizi, H., & Karrabi, M. (2016). A new approach in compatibilization of the poly (lactic acid)/ thermoplastic starch (PLA / TPS) blends. *Carbohydrate Polymers*, 144, 254–262.
- Al-Ittry, R., Lamnawar, K., & Maazouz, A. (2012). Improvement of thermal stability, rheological and mechanical properties of PLA, PBAT and their blends by reactive extrusion with functionalized epoxy. *Polymer Degradation and Stability*, 97(10), 1898–1914.
- Aliyu, M., & Hepher, M. J. (2000). Effects of ultrasound energy on degradation of cellulose material. *Ultrasonics Sonochemistry*, 7(4), 265–268.
- Alves, V. D., Mali, S., Beléia, A., & Grossmann, M. V. E. (2007). Effect of glycerol and amylose enrichment on cassava starch film properties. *Journal of Food Engineering*, 78(3), 941–946.
- Angellier-Coussy, H., Putaux, J. L., Molina-Boisseau, S., Dufresne, A., Bertoft, E., & Perez, S. (2009). The molecular structure of waxy maize starch nanocrystals. *Carbohydrate Research*, 344(12), 1558–1566.
- Arrieta, M. P., Fortunati, E., Dominici, F., & Ray, E. (2014). PLA-PHB / cellulose based fi lms : Mechanical , barrier and disintegration properties, 107.
- Arruda, L. C., Magaton, M., Bretas, R. E. S., & Ueki, M. M. (2015). Influence of chain extender on mechanical, thermal and morphological properties of blown films of PLA/PBAT blends. *Polymer Testing*, 43, 27–37.
- Auras, R., Singh, S., and Singh, J. (2006). No Title. *Journal of Testing and Evaluation*, 34(6).

Avérous L, B. N. (2004). Biocomposites based on plasticized starch: thermal and mechanical behaviour. *Carbohydrate Polymers*, 56(2), 111–122.

Azeredo, H. M. C. Antimicrobial nanostructures in food packaging. Trends in Food Science & Technology, v. 30, p. 56-69, 2013.

Bastioli, C. Global status of the production of biobased packaging materials. *Starch/Staerke*, v. 53, n. 8, p. 351–355, 2001.

Baxter, S., Zivanovic, S., & Weiss, J. (2005). Molecular weight and degree of acetylation of high-intensity ultrasonicated chitosan. *Food Hydrocolloids*, 19(5), 821–830.

Bel Haaj, S., Magnin, A., Pétrier, C., & Boufi, S. (2013). Starch nanoparticles formation via high power ultrasonication. *Carbohydrate Polymers*, 92(2), 1625–1632.

Bel Haaj, S., Thielemans, W., Magnin, A., & Boufi, S. (2016). Starch nanocrystals and starch nanoparticles from waxy maize as nanoreinforcement: A comparative study. *Carbohydrate Polymers*, 143, 310–317.

Belitz, H.-D., Grosch, Werner, Schieberle, P. *Food chemistry*, p.989, Springer, 2004

Berrios, J. D. J., Ascheri, J. L. R., & Losso, J. N. (2012). Extrusion Processing of Dry Beans and Pulses. In *Dry Beans and Pulses Production, Processing and Nutrition* (pp. 185–203). Oxford, UK: Blackwell Publishing Ltd.

Biasutti, E.A.R. Blendas poliméricas e nanocompósitos à base de amido: propriedades mecânicas, estruturais e de barreira e compostagem em solo simulado. Tese (Doutorado em Engenharia de Alimentos) UNICAMP, 2011.

Brandelero, R. P. H., Grossmann, M. V. E., & Yamashita, F. (2011). Effect of the method of production of the blends on mechanical and structural properties of biodegradable starch films produced by blown extrusion. *Carbohydrate Polymers*, 86(3), 1344–1350.

- Brito, G. F., Agrawal, P., Araújo, E. M., & Mélo, T. J. A. (2011). Biopolímeros , Polímeros Biodegradáveis e Polímeros Verdes. *Revista Eletrônica de Materiais E Processos*, 6(2), 127–139.
- Cameron, M., McMaster, L. D., & Britz, T. J. (2008). Electron microscopic analysis of dairy microbes inactivated by ultrasound. *Ultrasonics Sonochemistry*, 15(6), 960–964.
- Carvalho, A. J. F., Zambon, M. D., Da Silva Curvelo, A. A., & Gandini, A. (2005). Thermoplastic starch modification during melt processing: Hydrolysis catalyzed by carboxylic acids. *Carbohydrate Polymers*, 62(4), 387–390.
- Chang, Y. P., Abd Karim, A., & Seow, C. C. (2006). Interactive plasticizing–antiplasticizing effects of water and glycerol on the tensile properties of tapioca starch films. *Food Hydrocolloids*, 20(1), 1–8.
- Chen, D., Lawton, D., Thompson, M. R., & Liu, Q. (2012). Biocomposites reinforced with cellulose nanocrystals derived from potato peel waste. *Carbohydrate Polymers*, 90(1), 709–716.
- Chen, Y., Cao, X., Chang, P. R., & Huneault, M. A. (2008). Comparative study on the films of poly(vinyl alcohol)/pea starch nanocrystals and poly(vinyl alcohol)/native pea starch. *Carbohydrate Polymers*, 73(1), 8–17.
- Chen, Y., Liu, C., Chang, P. R., Cao, X., & Anderson, D. P. (2009). Bionanocomposites based on pea starch and cellulose nanowhiskers hydrolyzed from pea hull fibre: Effect of hydrolysis time. *Carbohydrate Polymers*, 76(4), 607–615.
- Condés, M. C., Añón, M. C., Mauri, A. N., & Dufresne, A. (2015). Amaranth protein films reinforced with maize starch nanocrystals. *Food Hydrocolloids*, 47, 146–157.
- Corradini, E., Lotti, C., Medeiros, E. S. De, Carvalho, A. J. F., Curvelo, A. a. S., & Mattoso, L. H. C. (2005). Estudo comparativo de amidos termoplásticos derivados do milho com diferentes teores de amilose. *Polímeros*, 15, 268–

- Corsello, F. A., Bolla, P. A., Anbinder, P. S., Serradell, M. A., Amalvy, J. I., & Peruzzo, P. J. (2017). Morphology and properties of neutralized chitosan-cellulose nanocrystals biocomposite films. *Carbohydrate Polymers*, 156, 452–459.
- Cortés-Rojas, D. F. *Encapsulação de compostos bioativos de Syzygium aromaticum em carreadores lipídicos sólidos*. Tese (Doutorado em Ciências Farmacêuticas) USP, 2015.
- Costa, D. L. M. G. Da. Produção por extrusão de filmes de alto teor de amido termoplástico de mandioca com poli(butileno adipato co-tereftalato) (pbat). Dissertação (Mestrado em Ciência de Alimentos) UEL, 2008.
- da Silva, J. B. A., Pereira, F. V., & Druzian, J. I. (2012). Cassava Starch-Based Films Plasticized with Sucrose and Inverted Sugar and Reinforced with Cellulose Nanocrystals. *Journal of Food Science*, 77(6), N14–N19.
- Dai, L., Qiu, C., Xiong, L., & Sun, Q. (2015). Characterisation of corn starch-based films reinforced with taro starch nanoparticles. *Food Chemistry*, 174, 82–88.
- Dainelli, D., Gontard, N., Spyropoulos, D., Zondervan-van den Beuken, E., & Tobback, P. (2008). Active and intelligent food packaging: legal aspects and safety concerns. *Trends in Food Science and Technology*, 19(SUPPL. 1).
- Dang, K. M., & Yoksan, R. (2016). Morphological characteristics and barrier properties of thermoplastic starch/chitosan blown film. *Carbohydrate Polymers*, 150, 40–47. <http://doi.org/10.1016/j.carbpol.2016.04.113>
- De Carvalho, R. A., & Grosso, C. R. F. (2006). Properties of chemically modified gelatin films. *Brazilian Journal of Chemical Engineering*, 23(1), 45–53.
- Del Nobile, M. A., Conte, A., Incoronato, A. L., & Panza, O. (2008). Antimicrobial efficacy and release kinetics of thymol from zein films. *Journal*

of Food Engineering, 89(1), 57–63.

Ermolovich, O. A., & Makarevich, A. V. (2006). Effect of compatibilizer additives on the technological and performance characteristics of biodegradable materials based on starch-filled polyethylene. *Russian Journal of Applied Chemistry*, 79(9), 1526–1531.

Fakhouri, F. M., Costa, D., Yamashita, F., Martelli, S. M., Jesus, R. C., Alganer, K., ... Innocentini-Mei, L. H. (2013). Comparative study of processing methods for starch/gelatin films. *Carbohydrate Polymers*, 95(2), 681–689.

Famá, L., Rojas, A. M., Goyanes, S., & Gerschenson, L. (2005). Mechanical properties of tapioca-starch edible films containing sorbates. *LWT - Food Science and Technology*, 38(6), 631–639.

Fan, H., Ji, N., Zhao, M., Xiong, L., & Sun, Q. (2016). Characterization of starch films impregnated with starch nanoparticles prepared by 2,2,6,6-tetramethylpiperidine-1-oxy (TEMPO)-mediated oxidation. *Food Chemistry*, 192, 865–872.

Fang, Z., & Bhandari, B. (2010). Encapsulation of polyphenols - A review. *Trends in Food Science and Technology*, 21(10), 510–523.

Félix, J. S., Manzoli, J. E., & Padula, M. (2008). Embalagem Plástica Contendo Poliamida 6 Para Produtos Cárneos E Queijos: Migração De Caprolactama E Efeito Da Irradiação . Uma. *Alim. Nutr. Araraquara*, 19(3), 361–370.

Fernandes, A. P. S.; Costa, J. B.; Soares, D. S. B.; Moura, C. J. DE; Souza, A. R. M. de. Application of biodegradable films produced from irradiated whey protein concentrate. *Pesquisa Agropecuária Tropical*, Goiânia-GO, v. 45, n. 2, p. 192-199, 2015.

Ferri, J. M., Fenollar, O., & Balart, R. (2016). The effect of maleinized linseed oil (MLO) on mechanical performance of poly (lactic acid) -thermoplastic starch (PLA-TPS) blends. *Carbohydrate Polymers*, 147, 60–68.

Fukushima, K., Wu, M. H., Bocchini, S., Rasyida, A., & Yang, M. C. (2012).

PBAT based nanocomposites for medical and industrial applications. *Materials Science and Engineering C*, 32(6), 1331–1351.

Garavand, F. et al. Improving the integrity of natural biopolymer films used in food packaging by crosslinking approach: a review. *International Journal of Biological Macromolecules*, Karaj, v. 104, p. 687-707, Nov. 2017.

Gómez-Estaca, J.; Montero, P.; Fernández-Martós, F.; Gímez-Guillín, M. C. Physico-chemical and film-forming properties of bovine-hide and tuna-skin gelatin: A comparative study. *Journal of Food Engineering*, v. 90, n. 4, p. 480–486, 2009.

Galdeano, M. C., Grossmann, M. V. E., Mali, S., Bello-Perez, L. A., Garcia, M. A., & Zamudio-Flores, P. B. (2009). Effects of production process and plasticizers on stability of films and sheets of oat starch. *Materials Science and Engineering C*, 29(2), 492–498.

Goffin, A.-L.; Raquez, J.-M.; Duquesne, E.; Siqueira, G.; Habibi, Y.; Dufresne, A., & Dubois, P. (2011). From Interfacial Ring-Opening Polymerization to Melt Processing of Cellulose Nanowhisker-Filled Polylactide-Based Nanocomposites. *Biomacromolecules*, 12(7), 2456–2465.

Gomez-Guillen, M. C., Gimenez, B., Lopez-Caballero, M. E., & Montero, M. P. (2011). Functional and bioactive properties of collagen and gelatin from alternative sources: A review. *Food Hydrocolloids*, 25(8), 1813–1827.

Gontard, N., Guilbert, S., & Cuq, J. L. (1993). Water and glycerol as plasticizers affect mechanical and water vapor barrier properties of an edible wheat gluten film. *Journal of Food Science*, 58(1), 206–211.

Hao Feng, Gustavo Barbosa-Canovas, J. W. Ultrasound technologies for food and bioprocessing. p. 218, Jochen, 2011.

Izidoro, D. R., Sierakowski, M. R., Haminiuk, C. W. I., De Souza, C. F., & Scheer, A. D. P. (2011). Physical and chemical properties of ultrasonically, spray-dried green banana (*Musa cavendish*) starch. *Journal of Food Engineering*, 104(4), 639–648.

Jambrak, A. R.; Herceg, Z.; Subaric, D.; Babic, J.; Brncic, M.; Brncic, S. R.; Bosiljkov, T.; Cvek, D.; Tripalo, B.; Gelo, J. Ultrasound effect on physical properties of corn starch. *Carbohydrate Polymers*, v. 79, n. 1, p. 91–100, 2010.

Jiang, S., Liu, C., Wang, X., Xiong, L., & Sun, Q. (2016). Physicochemical properties of starch nanocomposite films enhanced by self-assembled potato starch nanoparticles. *LWT - Food Science and Technology*, 69, 251–257.

Ke, T., Sun, S. X., & Seib, P. (2003). Blending of poly(lactic acid) and starches containing varying amylose content. *Journal of Applied Polymer Science*, 89(13), 3639–3646.

Kiatkamjornwong, S., Sonsuk, M., Wittayapichet, S., Prasassarakich, P., & Vejjajawiroth, P. C. (1999). Degradation of styrene-g-cassava starch filled polystyrene plastics. *Polymer Degradation and Stability*, 66(3), 323–335.

Kim, H. Y., Park, S. S., & Lim, S. T. (2015). Preparation, characterization and utilization of starch nanoparticles. *Colloids and Surfaces B: Biointerfaces*,

Krishna, M., Nindo, C. I., & Min, S. C. (2012). Development of fish gelatin edible films using extrusion and compression molding. *Journal of Food Engineering*, 108(2), 337–344.

Landim, P. A., M., Bernardo, C. O., Beatriz, I., Martins, A., Francisco, M. R., ... Ramos, N. (2016). Sustentabilidade quanto às embalagens de alimentos no Brasil Sustainability concerning food packaging in Brazil, 1–11.

Lautenschläger, B.I. 2001. Avaliação de embalagem de consumo com base nos requisitos ergonômicos informacionais. Florianópolis, SC. Dissertação de Mestrado. UFSC, 109 p. Le Corre, D., & Angellier-Coussy, H. (2014). Preparation and application of starch nanoparticles for nanocomposites: A review. *Reactive and Functional Polymers*, 85, 97–120.

Li, H., & Huneault, M. A. (2011). Comparison of sorbitol and glycerol as plasticizers for thermoplastic starch in TPS/PLA blends. *Journal of Applied*

Polymer Science, 119(4), 2439–2448.

- Li, J., Shin, G. H., Lee, I. W., Chen, X., & Park, H. J. (2016). Soluble starch formulated nanocomposite increases water solubility and stability of curcumin. *Food Hydrocolloids*, 56, 41–49.
- Li, X., Qiu, C., Ji, N., Sun, C., Xiong, L., & Sun, Q. (2015). Mechanical, barrier and morphological properties of starch nanocrystals-reinforced pea starch films. *Carbohydrate Polymers*, 121, 155–162.
- Liu, D., Wu, Q., Chen, H., & Chang, P. R. (2009). Transitional properties of starch colloid with particle size reduction from micro- to nanometer. *Journal of Colloid and Interface Science*, 339(1), 117–124.
- Liu, X. X., Wang, Y. F., Zhang, N. Z., Shanks, R. A., Liu, H. S., Tong, Z., ... Yu, L. (2014). Morphology and phase composition of gelatin-starch blends. *Chinese Journal of Polymer Science (English Edition)*, 32(1), 108–114.
- Loriot, C., Vannini, L., & Poustka, J. (2017). Testing of polybutylene succinate based films for poultry meat packaging a Vytej ckov a s V a, 60.
- Lourdin, D.; Coignard, L.; Bizot, H.; Colonna, P. Influence of equilibrium relative humidity and plasticizer concentration on the water content and glass transition of starch materials. *Polymer: The Chemistry, Physics And Technology Of High Polymer*, London, v.38, n.21, p.5401- 5406, Oct. 1997.
- Luckachan, G. E., & Pillai, C. K. S. (2011). Biodegradable Polymers- A Review on Recent Trends and Emerging Perspectives. *Journal of Polymers and the Environment*, 19(3), 637–676.
- Luzi, F., Fortunati, E., Jiménez, A., Puglia, D., Pezzolla, D., Gigliotti, G., ... Torre, L. (2015). Production and characterization of PLA_PBS biodegradable blends reinforced with cellulose nanocrystals extracted from hemp fibres. *Industrial Crops and Products*, 93, 276–289.
- Ma, P., Xu, P., Chen, M., Dong, W., Cai, X., Schmit, P., ... Lemstra, P. J. (2014). Structure–property relationships of reactively compatibilized PHB/EVA/starch blends. *Carbohydrate Polymers*, 108, 299–306.

- Ma, Q., Hu, D., & Wang, L. (2016). Preparation and physical properties of tara gum film reinforced with cellulose nanocrystals. *International Journal of Biological Macromolecules*, 86, 606–612.
- Mali, S., Grossmann, M. V. E., Garcia, M. A., Martino, M. N., & Zaritzky, N. E. (2002). Microstructural characterization of yam starch films. *Carbohydrate Polymers*, 50(4), 379–386.
- Mali, S., Grossmann, M. V. E., García, M. A., Martino, M. N., & Zaritzky, N. E. (2004). Barrier, mechanical and optical properties of plasticized yam starch films. *Carbohydrate Polymers*, 56(2), 129–135.
- Mali, S., Grossmann, M. V. E., García, M. A., Martino, M. N., & Zaritzky, N. E. (2005). Mechanical and thermal properties of yam starch films. *Food Hydrocolloids*, 19(1), 157–164.
- Mali, S., Grossmann, M. V. E., & Yamashita, F. (2010). Filmes de amido: Produção, propriedades e potencial de utilização. *Semina: Ciencias Agrarias*, 31(1), 137–156.
- Maliger, R. B., McGlashan, S. A., Halley, P. J., & Matthew, L. G. (2006). Compatibilization of starch–polyester blends using reactive extrusion. *Polymer Engineering & Science*, 46(3), 248–263.
- Malwela, T., & Sinha, S. (2015). International Journal of Biological Macromolecules Enzymatic degradation behavior of nanoclay reinforced biodegradable PLA / PBSA blend composites. *International Journal of Biological Macromolecules*, 77, 131–142.
- Manrich, S. Processamento de termoplásticos: rosca única, extrusão e matrizes, injeção e moldes. São Paulo: Artliber, 2005
- Mendes, J. F., Paschoalin, R. T., Carmona, V. B., Sena Neto, A. R., Marques, A. C. P., Marconcini, J. M., Oliveira, J. E. (2016). Biodegradable polymer blends based on corn starch and thermoplastic chitosan processed by extrusion. *Carbohydrate Polymers*, 137, 452–458.
- Mina-H, J., Valadez-G, A., & Toledano-T, T. (2013). Physico-Chemical Studied

of Thermoplastic Starch (TPS) and Polycaprolactone (PCL). *Biotecnología En El Sector Agropecuario Y Agroindustrial*, 2(2), 31–41.

Miranda, C. S., Ferreira, M. S., Magalhães, M. T., Santos, W. J., Oliveira, J. C., Silva, J. B. A., & José, N. M. (2015). Mechanical, Thermal and Barrier Properties of Starch-based Films Plasticized with Glycerol and Lignin and Reinforced with Cellulose Nanocrystals. *Materials Today: Proceedings*, 2(1), 63–69.

Miranda, V. R., & Carvalho, A. J. F. (2011). Blendas compatíveis de amido termoplástico e polietileno de baixa densidade compatibilizadas com ácido cítrico. *Polímeros*, 21(5), 353–360.

Mohanty, S., & Nayak, S. K. (2010). Starch based biodegradable PBAT nanocomposites: Effect of starch modification on mechanical, thermal, morphological and biodegradability behavior. *International Journal of Plastics Technology*, 13(2), 163–185.

Moon, R. J., Martini, A., Nairn, J., Simonsen, J., & Youngblood, J. (2011). *Cellulose nanomaterials review: structure, properties and nanocomposites*. *Chem. Soc. Rev. Chem. Soc. Rev* (Vol. 40).

Moraes, I., & Silva, G. (2008). Influência do grau de hidrólise do poli (vinil álcool) nas propriedades físicas de filmes à base de blendas de gelatina e poli (vinil álcool) plastificados com. *Ciência E Tecnologia*, 2008(2981), 738–745.

Mukerjea, R., Slocum, G., & Robyt, J. F. (2007). Determination of the maximum water solubility of eight native starches and the solubility of their acidic-methanol and -ethanol modified analogues. *Carbohydrate Research*, 342(1), 103–110.

Nasser, L. A. M., Maria, L., Lopes, X., & Monteiro, M. (2005). Oligômeros Em Embalagem De Pet Para Água Mineral E Suco De Fruta . Uma Revisão, 16(2), 183–194.

Nayak, S. K. (2010). Biodegradable PBAT/Starch Nanocomposites. *Polymer-Plastics Technology and Engineering*, 49(14), 1406–1418.

Nofar, M., Tabatabaei, A., Sojoudiasli, H., Park, C. B., Carreau, P. J., Heuzey, M., & Kamal, M. R. (2017). Mechanical and bead foaming behavior of PLA-PBAT and PLA-PBSA blends with different morphologies. *European Polymer Journal*, 90(March), 231–244.

Nossa, T. de S. Novas composições poliméricas obtidas a partir da modificação do amido por extrusão reativa. Tese (Doutorado em Engenharia de Materiais) USP, 2014.

Nur Hanani, Z. A., McNamara, J., Roos, Y. H., & Kerry, J. P. (2013). Effect of plasticizer content on the functional properties of extruded gelatin-based composite films. *Food Hydrocolloids*, 31(2), 264–269.

Nur Hanani, Z. A., Roos, Y. H., & Kerry, J. P. (2012). Use of beef, pork and fish gelatin sources in the manufacture of films and assessment of their composition and mechanical properties. *Food Hydrocolloids*, 29(1), 144–151.

Oliveira, T. A., Oliveira, R. R., Barbosa, R., Azevedo, J. B., & Alves, T. S. (2017). Effect of reprocessing cycles on the degradation of PP / PBAT-thermoplastic starch blends. *Carbohydrate Polymers*, 168, 52–60.

Pachekoski, W. M., & Dalmolin, C. (2014). Blendas Poliméricas Biodegradáveis de PHB e PLA para Fabricação de Filmes Biodegradable Polymeric Blends of PHB and PLA for Film Production, 24, 501–507.

Palsikowski, P. A. (2015). Estudo do comportamento da biodegradação em solo de blendas compatibilizadas de PLA/PBAT e seus efeitos genotóxicos e mutagênicos. 2015. 132 p. Dissertação (mestrado) - Universidade Estadual de Campinas, Faculdade de Engenharia Química, Campinas, SP.

Pellicano, M.; Pachekoski, W.; Agnelli, J. A. M. (2009) Influência da adição de amido de mandioca na biodegradação da blenda polimérica PHBV/ecoflex. *Polímeros*, v. 19, no.3, p. 212-217, 2009.

- Pelissari, F. M., Yamashita, F., & Grossmnn, M. V. E. (2011). Extrusion parameters related to starch/chitosan active films properties. *International Journal of Food Science & Technology*, 46(4), 702–710.
- Pereira, F. V., De Paula, E. L., De Mesquita, J. P., De Almeida Lucas, A., & Mano, V. (2014). Bionanocompósitos preparados por incorporação de nanocristais de celulose em polímeros biodegradáveis por meio de evaporação de solvente, automontagem ou eletrofiação. *Quimica Nova*, 37(7), 1209–1219.
- Pereira, V. A., de Arruda, I. N. Q., & Stefani, R. (2015). Active chitosan/PVA films with anthocyanins from Brassica oleraceae (Red Cabbage) as Time-Temperature Indicators for application in intelligent food packaging. *Food Hydrocolloids*, 43, 180–188.
- Petersson, M., & Stading, M. (2005). Water vapour permeability and mechanical properties of mixed starch-monoglyceride films and effect of film forming conditions. *Food Hydrocolloids*, 19(1), 123–132.
- Rajisha, K. R., Maria, H. J., Pothan, L. A., Ahmad, Z., & Thomas, S. (2014). Preparation and characterization of potato starch nanocrystal reinforced natural rubber nanocomposites. *International Journal of Biological Macromolecules*, 67, 147–153.
- Ramani, N., & Charles, P. (1999). Help define and grow a new biodegradable plastic industry. *ASTM Standardization News*, (December), 36–42.
- Reis, K. C., Pereira, J., Smith, A. C., Carvalho, C. W. P., Wellner, N., & Yakimets, I. (2008). Characterization of polyhydroxybutyrate-hydroxyvalerate (PHB-HV)/maize starch blend films. *Journal of Food Engineering*, 89(4), 361–369.
- Restuccia, D., Spizzirri, U. G., Parisi, O. I., Cirillo, G., Curcio, M., lemma, F., ... Picci, N. (2010). New EU regulation aspects and global market of active and intelligent packaging for food industry applications. *Food Control*, 21(11), 1425–1435.

- Rivero, S., García, M. A., & Pinotti, A. (2010). Correlations between structural, barrier, thermal and mechanical properties of plasticized gelatin films. *Innovative Food Science and Emerging Technologies*, 11(2), 369–375.
- Rodriguez-Gonzalez, F. J., Ramsay, B. A., & Favis, B. D. (2004). Rheological and thermal properties of thermoplastic starch with high glycerol content. *Carbohydrate Polymers*, 58(2), 139–147.
- Rudnik, E. (2008). *Compostable Polymer Materials*. 1º Ed. 224 pg.
- Sarazin, P., Li, G., Orts, W. J., & Favis, B. D. (2008). Binary and ternary blends of polylactide, polycaprolactone and thermoplastic starch. *Polymer*, 49(2), 599–609.
- Savadekar, N. R., & Mhaske, S. T. (2012). Synthesis of nano cellulose fibers and effect on thermoplastics starch based films. *Carbohydrate Polymers*, 89(1), 146–151.
- Scapim, M. R. da S. Produção, caracterização, aplicação e biodegradabilidade de filmes de blendas de amido e poli(butileno adipato co-tereftalato) produzidos por extrusão. Tese (Doutorado em Ciência de Alimentos) UEL, 2009
- Sebio, L. Desenvolvimento de plástico biodegradável a base de amido de milho e gelatina pelo processo de extrusão: avaliação das propriedades mecânicas, térmicas e de barreira. Tese (Doutorado em Engenharia de Alimentos) UNICAMP, 2003.
- Seligra, P. G., Moura, L. E., Famá, L., Druzian, J. I., & Goyanes, S. (2016). Influence of Incorporation of Starch Nanoparticles in PBAT/TPS Composites Films. *Polymer International*, (April).
- Shi, A. M., Wang, L. J., Li, D., & Adhikari, B. (2013). Characterization of starch films containing starch nanoparticles Part 1: Physical and mechanical properties. *Carbohydrate Polymers*, 96(2), 593–601.
- Shimazu, A. A., Mali, S., & Victória, M. V. E. (2007). Efeitos plastificante e antiplastificante do glicerol e do sorbitol em filmes biodegradáveis de

amido de mandioca Plasticizing and antiplasticizing effects of glycerol and sorbitol on biodegradable cassava starch films. *Semina: Ciências Agrárias*, 28(1), 79–88.

Shirai, M. A., Olivato, J. B., Demiate, I. M., Müller, C. M. O., Grossmann, M. V. E., & Yamashita, F. (2016). Poly(lactic acid)/thermoplastic starch sheets: effect of adipate esters on the morphological, mechanical and barrier properties. *Polímeros*, 26(1), 66–73.

Slavutsky, A. M., & Bertuzzi, M. A. (2014). Water barrier properties of starch films reinforced with cellulose nanocrystals obtained from sugarcane bagasse. *Carbohydrate Polymers*, 110, 53–61.

Soliman, E. A., & Furuta, M. (2014). Influence of Phase Behavior and Miscibility on Mechanical, Thermal and Micro-Structure of Soluble Starch-Gelatin Thermoplastic Biodegradable Blend Films. *Food and Nutrition Sciences*, 5(11), 1040–1055.

Stagner J.A., Alves, V.D. (2012). Application and Performance of Maleated Thermoplastic Starch–Poly(butylene adipate-co-terephthalate) Blends for Films. *Journal of Applied Polymer Science*, 126.

Sothornvit, R., Olsen, C. W., McHugh, T. H., & Krochta, J. M. (2007). Tensile properties of compression-molded whey protein sheets: Determination of molding condition and glycerol-content effects and comparison with solution-cast films. *Journal of Food Engineering*, 78(3), 855–860.

Stoyko Fakirov, D. B. *Handbook of engineering biopolymers: 'homopolymers, blends, and composites*. p.933, Hanser, 2007.

Tajuddin, S., Xie, F., Nicholson, T. M., Liu, P., & Halley, P. J. (2011). Rheological properties of thermoplastic starch studied by multipass rheometer. *Carbohydrate Polymers*, 83(2), 914–919.

Takinami, P. Y. I. Obtenção de Biopolímeros de Gelatina por Radiação Ionizante. Tese (Doutorado em Ciências na Área de Tecnologia Nuclear - Aplicações) IPEN, 2014.

Teixeira, E. de M., Pasquini, D., Curvelo, A. A. S., Corradini, E., Belgacem, M. N., & Dufresne, A. (2009). Cassava bagasse cellulose nanofibrils reinforced thermoplastic cassava starch. *Carbohydrate Polymers*, 78(3), 422–431.

Teixeira, E. M.; OLIVEIRA, C. R.; MATTOSO, L. H. C.; CORREA, A.C.; PALADIN, P. D. Nanofibras de algodão obtidos sob diferentes condições de hidrólise ácida. *Polímeros: Ciência e Tecnologia*, v. 20, n. 4, p. 264-268, 2010.

Teodoro, A. P., Mali, S., Romero, N., & De Carvalho, G. M. (2015). Cassava starch films containing acetylated starch nanoparticles as reinforcement: Physical and mechanical characterization. *Carbohydrate Polymers*, 126, 9–16.

Thakore, I. M., Desai, S., Sarawade, B. D., & Devi, S. (2001). Studies on biodegradability, morphology and thermo-mechanical properties of LDPE/modified starch blends. *European Polymer Journal*, 37(1), 151–160.

Thunwall, M., Kuthanová, V., Boldizar, A., & Rigdahl, M. (2008). Film blowing of thermoplastic starch. *Carbohydrate Polymers*, 71(4), 583–590.

Thuwall, M., Boldizar, A., & Rigdahl, M. (2006). Extrusion processing of high amylose potato starch materials. *Carbohydrate Polymers*, 65(4), 441–446.

Tongdeesoontorn, W., Mauer, L. J., Wongruong, S., Sriburi, P., & Rachtanapun, P. (2012). Mechanical and Physical Properties of Cassava Starch-Gelatin Composite Films. *International Journal of Polymeric Materials*, 61(October 2016), 778–792.

Van Soest, J. J. G., & Vliegenthart, J. F. G. (1997). Crystallinity in starch plastics: Consequences for material properties. *Trends in Biotechnology*, 15(6), 208–213.

Wei, D., Wang, H., Xiao, H., Zheng, A., & Yang, Y. (2015). Morphology and mechanical properties of poly(butylene adipate-co-terephthalate)/potato starch blends in the presence of synthesized reactive compatibilizer or

modified poly(butylene adipate-co-terephthalate). *Carbohydrate Polymers*, 123, 275–282.

Xie, F., Pollet, E., Halley, P. J., & Av??rous, L. (2013). Starch-based nano-biocomposites. *Progress in Polymer Science*, 38(10–11), 1590–1628.

Zainuddin, S. Y. Z., Ahmad, I., & Kargarzadeh, H. (2013). Cassava starch biocomposites reinforced with cellulose nanocrystals from kenaf fibers. *Composite Interfaces*, 20(3), 189–199.

Zullo, R., & Iannace, S. (2009). The effects of different starch sources and plasticizers on film blowing of thermoplastic starch: Correlation among process, elongational properties and macromolecular structure. *Carbohydrate Polymers*, 77(2), 376–383.

Wang, L.-F., Rhim, J-W, Hong, S-I. Preparation of poly(lactide)/poly(butylene adipate-co-terephthalate) blend films using a solvent casting method and their food packaging applicationLWT - Food Science and Technology 68 (2016) 454-461

APÊNDICE A

Curcumin loaded starch nanoparticles produced by solution mixing method

Abstract

Starch nanoparticles loaded with curcumin (CNP) were fabricated using a facile solution mixing method. Curcumin was encapsulated with 3 wt% loading of curcumin. In this concentration the results of mean diameter showed that the inclusion of curcumina an increase in the particles diameter and resulted PDI values hight. Zeta potential values of CNP was of the -14.66mv, which demonstrate lower stability of these nanoparticles. The encapsulation efficiency was 70% and Antioxidant capacity was of 35%. Differential scanning calorimetry and thermogravimetric analysis demonstrated interaction between starch and curcumin. X-ray diffraction showed disappearance of curcumin peaks and amorphous state of the CNP. The complete dissolution of CNP in water showed that these nanoparticle are an interesting option for application of curcumin in the food industry.

Keywords: Curcumin, starch, encapsulation.

1. Introduction

Curcumin is a yellow-orange a hydrophobic polyphenolic compound obtained from curcuma rhizomes, mainly *Curcuma longa* L. This compound has been associated with many pharmacological activities which include antiproliferative, anticancer, antiangiogenic, antidiabetic, antioxidant and antiinflammatory activities (Shome, Das, Dutta, & Kanti, 2016). In the food industry, the use of curcumin is restricted, as dyes in noodles, mustards, ice cream, cheeses and natural preservative in the treatment and preparation of foods such as pickles, Chips, margarines and meats and derivatives such as sausage. Due to the extremely low solubility in aqueous media which limits its use on a wider scale in food industry.

Different methods have been proposed and investigated with the aim of increasing its water solubility. Nanosystem represents one of the approaches more reported. Nevertheless, these systems are not suitable for food due to use of substances such as chloroform, surfactants, methylene chloride and others. Futhermore, the complicated preparation and hight cost render the majority of these methods inappropriate for food applications (Li, Shin, Lee, Chen, & Park, 2016). Methods without sophisticated fabrication and chemical modification and natural polymers based have been investigated (Aditya, Yang, Kim, & Ko, 2015; Esmaili et al., 2011; Patel, Heussen, Dorst, Hazekamp, & Velikov, 2013).

Polymeric nanoparticles are used in a variety of areas, such as food, cosmetics and pharmaceuticals (Lin, et al., 2011). In the food industry, these nanoparticles can be used as carriers for thermosensitive bioactive carriers, as mechanical reinforcement material in polymer films or even for improving the biodegradability and solubility of a given material.

The starch is the one of the most available natural polymers, presents an central role in human food, it is versatile, cheap and low cost. Recently, have been investigated its use for preparing emulsion and encapsulating hydrophobic compounds (Marefati, Dejmek, Rayner, Bertrand, & Sj, 2017; Yusoff & Murray, 2011). However, it is important highlight that researchs that report the use of starch to increase the functions of curcumin (solubility) as polymeric nanoparticle are recents and deserve attention.

In this context, the objective of this study was to produce curcumin loaded starch nanoparticles using a facile solution mixing method.

2. Methodology

Curcumin loaded starch nanoparticles (CNP) were produced according to the method adapted from (Li et al., 2016). Starch was dissolved in distilled water at the concentration of 5 mg/mL and heated at about 80°C to totally solubilize the starch. Then, curcumin ethanol solution (3 wt %) was pipetted slowly into the heated starch solution under stirring. Finally, colloidal suspension was sonicated at 50 W for 5 minutes and frozen and dried by freezing (lyophilization). Starch nanoparticles (SNP) without curcumin (same method) also were produced to compared the results.

The Figures 1a and 1b shows the colloidal suspension and curcumin loaded starch nanoparticles after lyophilization respectively.

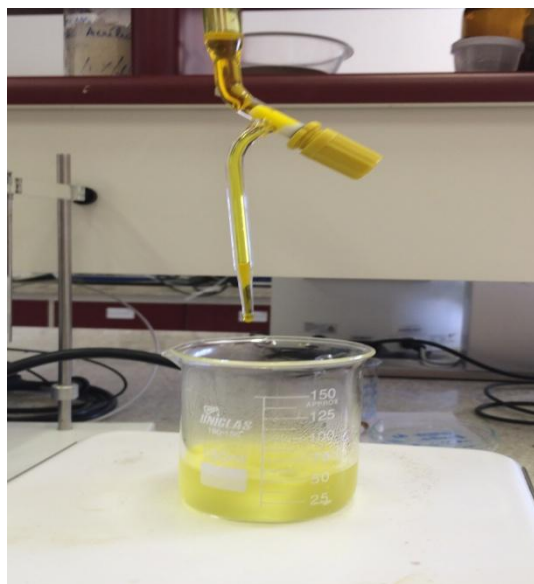


Figure 1a. Colloidal suspension.



Figure 1b. Curcumin loaded starch nanoparticles lyophilized.

2.1 Analysis

2.1.1 Mean diameter, polydispersity index and zeta potential

The mean diameter and size distribution were determined by dynamic light scattering using a Zetasizer Nano-ZS equipment (Malvern Instruments,

United Kingdom). Zeta potencial was also recorded on the same equipment. The reported values of the mean diameter are the average of the 3 (three) measures.

2.1.2 Loading ability and loading efficiency determination

The loading efficiency (LE) and loading ability (LA) were determined according to the (Su, Zhang, Wu, Tao, & Zang, 2010) and were determined using the following Equations 1 and 2.

$$LE = \frac{\text{detected curcumin weight}}{\text{original curcumin weight}} \times 100 \quad (1)$$

$$LA = \frac{\text{weight of curcumin}}{\text{weight of starch}} \times 100 \quad (2)$$

2.1.3 X-ray diffraction (XRD)

The measurement was conducted using a Rigaku, model Miniflex X-Ray Diffractometer (Japan), with a pace of 4°/min (SNP) or 2°/min (films) and copper radiation $\lambda = 1,5433 \text{ \AA}$, operating with 40 kV and a flow of 30 mA, scanning between 5°C and 40°C.

2.1.4 Thermal analysis

The thermogravimetric analysis (TGA) was made in a Perkin Elmer thermal analyzer, STA 6000 model (USA), assisted by Pyris Series software. In the tests for the CS, CNP and SNP of about 8 mg in an inert nitrogen atmosphere of 30mL/min were used, with a heat rate of 10°C/min, at a temperature interval of 25 to 600°C.

2.1.5 Antioxidant capacity

The 2, 2-Diphenyl-1-picrylhydrazyl (DPPH) was used to determine the free radical scavenging activity of CNP according to Kim et al. (2008) and Bitencourt et al. (2014). DPPH working solution was prepared by dissolving

DPPH reagent in ethanol at the concentration of 0.1 mM. To 4 mL of the above working solution, 1 mL of curcumin ethanoic solution or sample water solution was added and it was kept in the dark until the absorbance of the solution had stabilized (3h). Absorption at 517 nm was recorded on a UVvis spectrophotometer. The antioxidant capacity was calculated by using the equation 3:

$$\text{DPPH * scavenging effect (\%)} = \left[\left(\frac{\text{ABS}_{\text{DPPH}} - \text{ABS}_{\text{sample}}}{\text{ABS}_{\text{DPPH}}} \right) \right] \cdot 100 \quad (3)$$

Where ABS_{DPPH} = the absorbance of the DPPH radical solution and $\text{ABS}_{\text{sample}}$ = the absorbance of the sample.

2.1.5 Water solubility

The water solubility was determined according to (Li et al., 2016). 10 mg of nanoparticles was dissolved in 1 mL of distilled water and stirre for 30 min. Equally 0.279 mg of raw curcumin was dissolved in water.

3. Results and discussions

3.1 Mean diameter, polydispersity index (PDI) and zeta potential

In Table 1 the results of the mean diameter, population polydispersity index and SNP zeta potential are presented.

Table 1. Size, PDI, zeta potential values of the SNP and CNP.

Samples	Mean diameter (nm)	Population (%)	PDI	Zeta Potencial (mV)
SNP	92.57 \pm 8.39	93.1 \pm 4.33	0.2 \pm 0.01	-3.55 \pm 0.15
CNP	664.6 \pm 51.73	88.03 \pm 6.09	0.55 \pm 0.01	-14.66 \pm 0.17

*Values with different letters in the same column are significantly different ($p < 0.05$).

The SNP produced demonstrated a bimodal distribution with mean diameter ($D_{[4,3]}$) of approximately 92.57 ± 8.39 nm (93.1% of the major population). Meanwhile the curcumin loaded starch nanoparticles presented a

bimodal distribution with mean diameter ($D_{4,3}$) of 664.6 ± 51.73 nm (88.03% of the major population). This result indicates that the inclusion of curcumina caused an increase in the particles diameter and influenced PDI results, which were greater than 0.5 to this sample, indicating a relative heterogeneous dispersion (Gonçalves, Noreña, da Silveira, & Brandelli, 2014).

Zeta potential values of CNP (-14.66mv) were lower than that of SNP (-3.55 mv). This value can be indicate lower stability of curcumin loaded starch nanoparticles. It is believed that systems including nanoparticles, high zeta-potential value or its magnitude (negative or positive absolute value) usually means high degrees of stability (Li, Lee, Shin, Chen, & Park, 2015; Li, Shin, Chen, & Park, 2015).

3.2 Loading ability and loading efficiency determination

The low solubility of curcumin in aqueous means and its various health benefits make this lipophilic bioactive compound a target of numerous encapsulation studies. Different encapsulation methods and polimerics matrices have been tested (Bourbon, Cerqueira, & Vicente, 2016; Das, Kasoju, & Bora, 2010; Gandapu, Chaitanya, Kishore, Reddy, & Kondapi, 2011; Sari et al., 2015). In this work, the encapsulation efficiency was $70\% \pm 2.79$, different techniques and wall material can to influence the encapsulation efficiency. Furthermore, lower loading ability and efficiency than the theoretical values may be due to handling loss (Li et al. 2016).

3.3 X-ray diffraction (XRD)

The X-ray diffraction (XRD) patterns recorded for curcumin and CNP are shown in Figure 2. The curcumin exhibited sharp and intense peaks of crystallinity at 9.07° , 11.68° , 15.62° , 18.66° , 20.83° , 22° , 25.20° , 26.11° and 29.18° . On the other hand, diffractogram of CNP showed reduction in number of peak intensity as compared to the curcumin. According to Mangolim et al. (2014) when occurs the disappearance of curcumin peaks confirms the successful loading of curcumin into the nanoparticles.

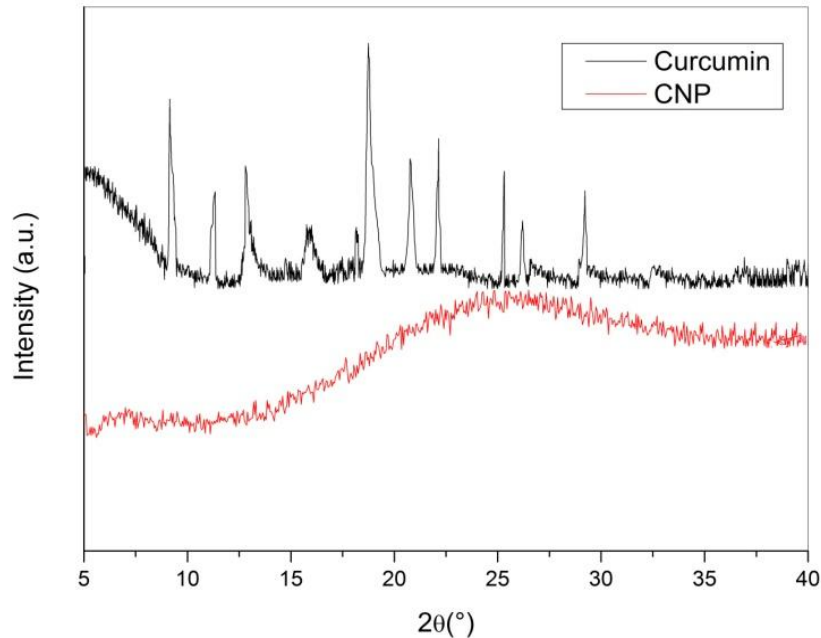


Figure 2. X-ray diffraction patterns for curcumin and curcumin loaded starch nanoparticles (CNP).

3.4 Thermal analysis

The thermal stability of curcumin and CNP are shown in Figure 3. The curcumin presents a single degradation process with a initial degradation temperature of 30°C and final degradation peak of 131.5°C (mass loss of 97.6%), this event has been related with the loss of volatile impurities during the melting of curcumin and with the loss of two water molecules owing to dehydroxylation of OH groups However, for CNP the thermogram curve shows three step degradation processes. There is an initial mass loss between 24 and 73°C followed by second stage of mass loss between 294–352°C and third stage between 469–500°C. Such result demonstrate that the curcumin loaded starch nanoparticles presents hight thermal stability when comparated to curcumin. This occurred probably due to the interaction of the colorant with the starch protecting the compound (DELGADO; VELÁSQUEZ, MOLINA, 2016).

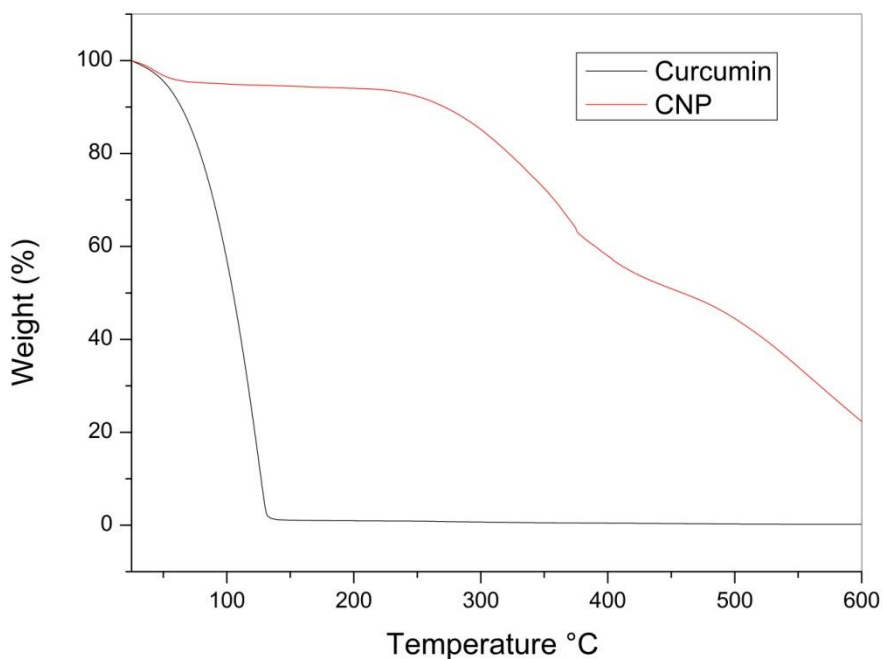


Figure 3. Thermogravimetric analysis (TG) of curcumin and curcumin loaded starch nanoparticles (CNP).

3.5 Antioxidant capacity

DPPH free radical scavenging method is based on the spectrophotometric determination of the radicals resulting from the reactions between DPPH radical and the antioxidant agent (hydrogen or electron donors) (Bitencourt, Fávaro-Trindade, Sobral, & Carvalho, 2014; Dawidowicz, Wianowska, & Olszowy, 2012; Re et al., 1999), it is reduced in the presence of curcumin, which decreases its coloring. Curcumin has high antioxidant ability and can effectively scavenge radicals like DPPH. However, it is very important for the curcumin loaded nanocomposite to retain the antioxidant ability and effectively release curcumin for reducing radicals (Neo et al., 2013).

The DPPH radical-scavenging activity of the curcumin was 84%, the antioxidant activity of curcumin due to mainly from the phenolic hydroxyl and a small fraction may result because of the single bond CH₂ single bond site (Priyadarsini et al., 2003). However, the CNP presented antioxidant activity of 35%. This result may be related to fact of both samples have been submitted the same time (3 hours) of stabilization. According to Jafari; Sabahi; Rahae

(2016), the encapsulated curcumin requires a more time to leach out into the DPPH solution for the scavenging activity, which may have influenced the result of this work.

3.6 Water solubility

The CNP were fully dissolved in water and no precipitate was observed after storage in refrigerator at 8°C for 24 h. The low solubility of curcumin is due to by its crystal nature and high hydrophobicity. In crystal state, curcumin forms both inter and intramolecular hydrogen bonding which inhibits curcumin dissolving in the aqueous solution. However, the curcumin loaded starch nanoparticles (amorphous character) are hydrophilic which allows for a greater interaction with the aqueous solvent and thus result in the increase of curcumin solubility in aqueous media (Chin, Mohd Yazid, & Pang, 2014; Li, Lee, et al., 2015; Vukićević & Tønnesen, 2015). Photographical images of curcumin and CNP, after storage in refrigerator, are shown in Figure 5.

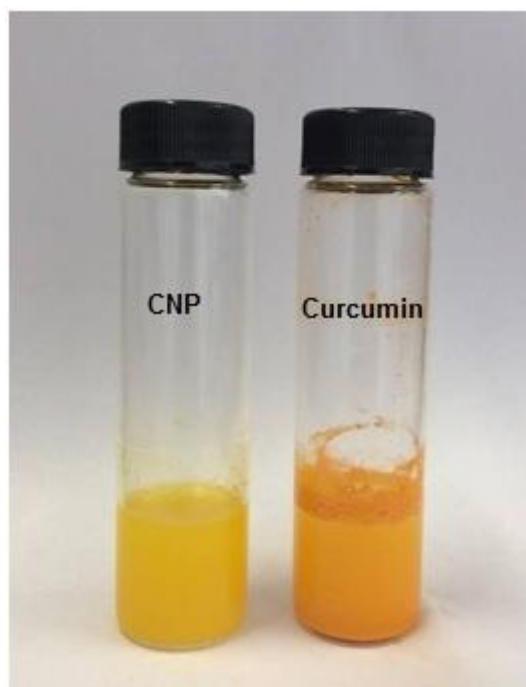


Figure 5. Photographical images of curcumin and CNP.

3 Conclusions

Curcumin loaded starch nanoparticles were successfully prepared using a facile solution mixing method. Encapsulation ability and efficiency was satisfactory. The thermal analysis showed that the CNP are more thermally stable when compared to curcumin. DSC analysis showed interaction between starch and curcumin. Furthermore, water solubility was greatly increased compared with curcumin due to amorphous character of CNP demonstrated by XRD analysis, which suggest that curcumin loaded starch nanoparticles can be used in food.

References

- Aditya, N. P., Yang, H., Kim, S., & Ko, S. (2015). Fabrication of amorphous curcumin nanosuspensions using β -lactoglobulin to enhance solubility, stability, and bioavailability. *Colloids and Surfaces B: Biointerfaces*, 127, 114–121.
- Athira, G. K., & Jyothi, A. N. (2015). Cassava starch-poly(vinyl alcohol) nanocomposites for the controlled delivery of curcumin in cancer prevention and treatment. *Starch - Stärke*, 67(5–6), 549–558.
- Bitencourt, C. M., Fávaro-Trindade, C. S., Sobral, P. J. A., & Carvalho, R. A. (2014). Gelatin-based films additivated with curcuma ethanol extract: Antioxidant activity and physical properties of films. *Food Hydrocolloids*, 40, 145–152.
- Bourbon, A. I., Cerqueira, M. A., & Vicente, A. A. (2016). Encapsulation and controlled release of bioactive compounds in lactoferrin-glycomacropeptide nanohydrogels: Curcumin and caffeine as model compounds. *Journal of Food Engineering*, 180, 110–119.
- Chin, S. F., Mohd Yazid, S. N. A., & Pang, S. C. (2014). Preparation and characterization of starch nanoparticles for controlled release of curcumin. *International Journal of Polymer Science*, 2014(January).

- Das, R. K., Kasoju, N., & Bora, U. (2010). Encapsulation of curcumin in alginate-chitosan-pluronic composite nanoparticles for delivery to cancer cells. *Nanomedicine: Nanotechnology, Biology and Medicine*, 6(1), 153–160.
- Dawidowicz, A. L., Wianowska, D., & Olszowy, M. (2012). On practical problems in estimation of antioxidant activity of compounds by DPPH method (Problems in estimation of antioxidant activity). *Food Chemistry*, 131(3), 1037–1043.
- Delgado, A. Y. C., & Alonso, Héctor José Ciro Velásquez, D. A. R. M. (2016). Thermal and thermodynamic characterization of a dye powder from liquid turmeric extracts by spray drying, 69(1), 7845–7854.
- Esmaili, M., Ghaffari, S. M., Moosavi-Movahedi, Z., Atri, M. S., Sharifizadeh, A., Farhadi, M., ... Moosavi-Movahedi, A. A. (2011). Beta casein-micelle as a nano vehicle for solubility enhancement of curcumin; food industry application. *LWT - Food Science and Technology*, 44(10), 2166–2172.
- Gandapu, U., Chaitanya, R. K., Kishore, G., Reddy, R. C., & Kondapi, A. K. (2011). Curcumin-Loaded Apotransferrin Nanoparticles Provide Efficient Cellular Uptake and Effectively Inhibit HIV-1 Replication In Vitro. *PLoS ONE*, 6(8), e23388.
- Gonçalves, P. M., Noreña, C. P. Z., da Silveira, N. P., & Brandelli, A. (2014). Characterization of starch nanoparticles obtained from Araucaria angustifolia seeds by acid hydrolysis and ultrasound. *LWT - Food Science and Technology*, 58(1), 21–27.
- Jafari, Y., Sabahi, H., & Rahaie, M. (2016). Stability and loading properties of curcumin encapsulated in Chlorella vulgaris. *Food Chemistry*, 211, 700–706.
- Li, J., Lee, I. W., Shin, G. H., Chen, X., & Park, H. J. (2015). Curcumin-Eudragit?? e PO solid dispersion: A simple and potent method to solve the problems of curcumin. *European Journal of Pharmaceutics and Biopharmaceutics*, 94, 322–332.

- Li, J., Shin, G. H., Chen, X., & Park, H. J. (2015). Modified curcumin with hyaluronic acid: Combination of pro-drug and nano-micelle strategy to address the curcumin challenge. *Food Research International*, 69, 202–208.
- Li, J., Shin, G. H., Lee, I. W., Chen, X., & Park, H. J. (2016). Soluble starch formulated nanocomposite increases water solubility and stability of curcumin. *Food Hydrocolloids*, 56, 41–49.
- Mangolim,C. S., Moriwaki, C., Claudia, A., Sato, F., Luciano, M., Medina, A., & Matioli, G. (2014). Curcumin – b -cyclodextrin inclusion complex : Stability , solubility , characterisation by FT-IR , FT-Raman , X-ray diffraction and photoacoustic spectroscopy , and food application, 153, 361–370.
- Marefati, A., Dejmek, P., Rayner, M., Bertrand, M., & Sj, M. (2017). Storage and digestion stability of encapsulated curcumin in emulsions based on starch granule Pickering stabilization € o, 63, 309–320.
- Neo, Y. P., Ray, S., Jin, J., Gizdavic-Nikolaidis, M., Nieuwoudt, M. K., Liu, D., & Quek, S. Y. (2013). Encapsulation of food grade antioxidant in natural biopolymer by electrospinning technique: A physicochemical study based on zein–gallic acid system. *Food Chemistry*, 136(2), 1013–1021.
- Patel, A. R., Heussen, P. C. M., Dorst, E., Hazekamp, J., & Velikov, K. P. (2013). Colloidal approach to prepare colour blends from colourants with different solubility profiles. *Food Chemistry*, 141(2), 1466–1471.
- Priyadarsini, K. I., Maity, D. K., Naik, G. H., Kumar, M. S., Unnikrishnan, M. K., Satav, J. G., & Mohan, H. (2003). Role of phenolic O-H and methylene hydrogen on the free radical reactions and antioxidant activity of curcumin. *Free Radical Biology and Medicine*, 35(5), 475–484.
- Re, R., Pellegrini, N., Proteggente, A., Pannala, A., Yang, M., & Rice-Evans, C. (1999). Antioxidant activity applying an improved ABTS radical cation decolorization assay. *Free Radical Biology and Medicine*, 26(9–10), 1231–1237.

- Sari, T. P., Mann, B., Kumar, R., Singh, R. R. B., Sharma, R., Bhardwaj, M., & Athira, S. (2015). Preparation and characterization of nanoemulsion encapsulating curcumin. *Food Hydrocolloids*, 43, 540–546.
- Shome, S., Das, A., Dutta, M., & Kanti, M. (2016). Curcumin as potential therapeutic natural product: a nanobiotechnological perspective, 68, 1481–1500.
- Su, Z. Q., Zhang, H. L., Wu, S. H., Tao, Y., & Zang, L. Q. (2010). Preparation and characterization of water-soluble chitosan nanoparticles as protein delivery system. *Journal of Nanomaterials*, 2010.
- Vukićević, M., & Tønnesen, H. H. (2015). Interaction between curcumin and human serum albumin in the presence of excipients and the effect of binding on curcumin photostability. *Pharmaceutical Development and Technology*, 1–9.
- Yusoff, A., & Murray, B. S. (2011). Modified starch granules as particle-stabilizers of oil-in-water emulsions. *Food Hydrocolloids*, 25(1), 42–55.

APENDICE B

Production and Characterization of Starch Nanoparticles

Normane Mirele Chaves Da Silva¹, Fernando Freitas de Lima², Rosana Lopes Lima Fialho¹, Elaine Christine de Magalhães Cabral Albuquerque¹, José Ignacio Velasco³ and Farayde Matta Fakhouri^{3,4*}

*Address all correspondence to: farayde@gmail.com

¹ Polytechnic School, Federal University of Bahia, Salvador, BA, Brazil

² School of Chemical Engineering, University of Campinas, Campinas, SP, Brazil

³ ESEIAAT, Universitat Politècnica de Catalunya - Barcelona TECH, Barcelona, Spain

⁴ Faculty of Engineering, Federal University of Grande Dourados, Dourados, MS, Brazil

Abstract

In recent years, the increasing interest in nanomaterials of natural origin has led to several studies in the area of nano-sized particles from natural polysaccharide polymers, such as cellulose, starch, and chitin. These nanomaterials are used especially as a reinforcement in a polymeric matrix to improve the mechanical and barrier properties of the materials. Starch is a sustainable, abundant biopolymer produced by many plants as a source of

storage energy; the main uses of starch are as food and industrial applications. However, recently their use as filler in polymeric matrix (nanoparticles) has attracted attention. Starch nanoparticles (SNPs) can be produced by many methods, using chemical, enzymatic, and physical treatments. The size distribution, crystalline structure, and physical properties of the SNPs may vary from one method to another. These nanoparticles are a very interesting alternatives not only for the polymeric filler but also for the renewability and biodegradability, since they show characteristics inherently of starch granules.

Keywords: methods, nanostarch, nanotechnology

1. Introduction

Nanotechnology is considered a study which involves science, medical, engineering, and ranging from 1 to 100 nm size [1]. In recent years, the use of nanotechnology for applications in the food industry has become more apparent, such as protection against biological and chemical deterioration, increasing bioavailability, enhancement of physical properties, and others [2]. However, the high cost of nanotechnology can make it difficult to its application in commercial scale. Therefore, the search for alternative materials and cheap to be used in the nanotechnology has been studied. Starch being a biodegradable natural polymer is a great alternative for the production of nanocrystals or nanoparticles. These materials can be produced by different methods, using chemical, enzymatic, and physical treatments and may be utilized as drug carriers, quality indicator for food products (nanoencapsulation), and reinforcement biodegradable and nonbiodegradable polymeric matrices [3].

2. Production and characterization methods of starch nanoparticles

The acid hydrolysis is the most commonly adopted method to produce starch nanocrystals (SNC). Usually, the starches submitted to this method have a two-step hydrolysis reaction: in the first step, a fast hydrolysis occurs, and in the second step, a slow hydrolysis occurs. For some authors there are three important steps of the acid hydrolysis: rapid, slow, and very slow [4–6]. In the first stage, the hydrolysis of the amorphous parts of the granules are attacked, while the slow step is the erosion of the crystalline regions [7]. Starch

nanocrystals produced for this method present high crystallinity and a platelet-like shape. In this process, starch is diluted in acid (hydrochloric or sulfuric) maintained under constant stirring for a prolonged period with temperature control. After the hydrolysis period, the nanocrystals are differentiated from the acid by centrifugation and washed with distilled water until neutrality of the eluent. Finally, for a homogeneous dispersion of the nanocrystals, the suspension is submitted to a mechanical procedure (ULTRA-TURRAX).

The botanic origin of starch influences the thickness of SNC, which can vary between 4 nm for wheat starch and 8 nm for potato starch and crystalline organization and consequently the size of SNC. This is related to the fact that the acid hydrolysis occurs in the amylose molecules of the starch granules, and depending on the botanic origin of starch, it can be occurred in different sites of granule structure, for example, in the amorphous region (wheat starch), interspersed among amylopectin clusters in both the crystalline and amorphous regions (maize starch), and in bundles between amylopectin clusters or co-crystallized with amylopectin (potato starch) [3]. Thus, depending on the crystalline organization (amylose content), SNC can present larger sizes, since amylose is believed to jam the pathways for hydrolysis. Generally, SNC presents platelet-like morphology.

The lengthy duration of the acid hydrolysis (until 40 days) implies in a low yield (around 5%) [6]. Thus, this method is not appropriate for practical applications due to the long treatment period, its low yield, and use of concentrated acid, which can cause a negative impact on the environment.

The study carried out by Gonçalves et al. [8] using the acid hydrolysis method used to modify the starch extracted from the crude seeds of the pinhão (*Araucaria angustifolia*) was effective, resulting in nanometric particles. The starch modified by this method showed the greatest differences compared to common starch, being the most soluble, translucent, and hygroscopic among the samples. The authors conclude that the greater solubility and reduced turbidity are interesting from a commercial standpoint, showing that pinhão starch nanoparticles could be useful for the development of coating materials or films. In another study, the method showed an ability to form a strong elastic gel

of starch nanocrystals [9]. Some recent studies by production of nanostarch by acid hydrolysis can be observed in **Table 1**.

Gamma radiation (γ -radiation) can be used to develop starch nanoparticles, since this technique can break large molecules into smaller fragments and is capable of cleaving glycosidic linkages. The technique consists in mixing starch and boiling water by stirring it for obtaining a homogenous paste, and then the suspension is irradiated using gamma ray, which generates active free radicals that are then responsible for the hydrolysis of starch. The fragmentation of starch results from the cleavage at the amorphous regions, instead of at the crystallite regions. In this sense, the gamma radiation method is very similar to that of the starch acid hydrolysis. Generally, the diameter of the nanoparticles obtained by this method is below 100 nm. Besides that, these nanoparticles also have nanocrystal aggregates, due to the large number of OH groups on their surface, which becomes strongly associated by hydrogen bonding, leading to fast thermal degradation [14]. The researches involving this method are still scarce and do not report the yield of process, which prevents the comparison with other methods.

Gamma radiation research demonstrates satisfactory results in the characterization and production of starch nanoparticles from cassava and waxy maize; the average sizes determined were (31 ± 5) nm and (41 ± 7) nm, respectively. The study shows that gamma radiation is a successful methodology to obtain starch nanoparticles able to be used as starch reinforcement and as a good alternative to production of starch nanoparticles, with low cost and using a simple and scalable methodology [14]. Gonzales Seligra et al. [28] also obtained average sizes less than 100 nm by producing starch nanoparticles by this same method. The insertion (0.6 wt%) of these nanoparticles in PBAT/TPS films improved the mechanical properties of the blend.

Starch source	Time of reaction (days)	Size or Size Distribution (nm)	Yield (%)	Morphology	Reference
Amaranth	10	376	3.6	Lamellar structure	Sanchez de la Concha et al. 121

					2018
Waxy maize	5	58	-	Platelet	Bel Haaj et al. 2016
Cassava	5	47-178	30	Spherical	Costa et al. 2017
Amadumbe	5	180-280	25	Platelet	Mukurumbira et al. 2017

Table 1. Starch source, time of reaction (days), size or size distribution (nm), yield (%), and morphology found in different studies on obtaining nanostarchs by acid hydrolysis.

The production of starch nanoparticles (SNPs) using physical treatments is still recent, with high-pressure homogenization and ultrasound treatment being more utilized methods. In these methods, there are no chemical treatments or addition of chemical reagents. Some advantages of these methods are that they are simple, effective, and environmentally friendly. Besides that, they might reduce the processing time to generate SNPs, increase the yield in NP production, and avoid various purification steps such as the acid hydrolysis [15]. In this context, ultrasound treatment shows up as a viable alternative. The method consists in sonication a starch suspension (starch and water) with controlled temperature for a fixed time, using ultrasound equipment. During the ultrasonication occurs a transfer the energy for to starch particles by cavitation, which is the collapse of microbubbles that burst and propagate as a sound wave through the solution. So microjets are formed with high velocities resulting the shear forces which may break covalent bonds of the starch and reduce the particle size. The ultrasonication process influences the crystalline structure of the starch (amylopectin), leading to nanoparticles with low crystallinity or an amorphous character. The ultrasonication in the starch can be affected by many factors such as ultrasonication power and frequency, time, and treatment temperature, besides the characteristics of starch dispersions, which are the concentration and botanical origin of starch and the dispersion solvent. Thus, the starch nanoparticles obtained for this method also can vary; for example, the size of the nanoparticles may vary between 30 nm and 200 nm. Some studies can be observed in **Table 2**.

The high-pressure homogenization is commonly in the chemical, pharmaceutical, food, and biotechnology industries. In this treatment, changes

not only in the products but also in the particles, colloids, or macromolecules which are product constituents may occur. Thus, novel applications for the high-pressure homogenization are researched [17] between the productions of starch nanoparticles. The method consists of the manipulation of a continuous flow of liquid through microfabricated channels; the starch slurry is passed by a microfluidizer, which can be intensified by external pressure sources, external mechanical pumps, integrated mechanical micropumps, or electrokinetic mechanisms, which result in the breakage of the hydrogen bonding inside the large particles by the mechanical shear forces. Homogenization pressures can reach up to 350 MPa. The nanoparticles obtained by this method may vary by 10 nm in size. In this method, the partial or complete destruction of the crystalline structure can also occur, and only a low concentration of starch slurry could be processed for homogenization.

Starch source	Concentration (w/t%)	Power (W)	Size or Size Distribution (nm)	Morphology	Reference
Waxy maize	2.0	400	40.0	Platelet	Boufi et al. 2018
Cassava	1.5	50	75.51	Spherical	Silva et al. 2017
Pinhão	20.0	100	454.3	Concave	Gonçalves et al. 2014
Potato	3.0	100	77.0	Spherical	Chang et al. 2017
Waxy maize	1.5	136	100-200	-	Bel Haaj et al. 2013

Table 2. Starch source, concentration (wt%), power (W), and size or size distribution (nm) found in different studies on obtaining nanostarchs by ultrasound treatment.

Recently, studies involving the ultrasound treatment and high-pressure homogenization methods show the development of nanoparticles of starch with nanometric scale sizes and the ability to form films [8, 18, 19]. The use of the ultrasound treatment method in pinhão (*Araucaria angustifolia*) seeds can be useful for the development of novel biocomposites, with improved properties to be employed such as coating materials or films [8]. In other researches, the study not only shows an easily controllable methodology to prepare starch

nano¹particles of small size and narrow distribution through precipitation but also provides an approach to produce starch nanoparticles with high efficiency and low cost, decreasing in viscosity of starch aqueous paste and not requiring any chemical treatment [18, 20].

The high-pressure homogenization researches have shown results of starch nanoparticles analyzed by transmission electron microscopy (TEM) and dynamic light scattering (DLS), which showed that starch nanoparticles had narrow size distribution, high dispersibility, and spherical shape [21] and films obtained from high-pressure homogenized dispersions had good moisture barrier capacity, better film transparency, and higher tensile strength but, however, lower elongation [19].

The utilization of the starch nanoparticles as polymeric filler is recent; however, the researchers showed satisfactory results. The nanoparticle presents at least one of its dimensions which is lower than 100 nm; thus, this nanometric dimension may result in a better dispersion and compactness of polymeric structure. The insertion of starch nanoparticle in a polymer results a new material, known as nanocomposite, with great properties that are not seen in traditional composites.

The incorporation of SNPs improves the mechanical properties and water vapor permeability (WVP) and also the biodegradability of the composites. The decrease in the WVP of nanocomposite films is attributed to compactness of the polymeric structure which is resulting in water vapor diffusion more difficult and consequently reducing permeability; in case the reinforcement is derived from the same material as the matrix, such as starch nanocrystals dispersed in starch films, it could have better compatibilization, since they show characteristics inherently from starch granules. It is worth pointing out that the concentration of starch nanoparticle inserted in a matrix polymeric must be carefully analyzed, once a lower nanoparticle concentration leads to better dispersion in the films and less clustering that hinders the passage of water and reduces permeability. On the other hand, the increase in WVP with a higher concentration of the SNPs can be related with a more nanoparticle grouping allowing diffusion of water molecules. Recently, some studies involving the use of SNP as filler in starch films showed that when the concentration of SNPs

inserted was less than 6%, the WVP presented a reduction. However, these same studies showed the use of a higher concentration of the SNPs resulting in an increase in WVP [22, 23]. The increase in WVP is not feasible for food packaging use; it offers increased food degradation rate. The WVP values are essential for the possible packaging application use of the biofilms. The material that where very permeable to water vapor may be suitable for the packaging of fresh food, whereas a slightly permeable biofilm may be useful for the packaging of dehydrated food [24].

The mechanical properties are proven be one the most important parameters for biofilm analysis, which usually presented poor mechanical properties. One alternative for improving these properties is the use of starch nanoparticle as reinforcement agent. For the mechanical properties, also the nanometric dimension of the starch nanoparticles can result in strong interactions with different matrices, once they have the capacity of occupying inter- or intramolecular space, resulting in densification of the film [25]. Besides that, the nanoparticle presents high specific surface area which can result in a better between filler and polymeric matrix interfacial interaction, which result in an increase of the nanocomposite strength [26]. So, the polymeric film incorporated with the SNP can present an increase in the tensile strength and modulus of elasticity, associated with decrease in the elongation percentage. These effects are heavily dependent on the SNP concentrations incorporated in the nanocomposites, because high concentrations of SNPs when incorporated in a matrix can cause aggregation, which leads to weaken the interface adhesion between the nanoparticle and matrix [27]. Li et al. [22] studied the incorporation of starch nanocrystals (SNC) in pea starch films. The authors concluded the concentrations bigger than 5% of SNC when incorporated in the films resulted in a decreased tensile strength associated with increase in elastic modulus.

Besides that, SNPs can speed up the biodegradation process. The influence of the SNP in the faster biodegradability of the composites is due to the fact that in soil, water diffuses into the polymer sample, causing swelling and enhancing biodegradation due to increases in microbial growths [28]. Costa et al. [12] studied the use of cassava starch nanocrystals (CSN) obtained by

acid hydrolysis to strengthen nanocomposite films from the same matrix. The authors conclude that the large percentage of loss of film mass was found over the biodegradability test and the film with 10% CSN showed a larger weight loss, which is probably associated with greater microorganism access.

Acknowledgements

The authors thank the Conselho Nacional de Desenvolvimento Científico e Tecnológico (CNPq) and the Coordenação de Aperfeiçoamento de Pessoal de Nível Superior (CAPES).

Conflict of interest

The authors declare no conflicts of interest.

References

- [1] Bera A, Belhaj H. Application of nanotechnology by means of nanoparticles and nanodispersions in oil recovery—A comprehensive review. *Journal of Natural Gas Science and Engineering*. 2016;34:1284-1309
- [2] He X, Hwang HM. Nanotechnology in food science: Functionality, applicability, and safety assessment. *Journal of Food and Drug Analysis*. 2016;24:671-681
- [3] Le Corre D, Angellier-Coussy H. Preparation and application of starch nanoparticles for nanocomposites: A review. *Reactive and Functional Polymers*. 2014;85:97-120
- [4] Putaux JL, Molina-Boisseau S, Momaur T, et al. Platelet nanocrystals resulting from the disruption of waxy maize starch granules by acid hydrolysis. *Biomacromolecules*. 2003;4:1198-1202
- [5] Angellier H, Putaux JL, Molina-Boisseau S, et al. Starch nanocrystal fillers in an acrylic polymer matrix. In: Macromolecular Symposia. 2005. pp. 95-104
- [6] Le Corre D, Bras J, Dufresne A. Starch nanoparticles: A review. *Biomacromolecules*. 2010;11:1139-1153

- [7] Kim HY, Park SS, Lim ST. Preparation, characterization and utilization of starch nanoparticles. *Colloids and Surfaces B: Biointerfaces*. 2015; **126**:607-620
- [8] Gonçalves PM, Noreña CPZ, da Silveira NP, et al. Characterization of starch nanoparticles obtained from Araucaria angustifolia seeds by acid hydrolysis and ultrasound. *LWT—Food Science and Technology*. 2014; **58**:21-27
- [9] Jiang S, Liu C, Han Z, et al. Evaluation of rheological behavior of starch nanocrystals by acid hydrolysis and starch nanoparticles by self-assembly: A comparative study. *Food Hydrocolloids*. 2016; **52**:914-922
- [10] de la Concha BBS, Agama-Acevedo E, Nuñez-Santiago MC, et al. Acid hydrolysis of waxy starches with different granule size for nanocrystal production. *Journal of Cereal Science*. 2018; **79**:193-200
- [11] Bel Haaj S, Thielemans W, Magnin A, et al. Starch nanocrystals and starch nanoparticles from waxy maize as nanoreinforcement: A comparative study. *Carbohydrate Polymers*. 2016; **143**:310-317
- [12] Costa ÉK de C, de Souza CO, da Silva JBA, et al. Hydrolysis of part of cassava starch into nanocrystals leads to increased reinforcement of nanocomposite films. *Journal of Applied Polymer Science*; 134. Epub ahead of print 2017. DOI: 10.1002/app.45311
- [13] Mukurumbira A, Mariano M, Dufresne A, et al. Microstructure, thermal properties and crystallinity of amadumbe starch nanocrystals. *International Journal of Biological Macromolecules*. 2017; **102**:241-247
- [14] Lamanna M, Morales NJ, Garcia NL, et al. Development and characterization of starch nanoparticles by gamma radiation: Potential application as starch matrix filler. *Carbohydrate Polymers*. 2013; **97**:90-97
- [15] Boufi S, Bel Haaj S, Magnin A, et al. Ultrasonic assisted production of starch nanoparticles: Structural characterization and mechanism of disintegration. *Ultrasonics Sonochemistry*. 2018; **41**:327-336
- [16] da Silva NMC, Correia PRC, Druzian JI, et al. PBAT/TPS composite films reinforced with starch nanoparticles produced by ultrasound. *International Journal of Polymer Science*. 2017;1-10
- [17] Wei B, Cai C, Xu B, et al. Disruption and molecule degradation of waxy maize starch granules during high pressure homogenization process. *Food Chemistry*. 2018; **240**:165-173

- [18] Chang Y, Yan X, Wang Q, et al. High efficiency and low cost preparation of size controlled starch nanoparticles through ultrasonic treatment and precipitation. *Food Chemistry*. 2017;227:369-375
- [19] Fu ZQ, Wang LJ, Li D, et al. Effects of high-pressure homogenization on the properties of starch-plasticizer dispersions and their films. *Carbohydrate Polymers*. 2011;86:202-207
- [20] Bel Haaj S, Magnin A, Pétrier C, et al. Starch nanoparticles formation via high power ultrasonication. *Carbohydrate Polymers*. 2013;92:1625-1632
- [21] Shi AM, Li D, Wang LJ, et al. Preparation of starch-based nanoparticles through highpressure homogenization and miniemulsion cross-linking: Influence of various process parameters on particle size and stability. *Carbohydrate Polymers*. 2011;83:1604-1610
- [22] Li X, Qiu C, Ji N, et al. Mechanical, barrier and morphological properties of starch nanocrystals-reinforced pea starch films. *Carbohydrate Polymers*. 2015;121:155-162
- [23] Jiang S, Liu C, Wang X, et al. Physicochemical properties of starch nanocomposite films enhanced by self-assembled potato starch nanoparticles. *LWT—Food Science and Technology*. 2016;69:251-257
- [24] Pagno CH, Costa TMH, De Menezes EW, et al. Development of active biofilms of quinoa (*Chenopodium quinoa W.*) starch containing gold nanoparticles and evaluation of antimicrobial activity. *Food Chemistry*. 2015;173:755-762
- [25] Shi Y, Jiang S, Zhou K, et al. Influence of g-C₃N₄ nanosheets on thermal stability and mechanical properties of biopolymer electrolyte nanocomposite films: A novel investigation. *ACS Applied Materials & Interfaces*. 2014;6:429-437
- [26] Wetzel B, Haupert F, Zhang MQ. Epoxy nanocomposites with high mechanical and tribological performance. *Composites Science and Technology*. 2003;63:2055-2067
- [27] Dai L, Qiu C, Xiong L, et al. Characterisation of corn starch-based films reinforced with taro starch nanoparticles. *Food Chemistry*. 2015;174:82-88

[28] González Seligra P, Eloy Moura L, Famá L, et al. Influence of incorporation of starch nanoparticles in PBAT/TPS composite films. Polymer International. 2016;65:938-945

APÊNDICE C

Figura 1 - Espectros de FTIR –ATR dos filmes de PBAT, PBAT/TPS e incorporados com SNP.

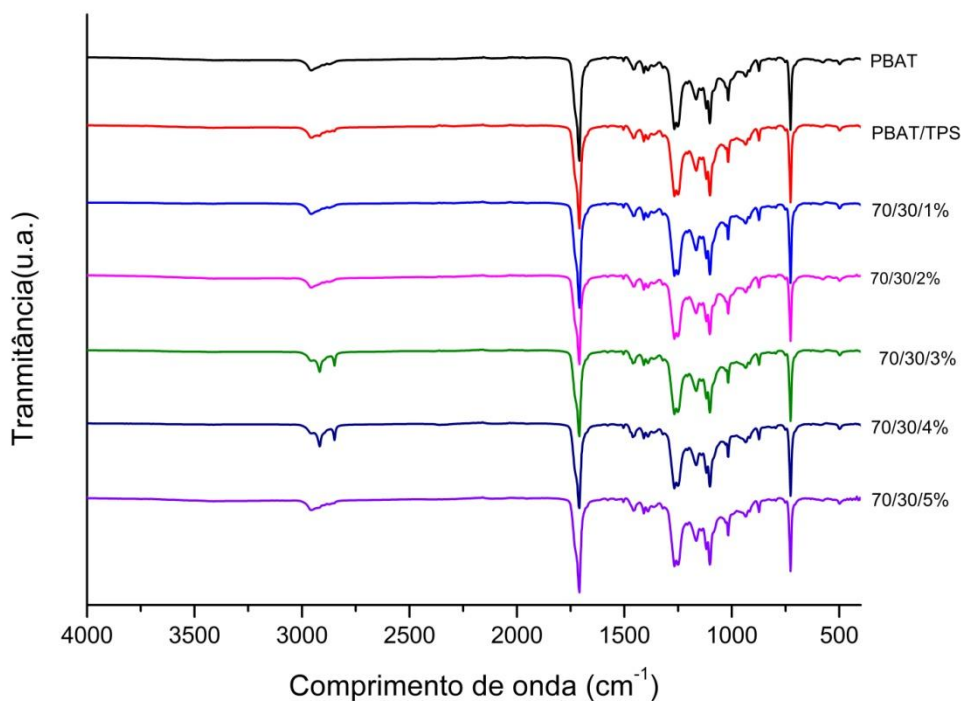


Figura 2 – Solubilidade em água dos filmes PBAT, PBAT/TPS e incorporados com SNP.

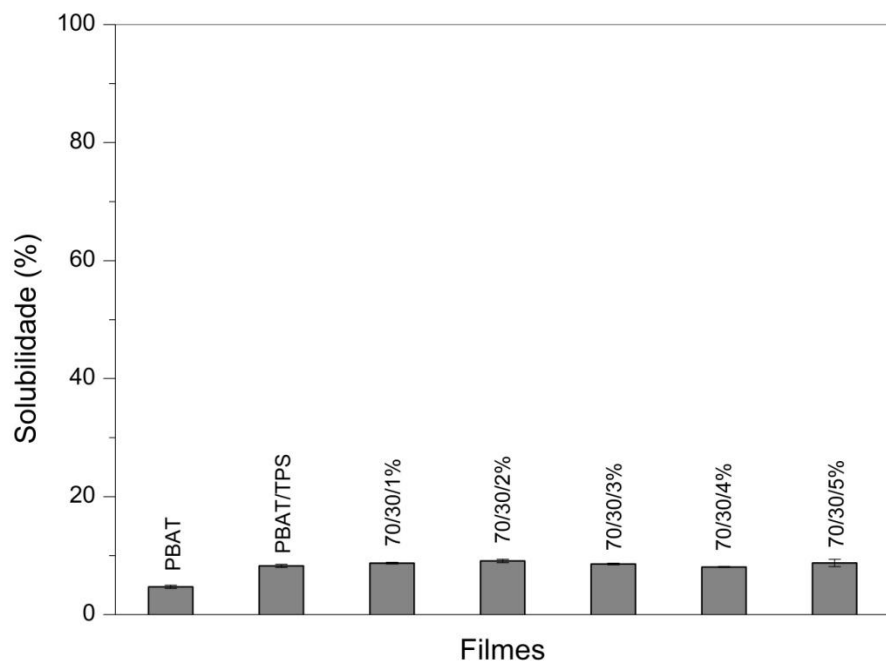


Figura 3 – Perda de massa dos filmes em contato com o solo simulado dos filmes de PBAT, PBAT/TPS e incorporados com SNP.

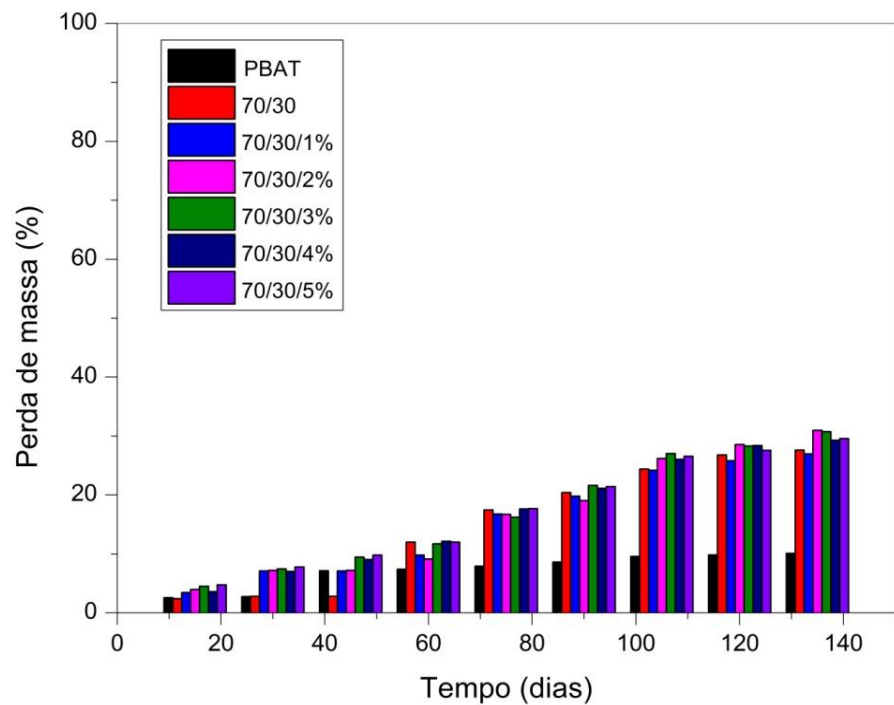


Figura 4 – Processamento de filmes de PBAT/ATP com curcumina pura.

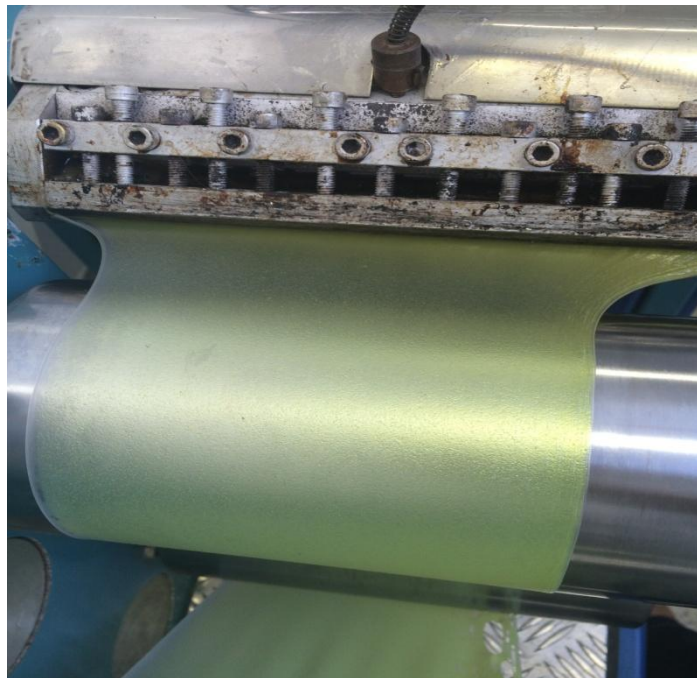


Figura 5 – Filmes de PBAT/ATP com curcumina pura e solução de NAOH.

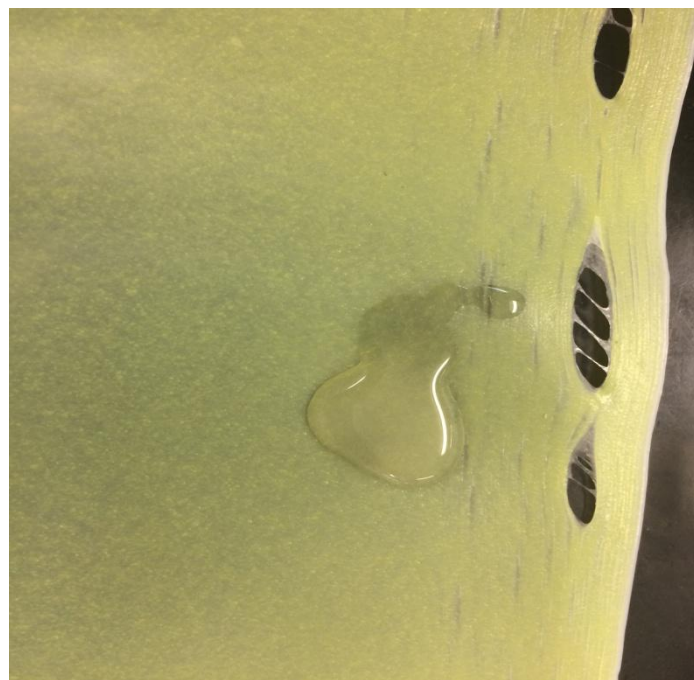


Figura 6 – Filme de PBAT/ATP com nanopartículas de amido carregadas com curcumina.





UFBA
UNIVERSIDADE FEDERAL DA BAHIA
ESCOLA POLITÉCNICA

PROGRAMA DE PÓS GRADUAÇÃO EM ENGENHARIA INDUSTRIAL - PEI

Rua Aristides Novis, 02, 6º andar, Federação, Salvador BA
CEP: 40.210-630
Telefone: (71) 3283-9800
E-mail: pei@ufba.br
Home page: <http://www.pei.ufba.br>